



TECHNICAL MEMORANDUM

TO: Chuck Reid, Manager, CCBWQA
FROM: Christine Hawley and Jean Marie Boyer, PhD, PE; Hydros Consulting Inc.
SUBJECT: DRAFT 2014-2017 Update to the Cherry Creek Reservoir Water-Quality Model
DATE: March 8, 2019

The Cherry Creek Basin Water Quality Authority (Authority) requested that Hydros Consulting (Hydros) update the existing reservoir water-quality model, extending the original simulation period (2003 through 2013) to include four more years of record (2014-2017). Additionally, the Authority asked Hydros to provide a discussion of key drivers of reservoir water-quality response in terms of chlorophyll *a*, cyanobacteria blooms, and dissolved oxygen concentrations in each of the four added years.

This technical memorandum presents the results of that effort. The memo is organized in six sections that follow and Executive Summary:

1. Introduction;
2. Observed Data Overview;
3. Model Extension Results;
4. Water-Quality Response Overview, 2014 – 2017;
5. Summary of Findings; and
6. References.

The discussions are supported by two attachments containing additional graphics:

Attachment A: Observed and simulated temperature profiles; and
Attachment B: Observed and simulated dissolved oxygen profiles.

Executive Summary

At the request of the Authority, Hydros conducted a data evaluation and extension of the reservoir model for the years 2014 through 2017. The following summarizes key findings and recommendations generated from that effort.

- **The Model Extension (Validation) Successfully Met All Original Calibration Criteria** - The extended reservoir water-quality model, with no changes to the original calibration settings, successfully met all calibration targets for the added four years (2014 – 2017) as well as for the full 15-year simulation (2003 – 2017). As an example of the results, average

summertime chlorophyll *a* concentrations for 2003 – 2017 (Figure ES-1) were predicted with a mean absolute error (MAE) of 2.7 µg/L, compared to an MAE of 2.8 µg/L for 2003 – 2013.

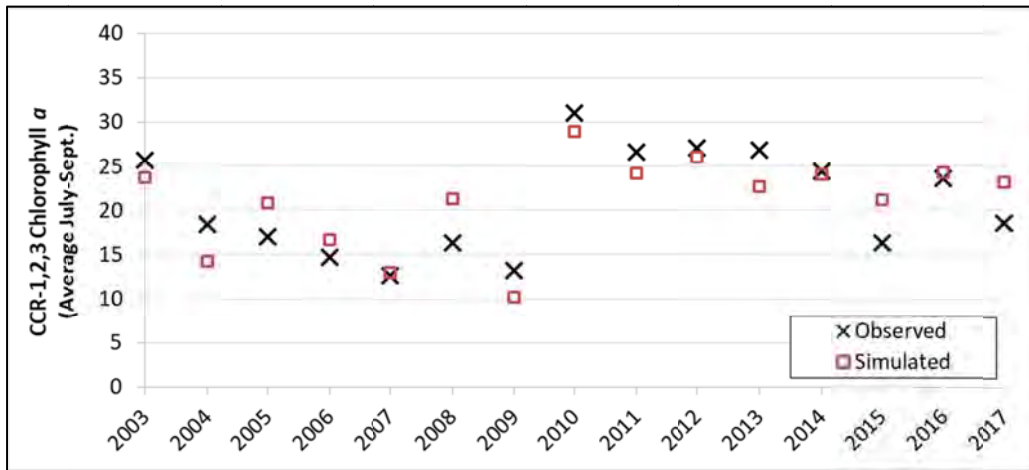


Figure ES-1. Simulated and Observed Summertime Average Chlorophyll *a*, µg/L, 2003 – 2017

- A Slight Adjustment to Model Settings Was Found to Improve Simulated Timing of Spring Cyanobacteria Blooms** – Data from 2014 through 2017 provided an opportunity to simulate (and refine calibration for) major spring cyanobacteria blooms not present in the previous observed biovolume dataset. The model adjustment improved the simulated timing of spring *Anabaena* blooms. All other results were similar to those from the unadjusted model, meeting all calibration criteria. For example, the MAE for 2003 – 2017 summertime chlorophyll *a* was 2.5 µg/L (Figure ES-2). The adjusted model is recommended for use moving forward.



Figure ES-2. Simulated and Observed Summertime Average Chlorophyll *a* for Unadjusted Simulation and Proposed Calibration Refinement Run, µg/L, 2003 - 2017

- The Extended Dataset Indicates Possible Beneficial Effects of the Existing Destratification System in May and Early June:** The data suggest the destratification system can reduce thermal stratification in May and early June and that mixing may help limit cyanobacteria blooms at that time. The observed mixing, however, does not appear to be adequate to maintain oxygenated conditions at the bottom or reduce internal anaerobic loading at that

time. Further, the full dataset continues to indicate that the current destratification system has no significant effect on chlorophyll *a* or cyanobacteria through the summer months.

- **Recommendation: Install Continuous Dissolved Oxygen Probes at CCR-2** at the top and bottom or install an automated profiler for daily dissolved oxygen profiles. This is needed to better understand oxygen dynamics and to support possible future upgrades to the destratification system.
- **Recommendation: Test Smaller Filter Sizes for SRP Samples** to help evaluate the potential significance of inflowing colloidal phosphorus. Analysis of SRP from samples filtered at 0.02 μm (in addition to currently conducted 0.45 μm filtered analyses) should be performed at CC-10 and CCR-2 over at least one average or wet year sampling season.

1 Introduction

Cherry Creek Reservoir (Figure 1) is a 13,000 acre-ft flood-control reservoir near Denver, Colorado. The reservoir is a popular recreation area and a high-quality walleye fishery. The Cherry Creek Basin Water Quality Authority (Authority) exists to protect and improve water quality in the reservoir to meet applicable water-quality standards. Key water-quality concerns for the reservoir include periodic nuisance cyanobacteria (blue-green algae) blooms and high chlorophyll *a* concentrations. The reservoir has failed to consistently meet the current site-specific chlorophyll *a* standard of 18 ug/L, assessed as a July through September average.



Figure 1. Cherry Creek Reservoir and Destratification System Footprint (*Background aerial image from Google Earth; imagery date May 13, 2017*)

In efforts to improve water quality, the Authority has implemented major watershed and in-reservoir monitoring and mitigation projects. In-reservoir efforts include installation of a compressed-air destratification system (in-reservoir footprint shown in Figure 1). Mixing from the destratification system was intended to increase dissolved oxygen at the bottom, thereby reducing internal loading of nutrients and chlorophyll *a* concentrations. The mixing from the destratification system was also intended to reduce cyanobacteria concentrations by disrupting their buoyancy advantage over other algal types. The destratification system was operated from 2008 through 2013 (from roughly April through November each year) and in 2017 (May and June only).

In 2015, based on ongoing water-quality concerns, the Authority identified a need to develop a water-quality model of the reservoir to:

- Better understand the causes of chlorophyll *a* standard exceedances and cyanobacteria blooms;

- Determine the impacts of the destratification system; and
- Provide a tool to help predict the effects of future management strategies.

To meet that need, a two-dimensional hydrodynamic and water-quality model of Cherry Creek Reservoir was developed (Figure 2) using CE-QUAL-W2 (Cole and Wells, 2017). The model and supporting data analysis (Hydros, 2017) identified the following as key drivers of the observed chlorophyll *a* and cyanobacteria response in the reservoir:

- Relatively shallow depth and resulting polymixis,
- High levels of internal and external phosphorus loading, and
- Nitrogen limitation creating favorable conditions for nitrogen-fixing cyanobacteria.

In addition to identifying key drivers of algal and cyanobacteria response, the model and associated data analysis (including data from 2003 through 2013) indicated that the current destratification system was under-designed to meet its objectives.

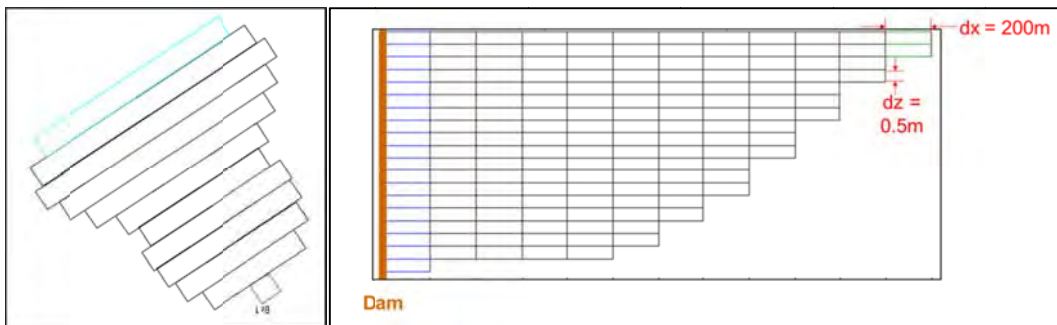


Figure 2. Plan and Profile Views of Cherry Creek Reservoir Model Segmentation

The Authority has continued extensive data collection in the reservoir and watershed. In 2018, the Authority requested that the reservoir model be extended to include 2014 through 2017 without recalibration. This would provide an opportunity to evaluate model performance and identify areas that may be in need of further calibration. The robust dataset of 2014 through 2017 allows for evaluation of model simulation results over a wider range of hydrologic conditions, including an extended period during which the destratification system was not operated (2014 through 2016). Previously, the more robust portion of the dataset (2009-2013) corresponded only to years when the destratification system was operated. These additional years of data are expected to provide a greater understanding of the effectiveness of the destratification system.

This technical memorandum presents the results of the model extension through 2017 and discussions of the observed water-quality response for 2014 through 2017, with a primary focus on chlorophyll *a* and cyanobacteria blooms.

2 2014 - 2017 Observed Data Overview

Observed data for 2014 through 2017 were reviewed to develop model inputs. The recent four years of data were compared to observations from 2003 through 2013, where available, to note any possible changing conditions. Additionally, data were reviewed for patterns to support critical review of and ongoing development of the conceptual system understanding presented in the original model documentation (Hydros, 2017). This included further evaluation of the effectiveness of the current destratification system. The following subsections summarize findings regarding water balance, meteorological conditions, inflow water quality, and in-reservoir water quality. Data sources matched those described in the original model documentation, except where noted.

2.1 Water Balance

The water balance for 2014 through 2017 was developed for the same major inflow and outflow terms simulated in the 2003 - 2013 model documentation:

Inflows:

- Cherry Creek (gaged);
- Cottonwood Creek (gaged);
- Alluvial inflow;
- Ungaged surface inflow from the direct watershed; and
- Precipitation.

Outflows:

- Reservoir releases from the dam;
- Outflow seepage; and
- Evaporation.

The water balance for 2014 through 2017 generally shows patterns similar to those noted for 2003 through 2013 in the original model documentation (Hydros, 2017). The daily inflows for 2014 through 2017 continued to exhibit a wide range of flow rates, characterized by periodic storm event hydrograph peaks (Figure 3). The highest peak inflow of the 15-year period occurred in 2015, estimated by water balance to be 1,003 AF/d in Cherry Creek on June 12. On an annual basis, Cherry Creek was the dominant source of water into the reservoir for 2014 through 2017, averaging more than 60% of total inflows (Figure 4). Cottonwood Creek and alluvial inflow comprised the next largest fractions.

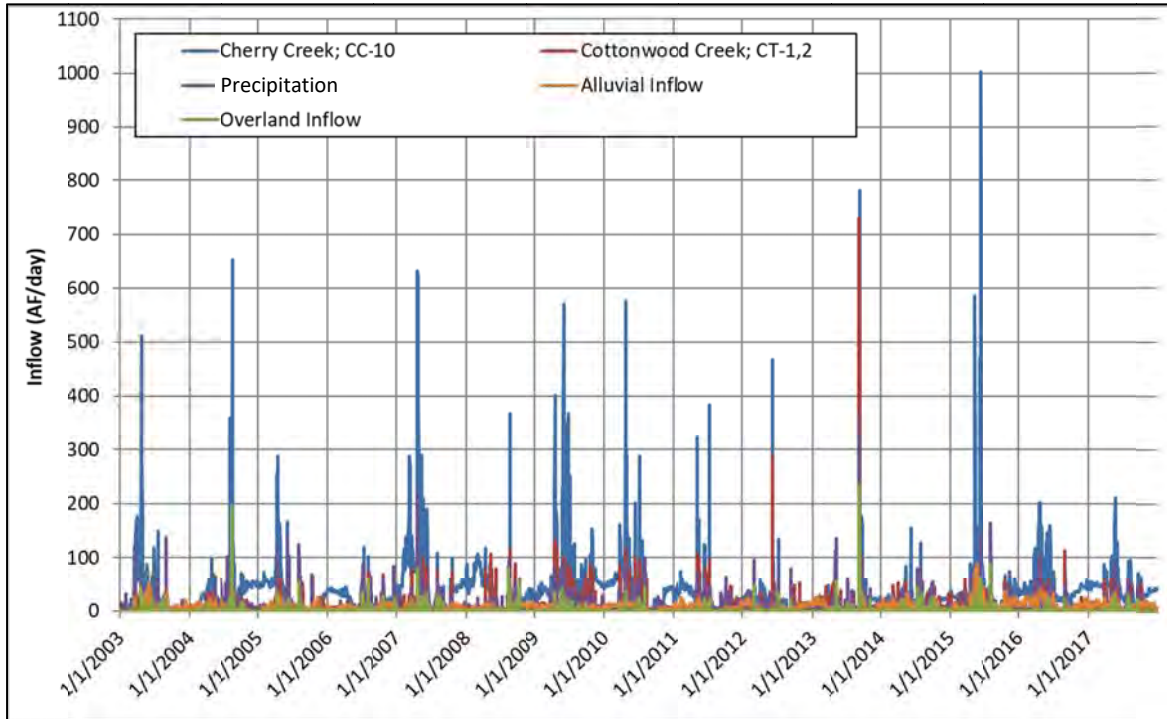


Figure 3. Cherry Creek Reservoir Daily Inflow Rates, 2003 – 2017

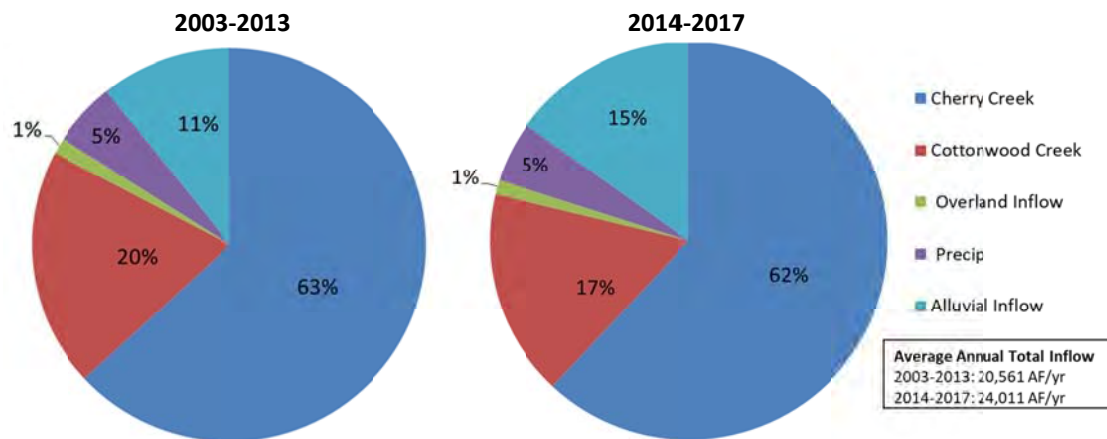


Figure 4. Relative Fractions of Cherry Creek Total Inflows, 2003 – 2013 and 2014 – 2017

On closer inspection, a change was identified in the ratio of Cottonwood Creek inflow to Cherry Creek. From 2003 through 2011, there was a seasonal pattern to the ratio, indicating that Cottonwood Creek typically comprised an equal or greater portion of inflow relative to Cherry Creek through much of the summer months (Figure 5). However, that seasonal increase in the ratio is less apparent from 2012 through 2017, due to lower flow rates from Cottonwood Creek (Figure 6). The exact cause of this change in the summer ratio is uncertain but may be due to wetlands upgrades in 2012 on Cottonwood Creek, effectively reducing low-flow rates through increased evaporation/transpiration, particularly in the summer months. Given the differing

water quality of the two inflows (discussed in Section 2.3), this changing ratio could affect reservoir water quality, including algal response.

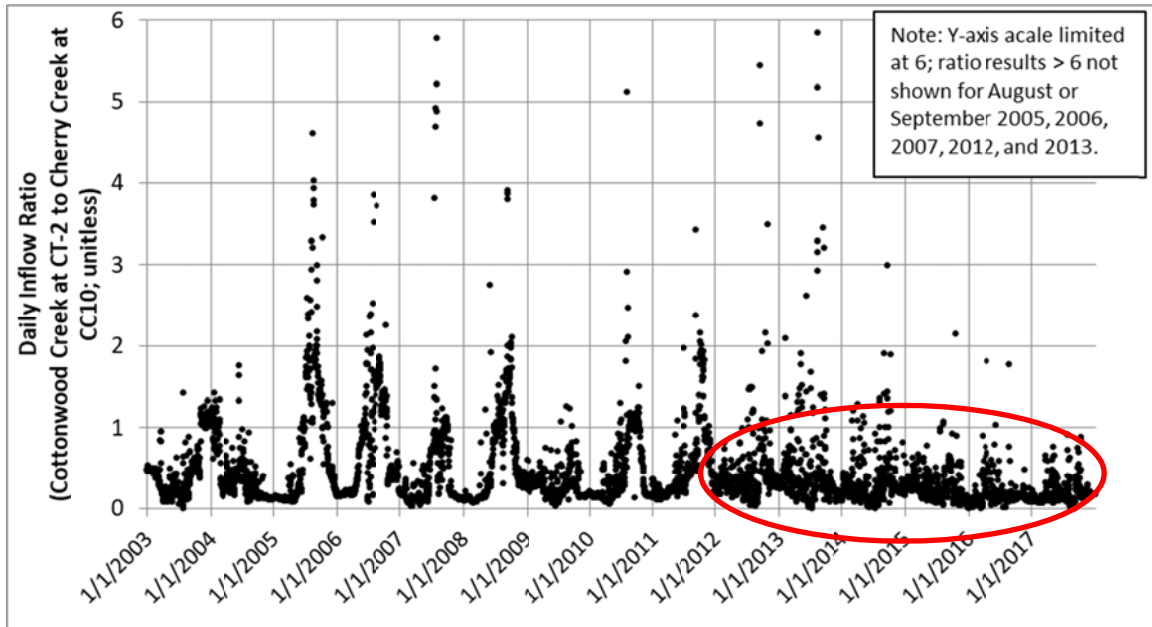


Figure 5. Ratio of Daily Inflow Rates for Cottonwood Creek to Cherry Creek, 2003 – 2017 (Red circle indicates timing of change in summer low-flow pattern.)

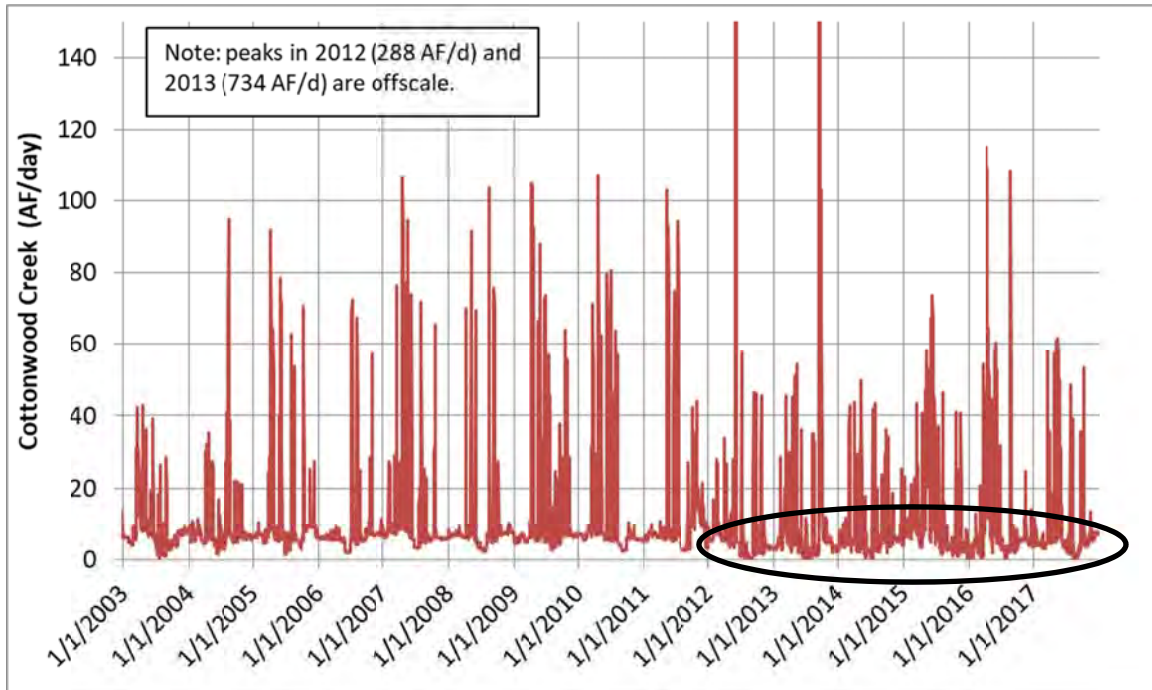


Figure 6. Daily Inflow from Cottonwood Creek, 2003 – 2017 (Black circle indicates timing of change in summer low-flow pattern.)

As noted for inflows, outflows for 2014 through 2017 were similar to those for 2003 through 2013 (Figure 7). The primary annual outflow (>80%) was the release from the dam. From 2014

through 2017, daily outflow from the dam generally paralleled daily inflows, resulting in limited variation in surface water elevation over the four years (roughly ± 1 ft), with the exception of the 2015, which had very high inflows (Figure 8).

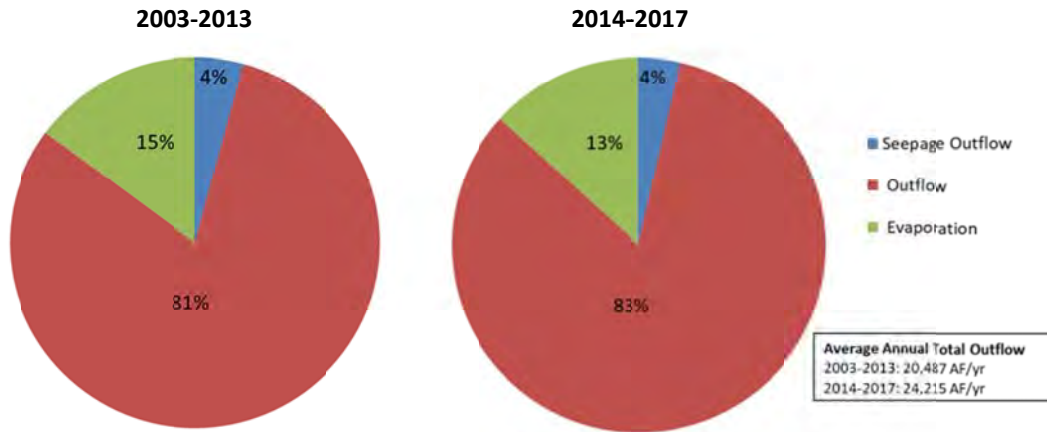


Figure 7. Relative Fractions of Cherry Creek Total Outflows, 2003 – 2013 and 2014 – 2017

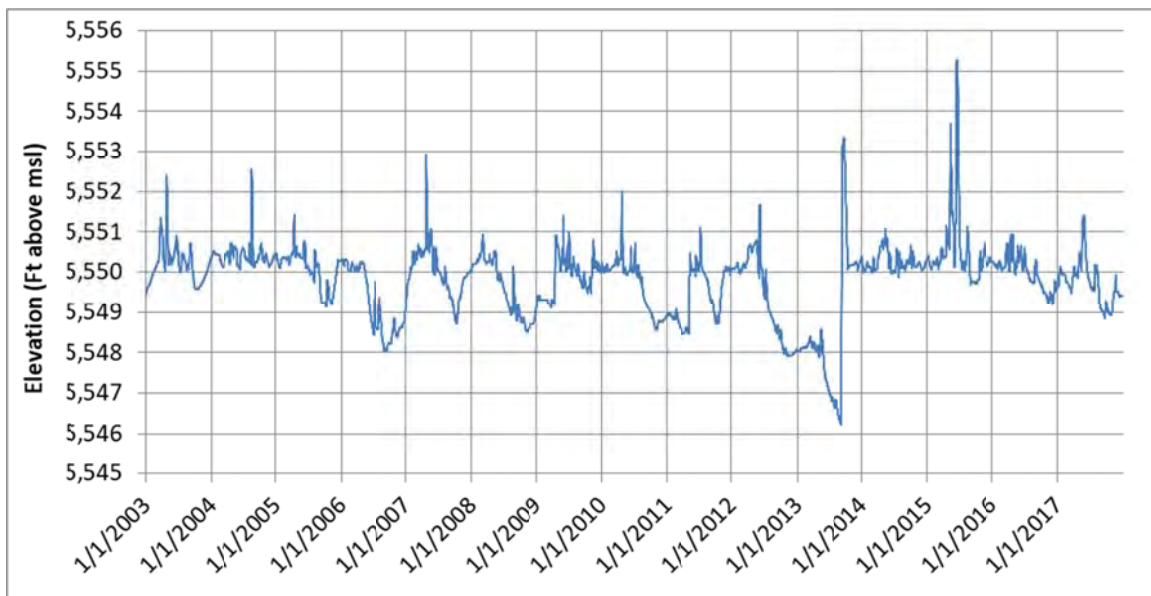


Figure 8. Daily Surface Water Elevation in Cherry Creek Reservoir, 2003 – 2017 (Feet above mean sea level [msl])

Total annual inflows and outflows vary widely from year to year (Figure 9). Of the four years to be added to the water-quality model, three were relatively high flow years (2015, 2016, and 2017), and one was a relatively low flow year (2014). Estimated annual hydraulic residence times were correspondingly variable (Figure 10), ranging from six months in 2009 to just over 14 months in 2014 (Figure 10). The average residence time for the entire 15-year period was 10 months.

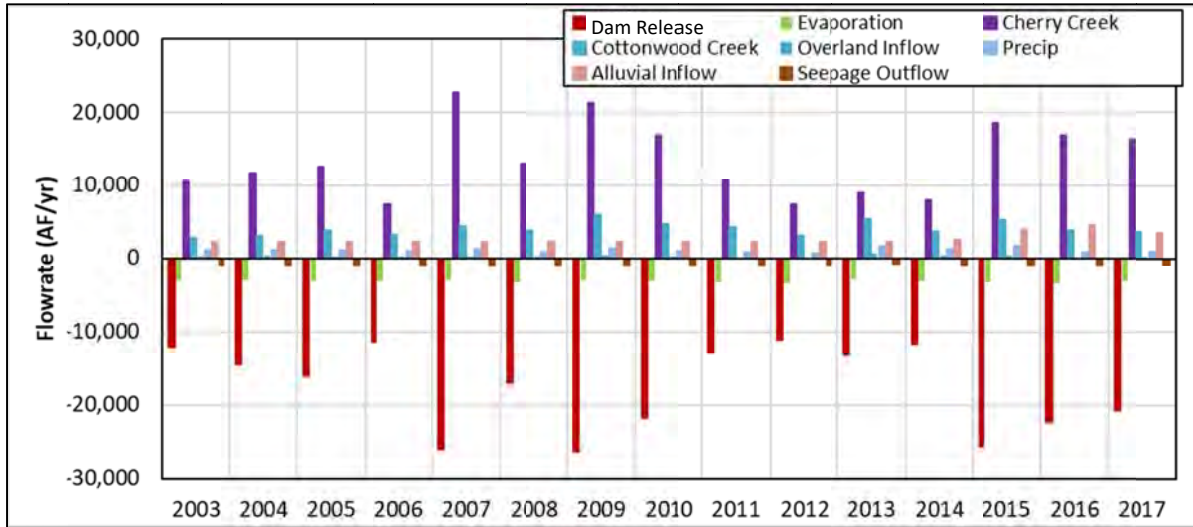


Figure 9. Cherry Creek Reservoir Annual Water Balance, 2003 - 2017

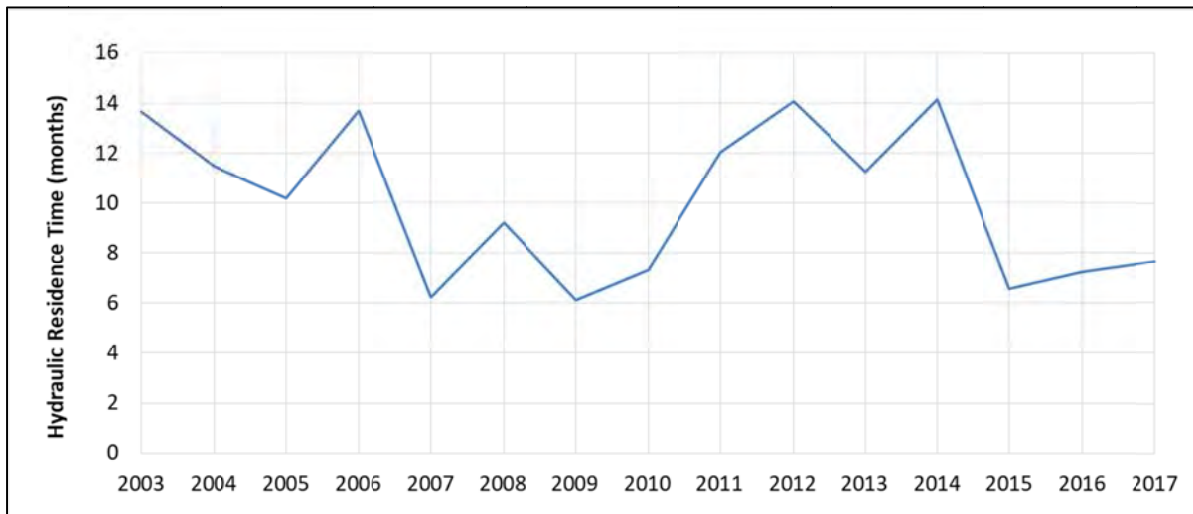


Figure 10. Annual Hydraulic Residence Time (Based on Average Annual Storage / Annual Reservoir Releases)

2.2 Meteorological Conditions

To evaluate the observed water-quality response and to update the model, meteorological data for 2014 through 2017 were compiled from the KAPA station (located ~4 miles south of the reservoir at the Centennial Airport [Figure 11]) for air temperature, windspeed, wind direction, dew point, and cloud cover. Solar radiation data were retrieved from the National Renewable Energy Labs (NREL) SolarTAC site (located ~15 miles NW of the reservoir [Figure 11]; Andreas and Wilcox, 2011). Previously, data from the Colorado Parks and Wildlife (CPW) meteorological station adjacent to the reservoir were used for air temperature and solar radiation, but CPW data were not available for recent years and are understood to have been discontinued. Modeling 2014 through 2017 with meteorological data sources located farther from the reservoir adds some uncertainty and is therefore is not ideal. Fortunately, the Authority is in the

process of installing a meteorological data collection station at the reservoir, which will benefit future model updates.

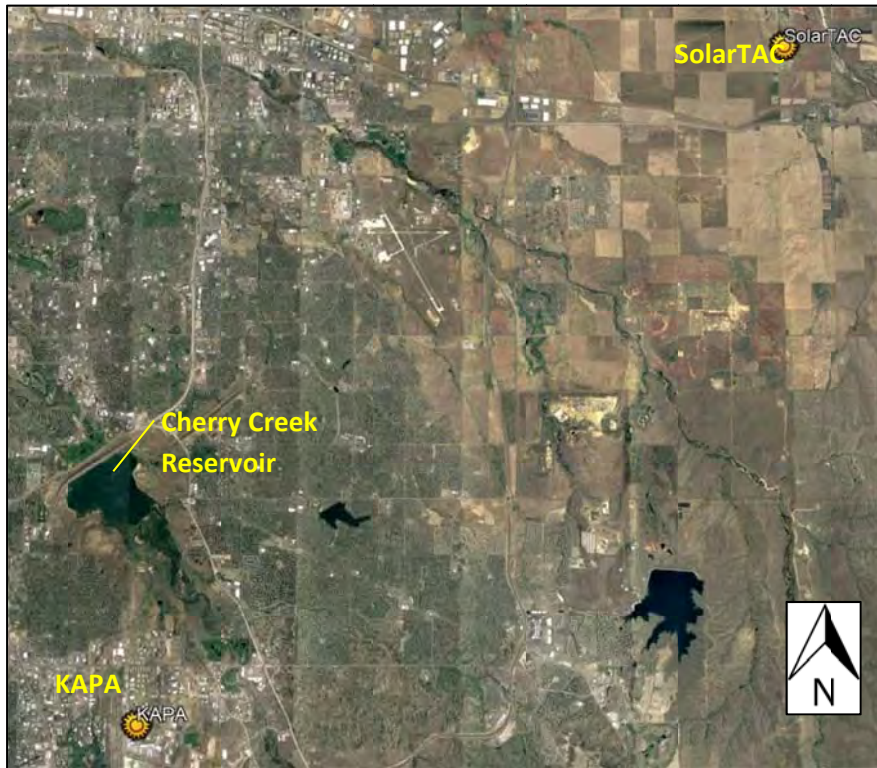


Figure 11. Location of Meteorological Data Sources for 2014 – 2017 (Background Google Earth® image from May 31, 2018)

Air temperature, solar radiation, and windspeed data compiled for 2014 through 2017 generally exhibit seasonal patterns seen in the 2003 – 2013 data, with a few noteworthy differences. Air temperatures were slightly below average for the key months of April through August (Figure 12), while solar radiation was above average (Figure 13). These differences may or may not be attributable to the use of different meteorological data stations for 2014 – 2017. Windspeeds were generally below the 2003 – 2013 average for 2015, 2016, and 2017 (Figure 14).

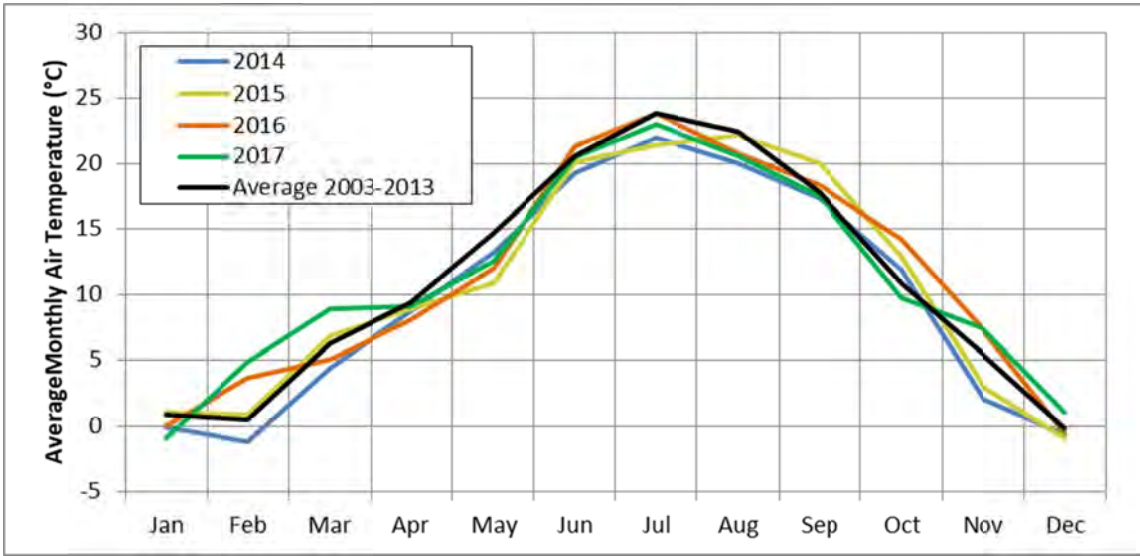


Figure 12. Average Monthly Air Temperatures for 2014 - 2017 Compared to 2003 - 2013 Averages

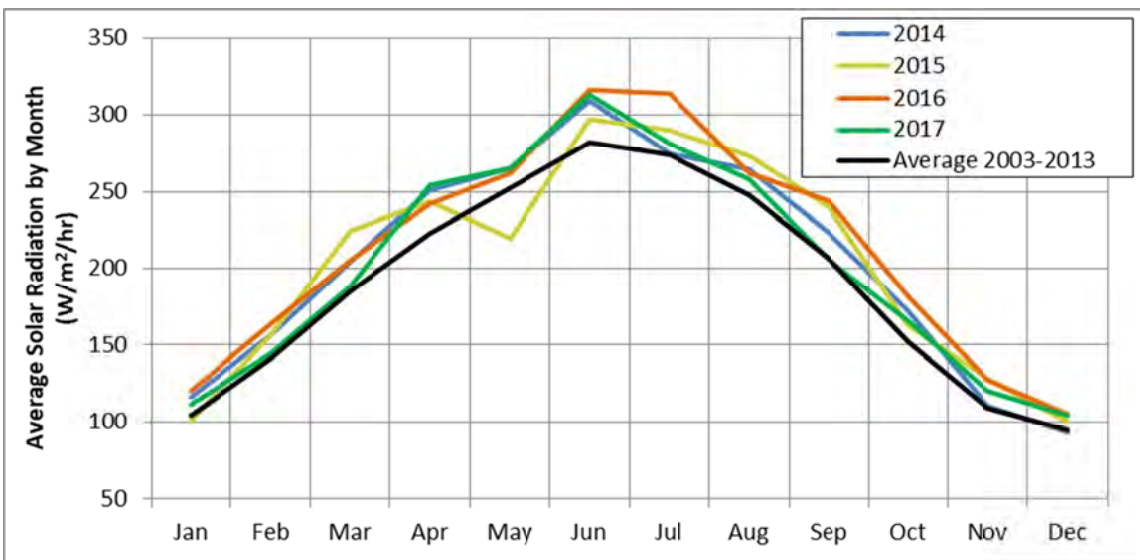


Figure 13. Average Monthly Solar Radiation for 2014 - 2017 Compared to 2003 - 2013 Averages

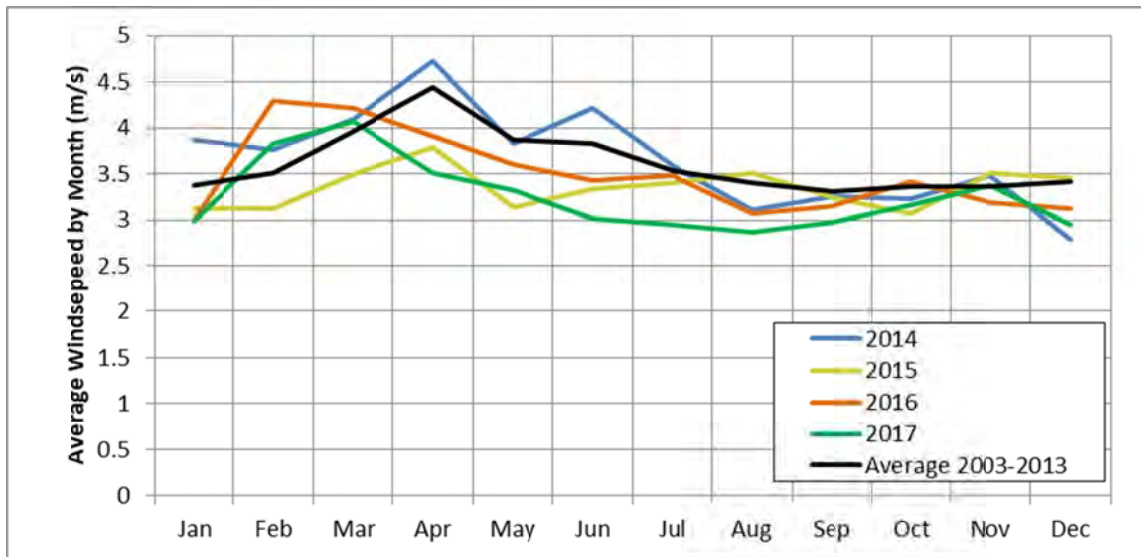


Figure 14. Average Monthly Windspeeds for 2014 - 2017 Compared to 2003 - 2013 Averages

2.3 Inflow Nutrients

Water-quality data are collected at the inflow locations to the reservoir on Cherry Creek and Cottonwood Creek at gages CC-10 and CT-2, respectively. Inflow water quality is characterized by high nutrient concentrations and has been the subject of numerous water-quality improvement projects implemented by the Authority in the watershed. The following subsections describe inflow nitrogen and phosphorus concentrations for 2014 – 2017 in comparison to observations from 2003 – 2013.

2.3.1 Inflow Nitrogen

Observed data for nitrogen indicate higher concentrations from Cottonwood Creek than from Cherry Creek for 2014 through 2017 (Figure 15). The data for recent years generally match patterns and ranges observed in the previous years, with nitrate+nitrite comprising the majority of the inflow total inorganic nitrogen (TIN, which is bioavailable and equals the sum of ammonia and nitrate+nitrite) concentrations. Both nitrate+nitrite and total nitrogen concentrations tend to be higher in winter months in both tributaries, though concentrations in Cherry Creek were relatively low in the winter of 2014/2015 and 2015/2016.

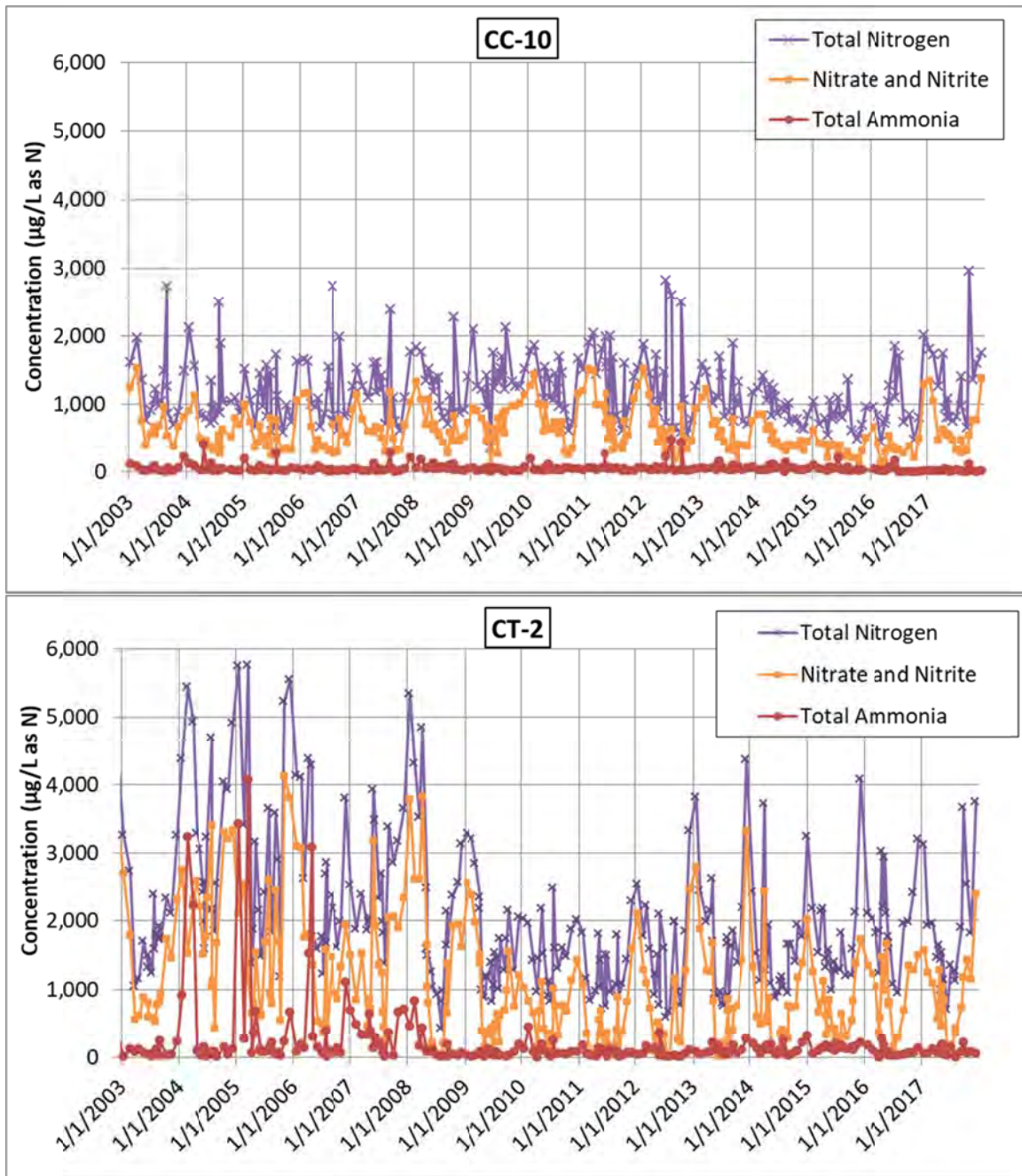


Figure 15. Inflow Total Nitrogen, Nitrate+Nitrite, and Ammonia Concentrations for Cherry Creek (top graph) and Cottonwood Creek (bottom graph), 2003 – 2017; Y-Axis Scales Identical to Allow for Direct Comparison of Magnitudes

Volume-weighted average concentrations of ammonia, nitrate+nitrite, and total nitrogen were lower in both Cherry Creek and Cottonwood Creek for 2014 – 2017 compared to 2003 – 2013 (Figure 19). However, average annual loading was only slightly below that for 2003 - 2013 (Figure 17), due to greater average inflow volumes for 2014 – 2017. Nitrogen loading should be interpreted with caution, recognizing the other factors that can limit or increase its significance to algal growth, including inflow timing, inflow location, nutrient ratios, water temperatures, clarity, settling (for total nitrogen), and outflows.

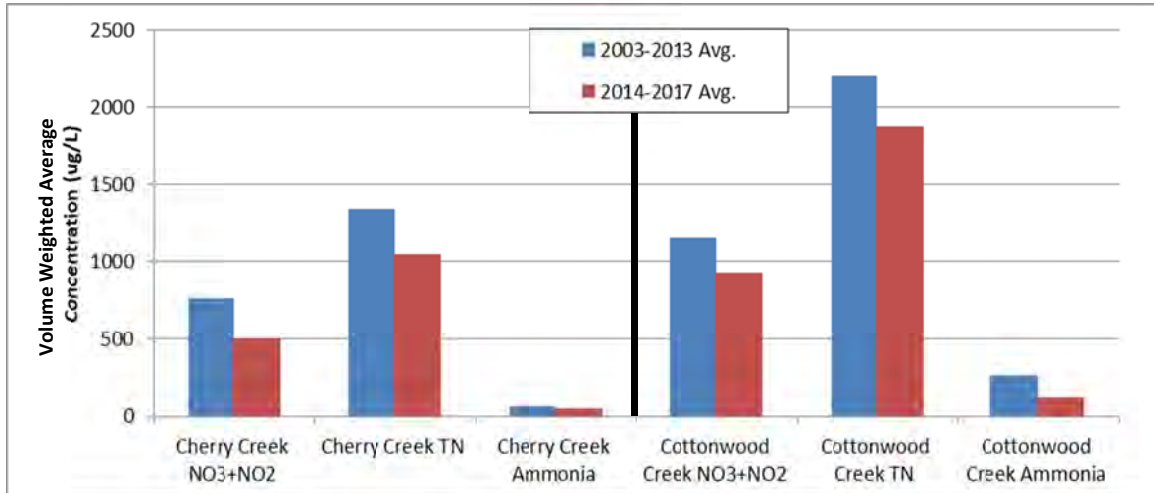


Figure 16. Comparison of 2003 - 2013 and 2004 - 2017 – Volume-Weighted Average Concentrations; Nitrate+Nitrite, Total Nitrogen, and Ammonia

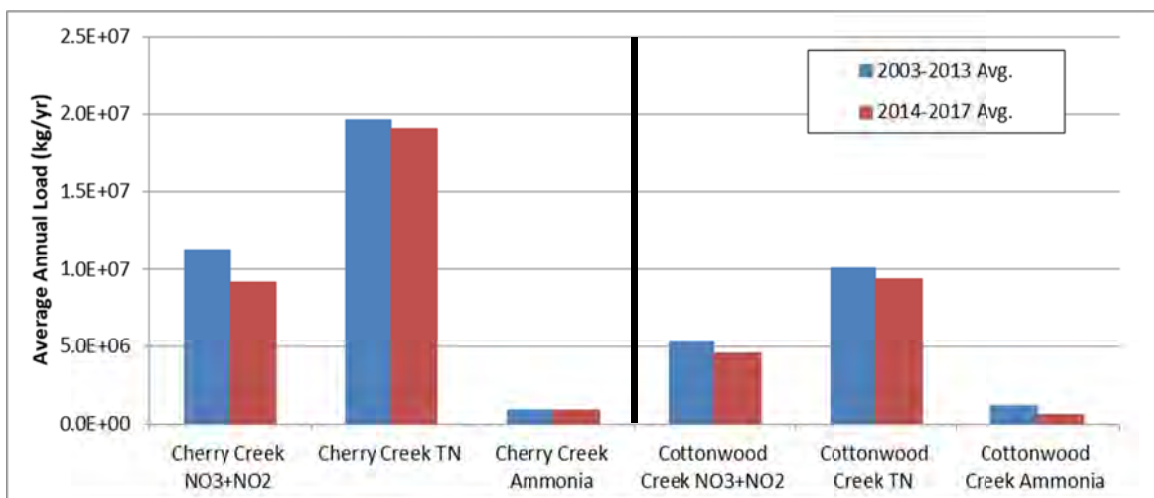


Figure 17. Comparison of 2003 - 2013 and 2004 - 2017 - Average Annual Load; Nitrate+Nitrite, Total Nitrogen, and Ammonia

2.3.2 Inflow Phosphorus

Inflow concentrations of total phosphorus and soluble reactive phosphorus (SRP) for 2014 through 2017 followed similar patterns and ranges to data from the recent preceding years (particularly since ~2009; Figure 18). Both total phosphorus and SRP concentrations are consistently higher in Cherry Creek than Cottonwood Creek. Further, Cherry Creek inflow concentrations exhibit seasonal patterns of higher summer concentrations for both SRP and total phosphorus, with storm-associated peaks for total phosphorus (likely due to association with suspended solids).

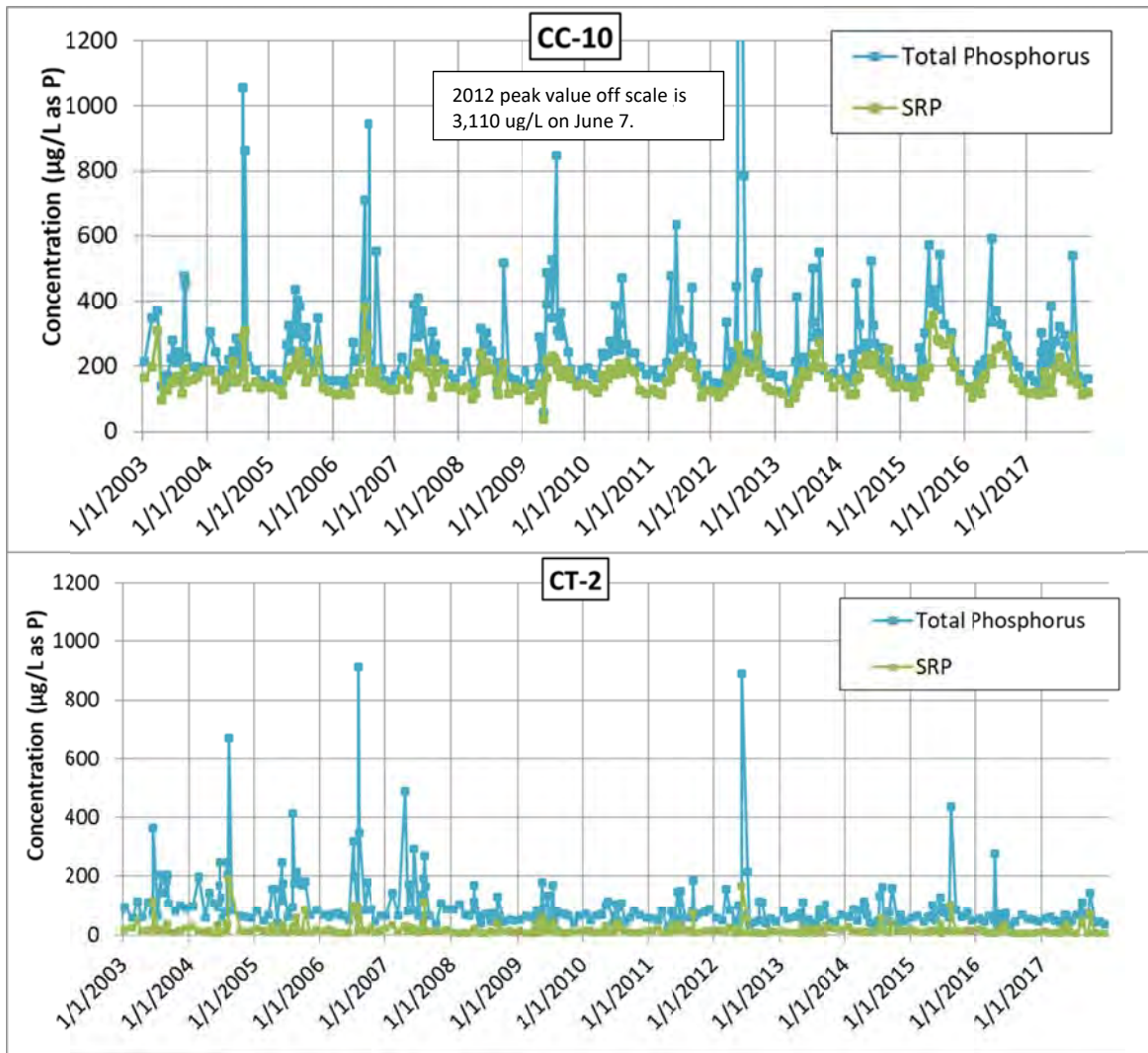


Figure 18. Inflow Total Phosphorus and SRP Concentrations for Cherry Creek (top graph) and Cottonwood Creek (bottom graph), 2003 – 2017; Y-Axis Scales Identical to Allow for Direct Comparison of Magnitudes

Volume-weighted average concentrations of SRP and total phosphorus were similar for 2014 – 2017 compared to 2003 – 2013 for Cherry Creek but slightly lower for Cottonwood Creek (Figure 19). In spite of similar concentrations, average annual phosphorus loading for Cherry Creek was higher for 2014 – 2017 (Figure 20), due to greater inflow volumes. As noted for nitrogen, the effects of loading should be interpreted with caution. Algal response in the reservoir depends on the timing and location (underflow, overflow, etc.) of inflow loads as well as nutrient ratios, water temperatures, etc. Additionally, phosphorus can be subject to significant loss mechanisms, including sorption/settling and outflows, all of which can confound simple correlation of annual or seasonal loading to algal growth/chlorophyll *a*.

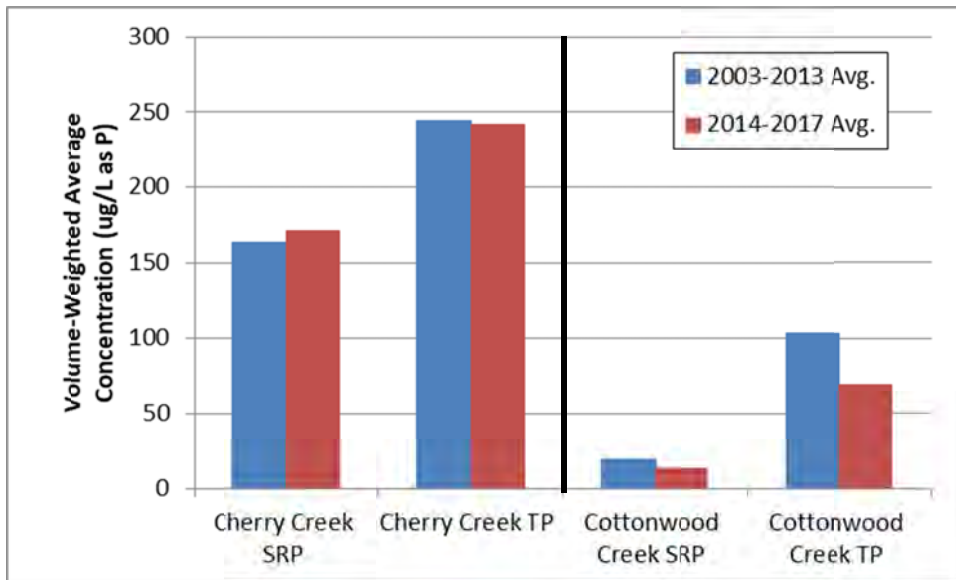


Figure 19. Comparison of 2003 - 2013 and 2004 - 2017 – Volume-Weighted Average Concentrations, SRP and Total Phosphorus

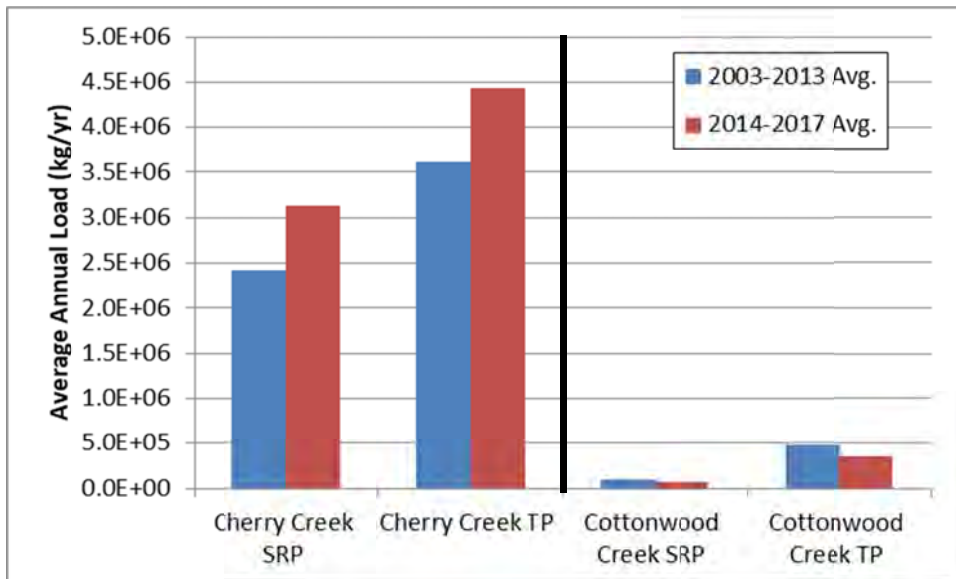


Figure 20. Comparison of 2003 - 2013 and 2004 - 2017 - Average Annual Load, SRP and Total Phosphorus

2.3.2.1 Colloidal Phosphorus in Cherry Creek

Detailed review of the observed data and existing literature has raised a question about the SRP data, and a recommendation is offered for additional water-quality analyses in the coming sampling year (2019). It is assumed that SRP results reflect the concentration of orthophosphate concentration in the water, which is the most readily-available form of phosphorus for algal growth (high bioavailability). This is a reasonable assumption for many systems; however, SRP is not always a reliable estimate of bioavailable phosphorus, particularly in systems with higher SRP (Twinch and Breen, 1982). This is because SRP can include colloidal

phosphorus which can have very limited bioavailability¹ (Li and Brett, 2015). For example, in some Canadian lakes, SRP has been found to be two to three orders of magnitude higher than the actual orthophosphate concentration (Hudson et al., 2000).

This is potentially significant for Cherry Creek given the emphasis on managing phosphorus inflows to the reservoir to control algal growth. Costly efforts to reduce phosphorus that do not target the bioavailable fraction of phosphorus may not produce the desired results of reduced algal and cyanobacterial growth in the reservoir. Further, because ~70% of the total phosphorus from Cherry Creek is identified as SRP, it is important to understand what the SRP measure actually contains.

There is currently no definitive evidence that SRP overestimates bioavailable phosphorus in Cherry Creek; however, there are possible indications:

- SRP concentrations in Cherry Creek through the spring and summer are routinely ten times higher than the 20 µg/L value noted in Twinch and Breen (1982) as a threshold for possible overestimation of bioavailable phosphorus by SRP analysis.
- In many systems there is an inverse relationship between SRP and flow rate, since runoff can dilute major sources of dissolved orthophosphate such as WWTP effluent. There is no such relationship in Cherry Creek. Instead, SRP concentrations have been observed to increase with flow rate at times (Figure 21), which might suggest that the SRP includes fractions that are particulate (colloidal) in nature and can be mobilized at higher flow rates.
- There has been speculation (though without definitive documentation) that there is a geological source in the basin providing the high levels of phosphorus to Cherry Creek (based on relatively high SRP concentrations in the upper basin per JCHA [2007]). Mineral forms of phosphorus can be colloidal in size, and mineral forms such as apatite and ferric pyrophosphate have been shown to have very low bioavailability (Li and Brett, 2013). Such mineral colloids could be included as “false positives” in the SRP analysis, resulting in an overestimate of the bioavailable phosphorus concentration (Li and Brett, 2015).

¹ Colloids are very small particles, generally defined as being between 1 nm and 1 µm in size (Kretzschmar et al., 1999). Colloidal phosphorus can be part the molecular structure or sorbed to mineral or organic colloids. Typical measurement of SRP (as done for Cherry Creek Reservoir) is conducted by acid molybdate colorimetry of the filtered (0.45 µm) fraction. The acidification step of the analysis can liberate phosphorus which would otherwise be recalcitrant (not reactive or bioavailable), thereby resulting in an overestimate of orthophosphate in the sample. In the reservoir, however, the recalcitrant phosphorus released by acidification may not be bioavailable under the typical neutral-pH conditions in the reservoir.

Ideally, inflowing water quality would be characterized in terms of bioavailable phosphorus (BAP) to best reflect effects on algal growth; however, this would require use of bioassay experiments, which can be costly and time-consuming (Ekholm et al., 2007). Instead, more refined filtration would be a logical first step in evaluating whether colloidal phosphorus may be present in the SRP results for Cherry Creek. Assuming 2019 will be a typical hydrologic year (and not a low-flow year, in particular), it is recommended that inflow SRP samples for March through November of 2019 be measured in 0.2 μm and 0.02 μm filtered samples (or 0.02 μm at a minimum) in addition to the already-measured 0.45 μm -filtered results. This should be conducted for CC-10 and CCR-2 SRP samples. If concentrations of SRP are significantly higher in the 0.2 μm or 0.45 μm -filtered fractions, that would indicate the presence of colloidal phosphorus, presuming that the 0.02 μm fraction better reflects the truly dissolved orthophosphate fraction. If the analysis does indicate significant colloidal phosphorus, further characterization can be conducted on subsequent samples to determine the bioavailable fraction. That information can be used to support appropriately-targeted management of inflow water quality to control algal/cyanobacterial growth in the reservoir.

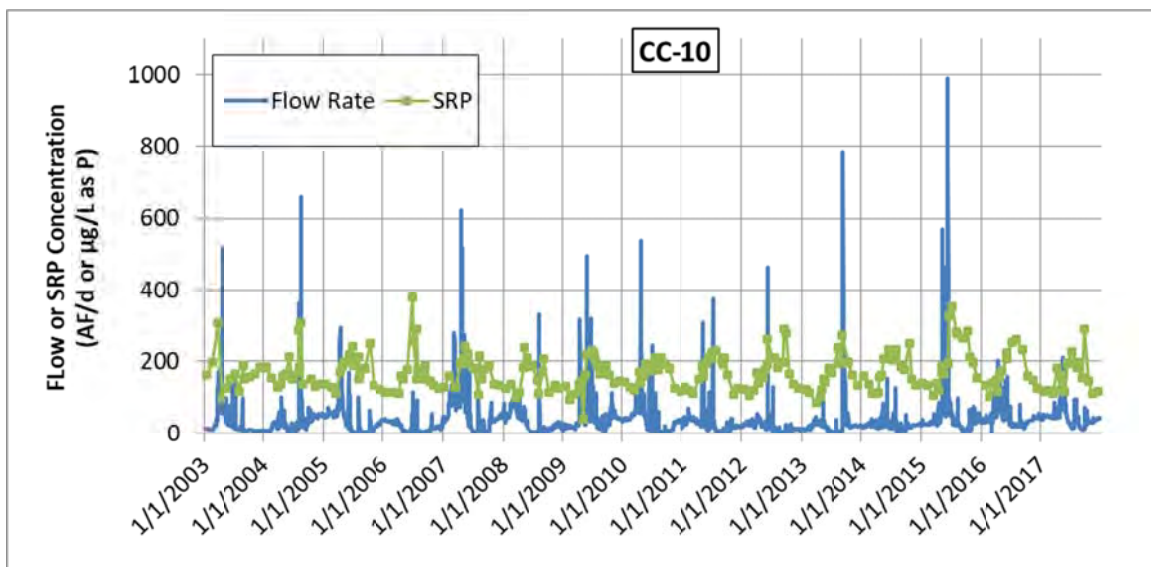


Figure 21. Cherry Creek SRP Concentrations and Flow Rate, 2003 – 2017

2.4 In-Reservoir Water Quality

Water-quality data from stations CCR-1, CCR-2, and CCR-3 (Figure 22) were reviewed in detail for 2014 – 2017. Data were also compared to previous years (2003 – 2013). This section presents highlights focusing primarily on CCR-2, the deepest sampling location, focusing on temperature, dissolved oxygen, nutrients, and algal growth.

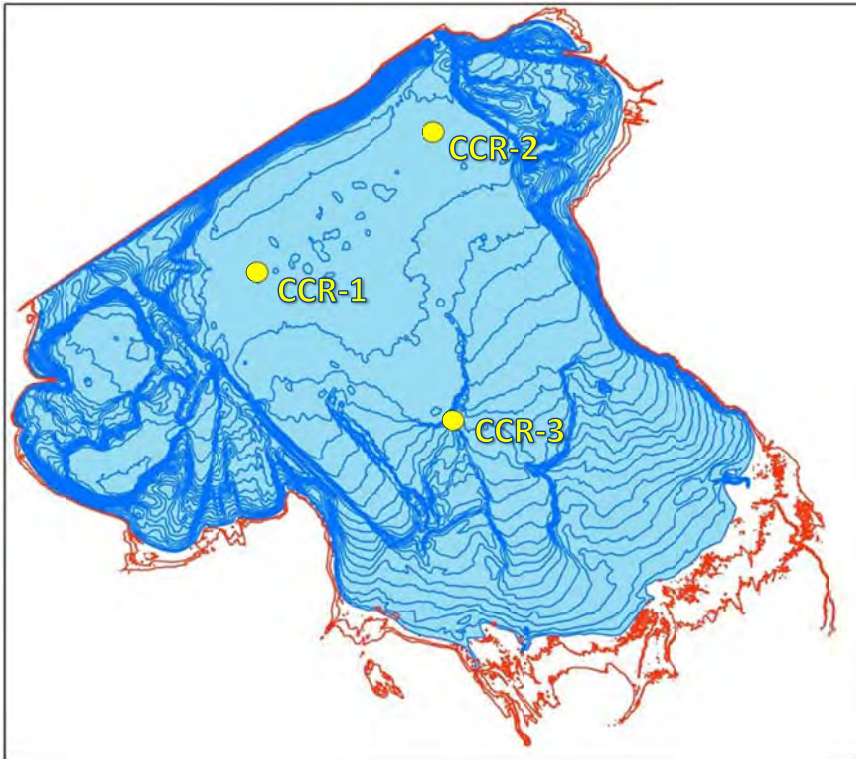


Figure 22. Cherry Creek Reservoir Sampling Location Presented on 1 ft. Bathymetric Contours, and In-Reservoir Sampling Locations

2.4.1 Temperature

Water temperature is an important water-quality metric because it affects the growth rate of algae and cyanobacteria as well as the rates of many reactions including organic matter decay. Temperature data also provide information on thermal stratification. Temperature data from the top of the reservoir indicate that 2014 through 2017 followed typical seasonal thermal patterns, with average daily temperatures peaking in July (June for 2015) between ~24-25 °C (Figure 23 and Figure 24). Of the four recent years, peak temperatures were warmest in 2016 and coolest in 2014. For 2015, 2016, and 2017, surface temperatures in June were above the 2003 – 2013 average (Figure 24).

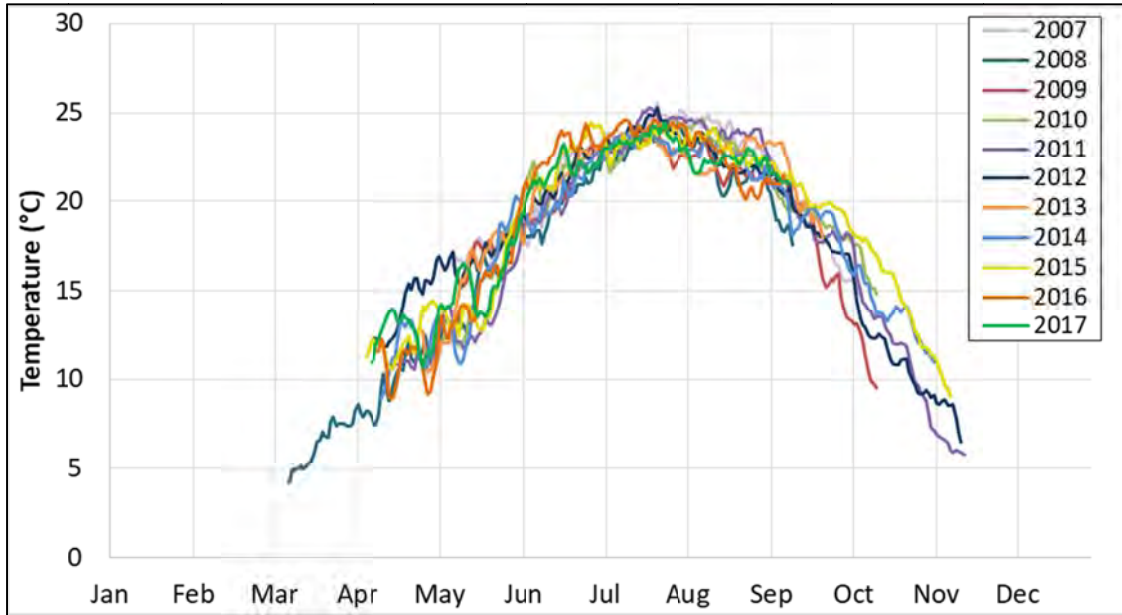


Figure 23. Daily Average Thermistor Temperatures at 1 m at CCR-2, 2007 - 2017

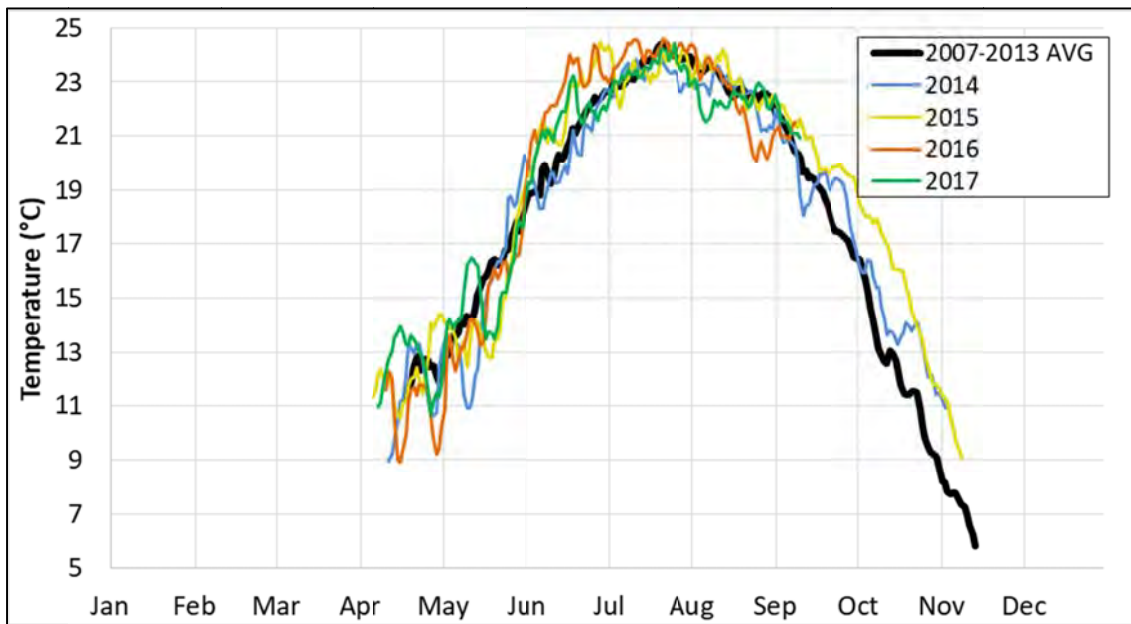


Figure 24. Comparison of Daily Average Thermistor Temperatures at 1 m at CCR-2 for 2014 through 2017 to the 2007 – 2013 Average (Note: 2 m data are shown for April 15 – June 23, 2014, due to lack of 1 m data.)

Differences in temperature between the top and the bottom at CCR-2 were compiled from the in-reservoir thermistor data to evaluate thermal stratification patterns. Results for 2014 through 2017 look similar to the range of results from 2007 through 2013, through differences were on the higher end of previously observed ranges for 2014 through 2016 (Figure 25). For all years, temperature differences indicate periods of weak stratification of varying durations through the spring and summer, indicative of a polymictic reservoir.

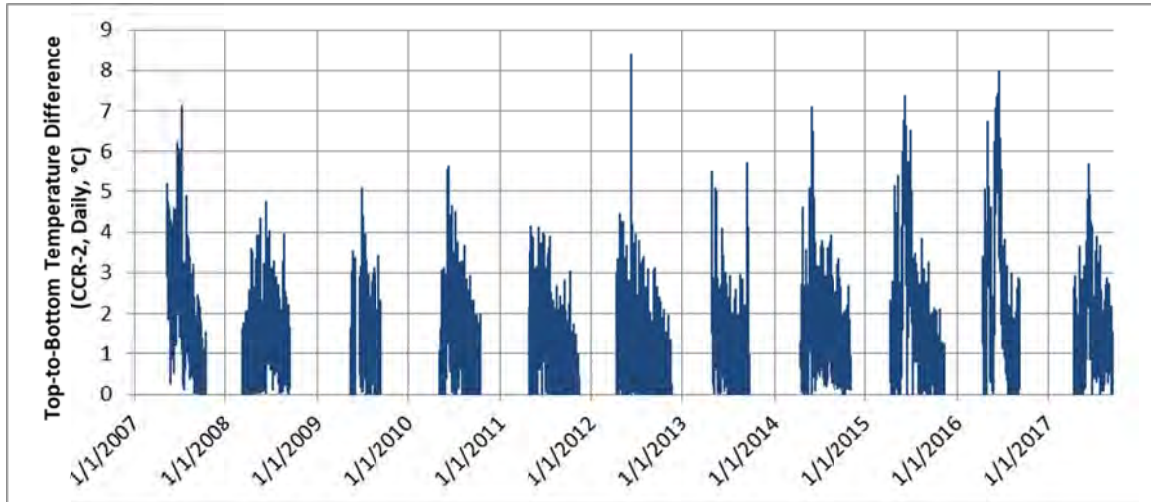


Figure 25. Top to Bottom Temperature Differences at CCR-2, 2007 - 2017

For the original calibration, thermistor data were only available for 2007 through 2013, which includes only one year when the destratification system was not operated. For this analysis, there are three additional years of thermistor data during which the destratification system was not operated (2014, 2015, and 2016), and one additional year with operation (2017, though only operated in May and June). These added years of data offer an opportunity for closer evaluation of the thermal data for evidence of destratification system effects on stratification.

There are apparent differences in the years with and without destratification system operation. The four years without destratification system operations show a greater overall range of top-to-bottom temperature differences as compared to the seven years of record without destratification system operations (Figure 26 compared to Figure 27). Comparing the average difference for each set of years, there is a clear pattern of greater thermal stratification in May and early June in years without destratification system operations (Figure 28). There is, however, no apparent difference in stratification patterns from mid-June through October². These patterns indicate that the destratification system appears to have a notable mixing effect in May and early June, but not later in the season.

The lack of effectiveness of the destratification system in summer months is in agreement with previous findings (Hydros, 2017). The greater relative effect in the spring makes sense considering the lower thermal resistance to mixing at that time (compared to the summer) due to typical water temperatures and associated densities, as noted in Hydros (2014). This finding is also evaluated relative to dissolved oxygen and algal/cyanobacteria response in Sections 2.4.2 and 2.4.4, respectively.

² Note that this statement also holds even if 2017 (during which the destratification system was only operated for May and June) is excluded from the destratification-system-operating group.

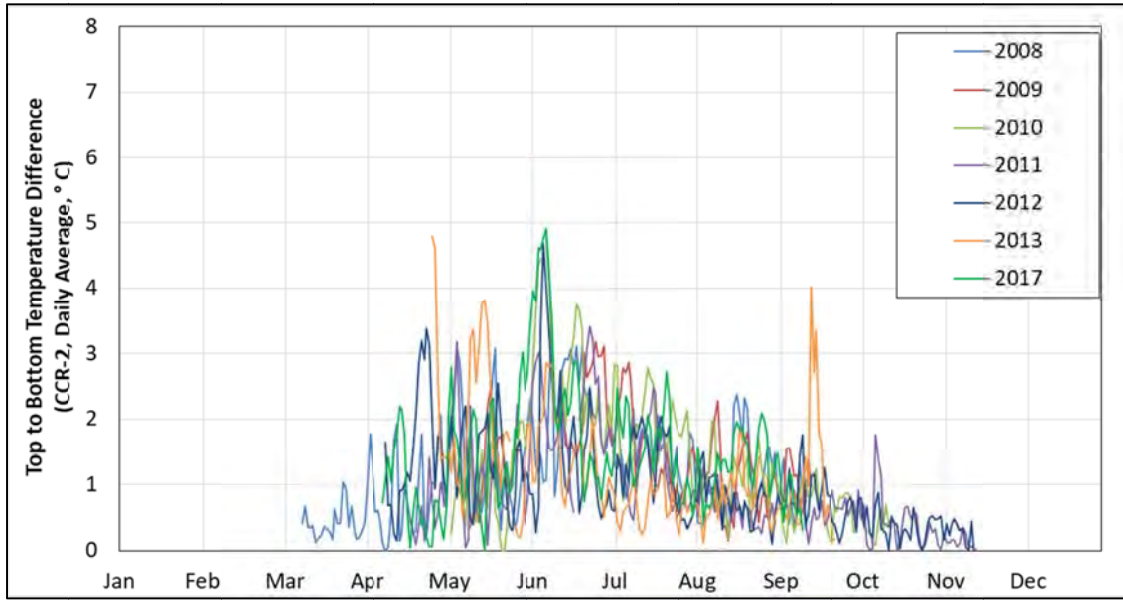


Figure 26. Top-to-Bottom Temperature Differences at CCR-2 for Years with Destratification System Operations; 2008 – 2013, 2017

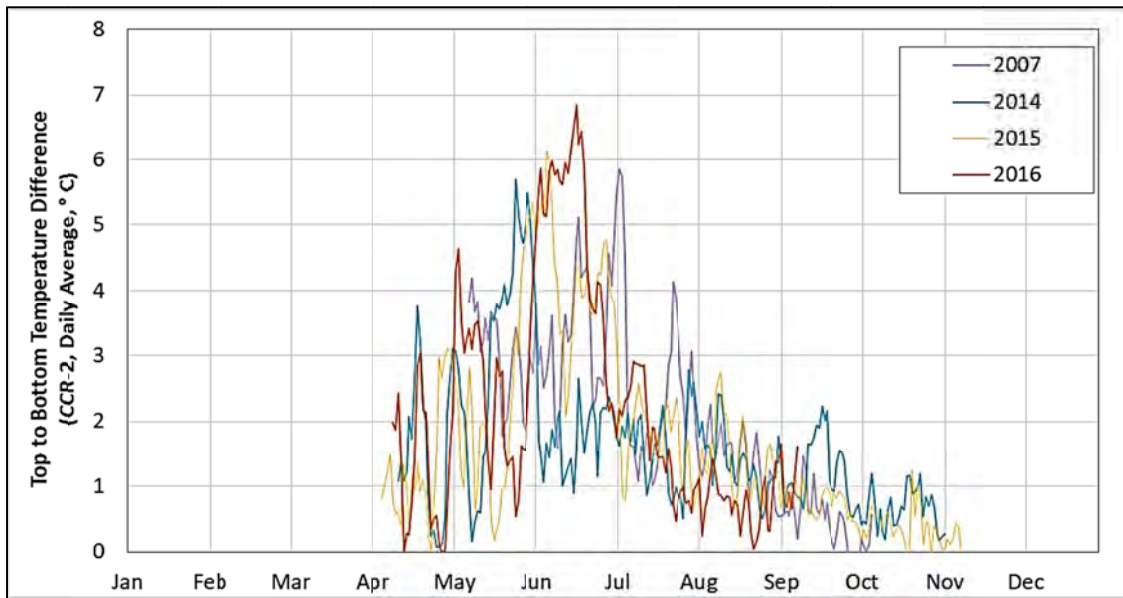


Figure 27. Top-to-Bottom Temperature Differences at CCR-2 for Years without Destratification System Operations; 2007, 2014 - 2016

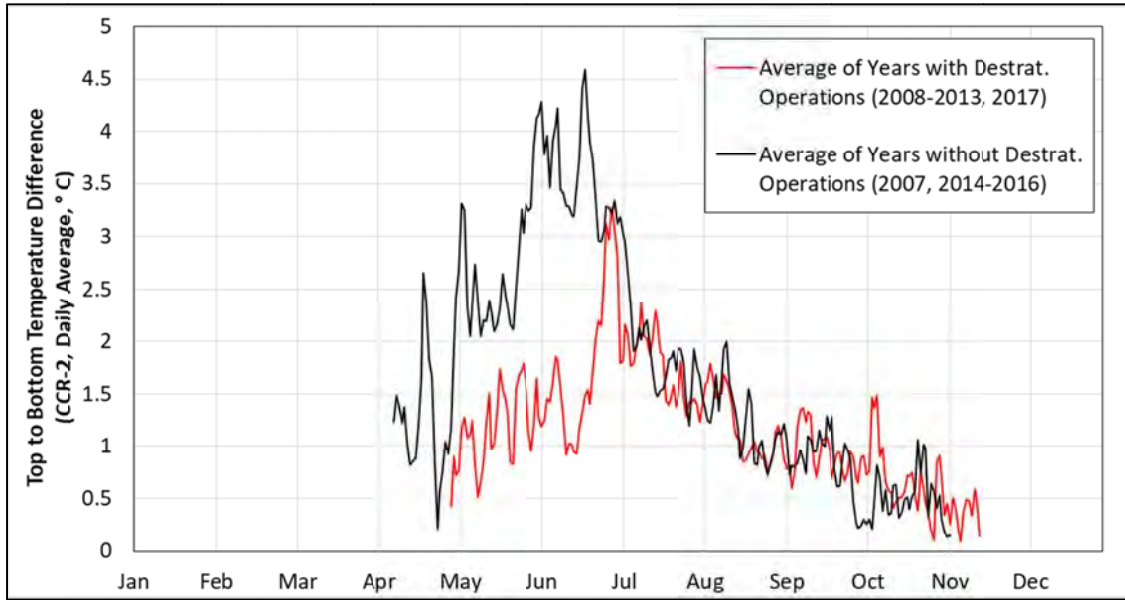


Figure 28. Average Top-to-Bottom Temperature Differences at CCR-2 for Years with and without Destratification System Operations

2.4.2 Dissolved Oxygen

Dissolved oxygen is a critical in-reservoir measure of water quality for aquatic life. Dissolved oxygen at the bottom of the reservoir is also useful to identify anaerobic internal loading of nutrients from the sediments. Concentration of dissolved oxygen at the top of Cherry Creek Reservoir in 2014 – 2017 followed similar patterns to those observed in previous years (Figure 29). The recent four years of data agree better with the 2011 – 2013 data, which did not include the high values recorded in the 2003 – 2010³ dataset). From 2014 through 2017, there was only one case of dissolved oxygen concentrations at the top dipping below the 5 mg/L standard at all three sampling locations in the reservoir. This occurred on August 4, 2015, with values ranging from 4.8 to 4.9 mg/L, following a period of brief stratification where anoxic conditions were observed at the bottom during warmest part of summer. There were no reports of fish kill associated with these observations.

³ Note that the Model Calibration Report (Hydros, 2017) called out the higher dissolved oxygen values from 2003 – 2010 as being somewhat uncertain given lack of explanation in terms of elevated relative algal biovolume or chlorophyll *a* levels.

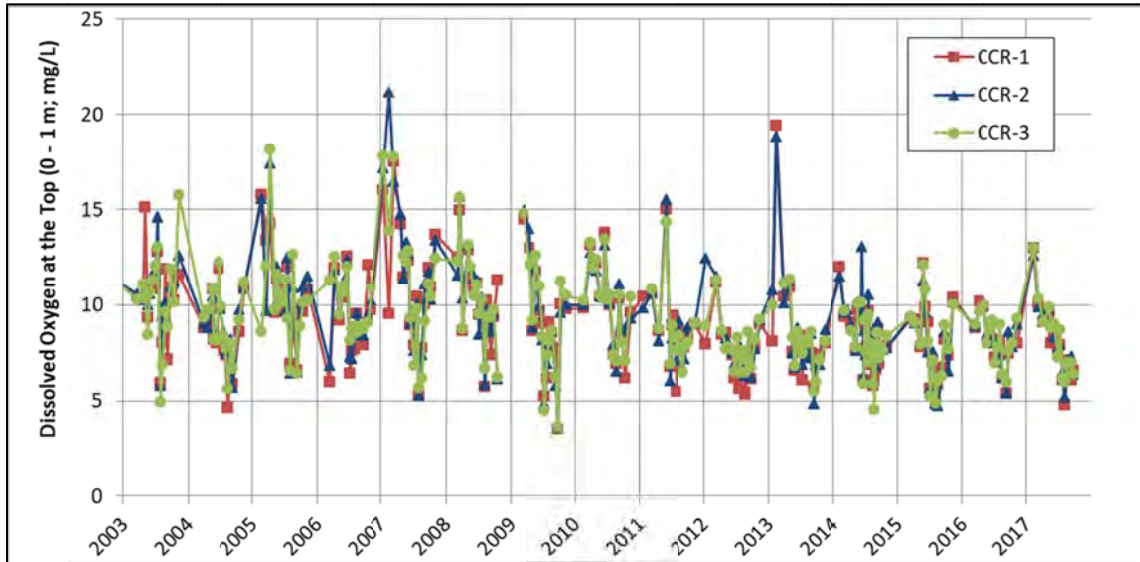


Figure 29. Dissolved Oxygen Concentrations Observed at the Top of Cherry Creek Reservoir, 2003 – 2017

Concentrations of dissolved oxygen from 2014 – 2017 at the bottom of the deepest portion of the reservoir (CCR-2; Figure 30) also agreed well with patterns and ranges from previous recent years (particularly 2011 – 2013). Further, the extended dataset continues to show no apparent effect of the destratification system on dissolved oxygen at the bottom of the reservoir in the deepest areas (Figure 30). Dissolved oxygen observations from the shallower location (CCR-3) for 2014 – 2017 also agree well with ranges observed in previous years.

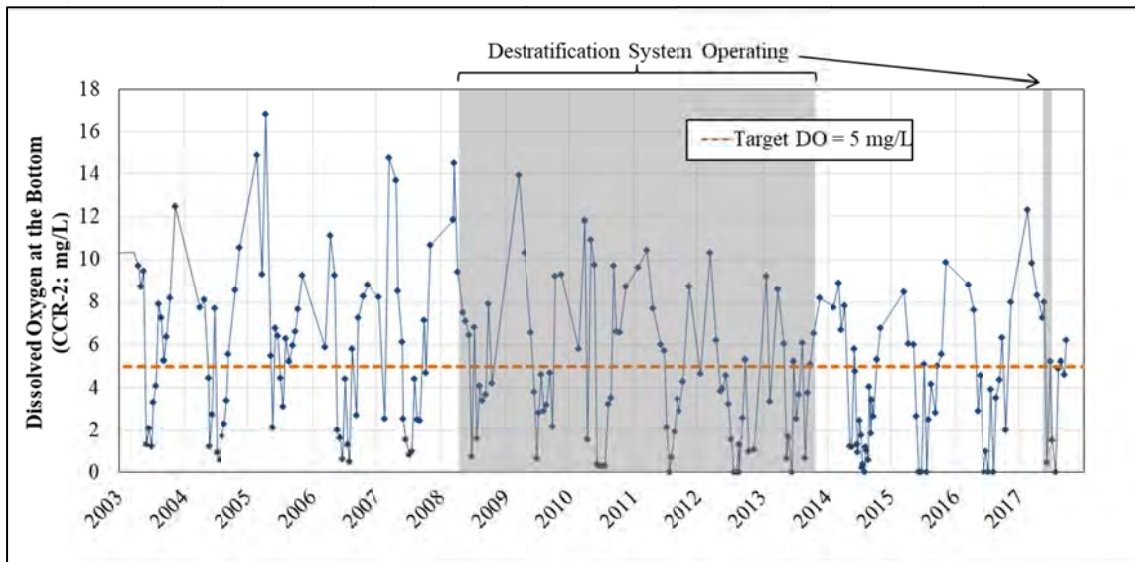


Figure 30. Dissolved Oxygen Concentrations Observed at the Bottom of Cherry Creek Reservoir at CCR-2, 2003 – 2017

The extended dataset continues to show a possible effect of increased dissolved oxygen concentrations at the bottom at this shallower location during destratification system operations (Figure 31), an effect that was also noted in Hydros (2017). Generally the minimum

dissolved oxygen concentration in the summer at CCR-3 at the bottom is above 2 mg/L in years when the destratification system is operated and less than 2 mg/L in most years that the system was not operated. The two exceptions are 2007 and 2015, which were very high inflow years. Inflows during warm months tend to be underflows because they are cooler than the reservoir surface temperatures. Those underflows may be increasing the dissolved oxygen at CCR-3 in high inflow years, though the effect does not appear to extend all the way through the reservoir to CCR-2.

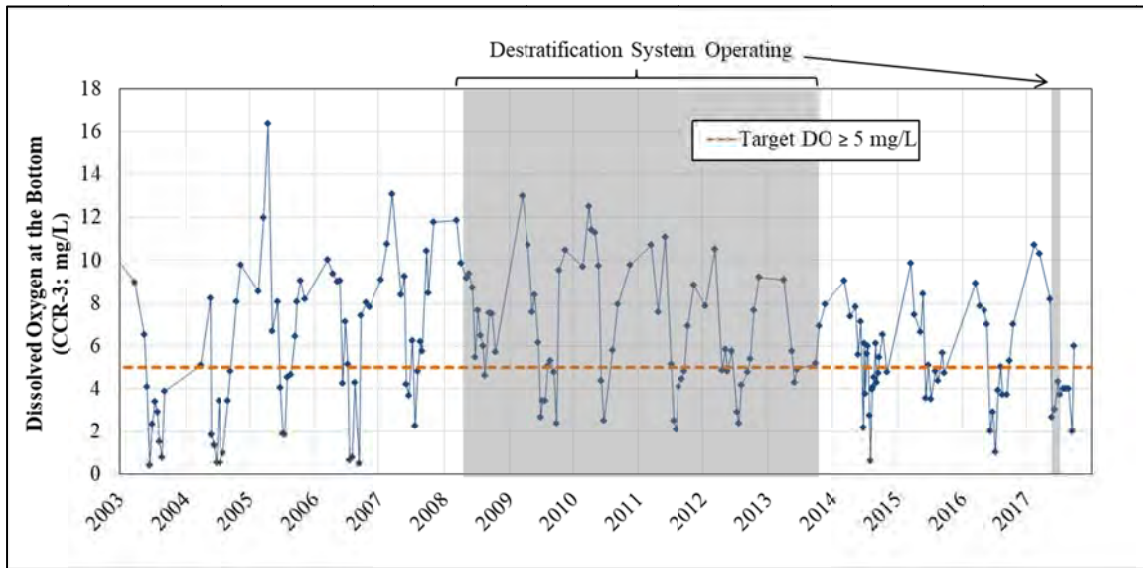


Figure 31. Dissolved Oxygen Concentrations Observed at the Bottom of Cherry Creek Reservoir at CCR-3, 2003 – 2017

The dissolved oxygen data at the bottom at CCR-2 were reviewed further to determine whether there was any indication that the destratification system may increase dissolved oxygen concentrations in May/early June, corresponding to the finding from the temperature analysis (Section 2.4.1). Comparison of dissolved oxygen data for years with destratification system operation (Figure 32) and years without (Figure 33) does not show a clear effect. Conditions still reach hypoxia (<2 mg/L DO) and anoxia in May and early June of in some years when the destratification system was operated at that time. These data suggest that while the destratification system may be capable of decreasing thermal stratification when the thermal resistance to mixing is lower (i.e., May/early June), it cannot induce enough mixing to bring enough oxygenated water from the surface to overcome the sediment oxygen demand in the deeper areas of the reservoir.

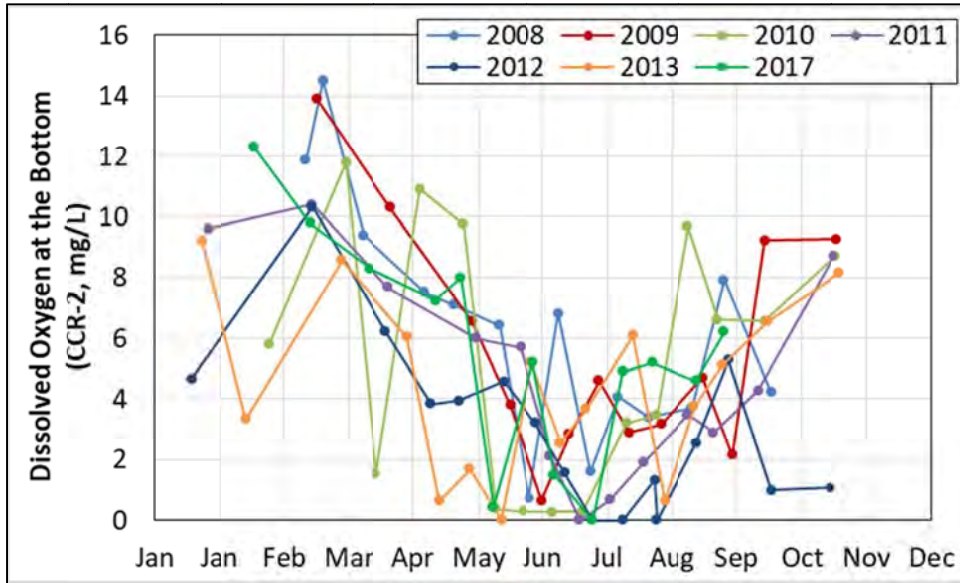


Figure 32. Bottom Dissolved Oxygen Concentrations at CCR-2 for Years with Destratification System Operations; 2008 - 2013, 2017

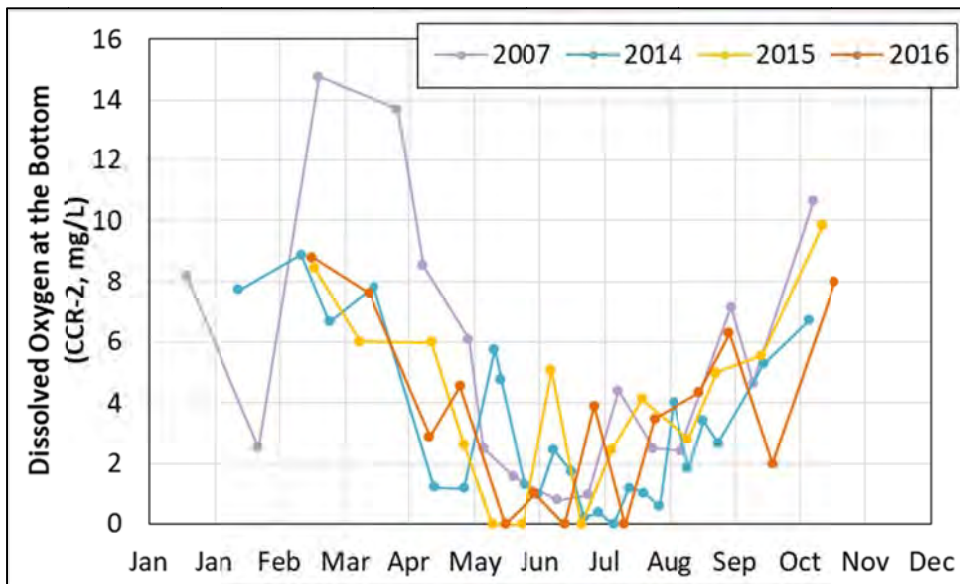


Figure 33. Bottom Dissolved Oxygen Concentrations at CCR-2 for Years without Destratification System Operations; 2007, 2014 - 2016

2.4.3 Nutrients

Nutrient concentrations at the top and bottom of Cherry Creek Reservoir for 2014 through 2017 exhibit similar patterns and ranges to the dataset from 2003 – 2013 (Figure 34 through Figure 36). As seen in previous years, while nitrate+nitrite concentrations comprise the majority of inflowing total inorganic nitrogen (Section 2.3.1), ammonia comprises the majority of total inorganic nitrogen in the reservoir. This pattern reflects uptake of inflowing nitrate+nitrite by algae and in-reservoir production of ammonia from decay of organic matter in the water column

and internal loading from sediments. Algal uptake and internal loading of SRP are also apparent in the full combined observed dataset. In-reservoir SRP concentrations, particularly in the photic zone, are well below inflow volume-weighted average SRP concentrations (see Section 2.3.1) indicating algal uptake. Further, SRP concentrations at the bottom of the reservoir show seasonal patterns of elevated concentrations relative to the photic zone indicative of internal loading (Figure 36).

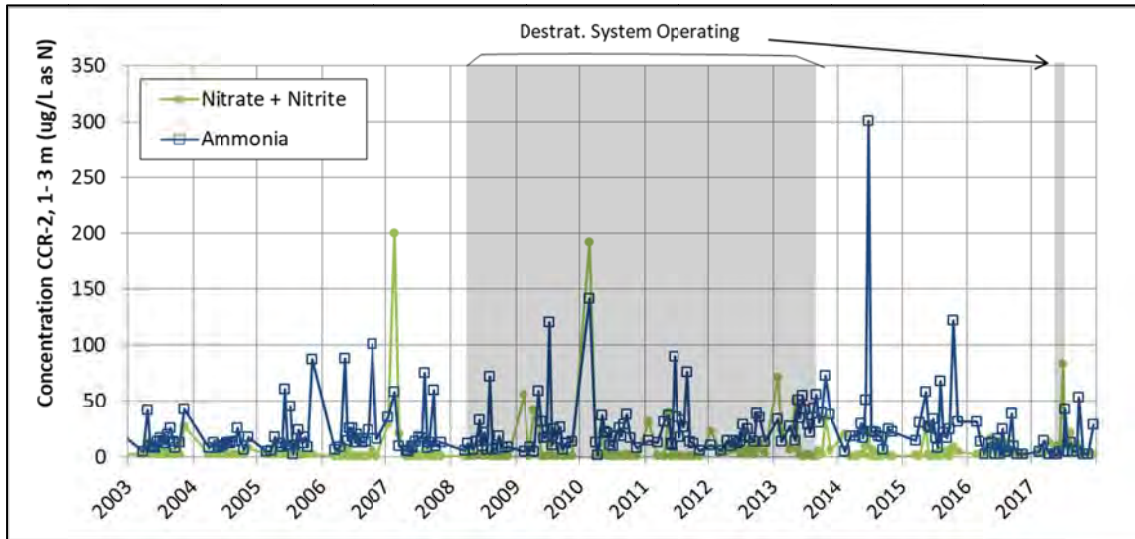


Figure 34. Observed of Nitrate+Nitrite and Ammonia Concentrations in the Photic Zone (1 – 3 m) at CCR-2, 2003 - 2017

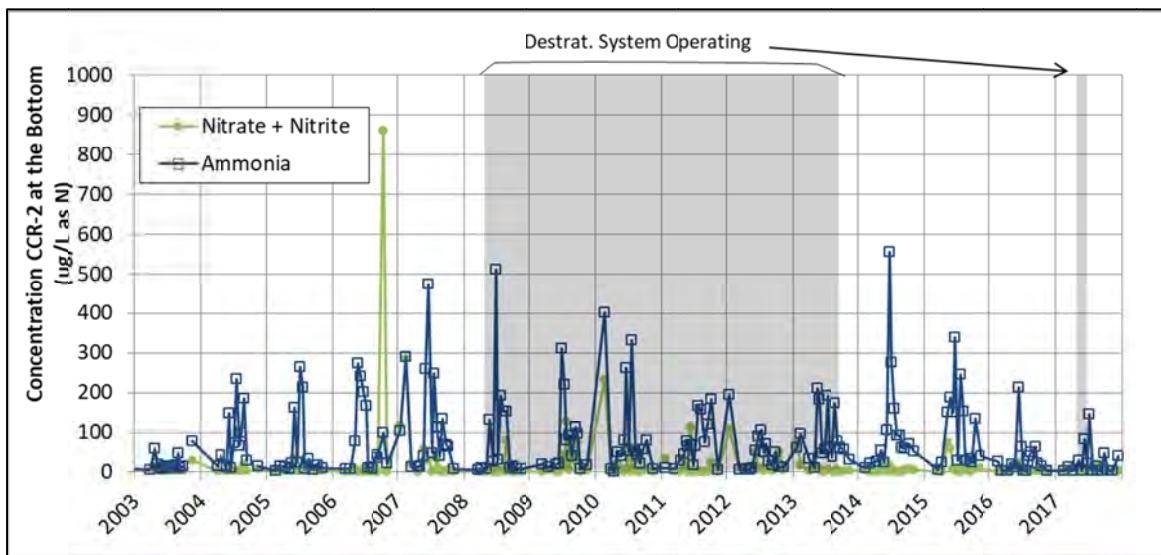


Figure 35. Observed of Nitrate+Nitrite and Ammonia Concentrations at the Bottom at CCR-2, 2003 - 2017

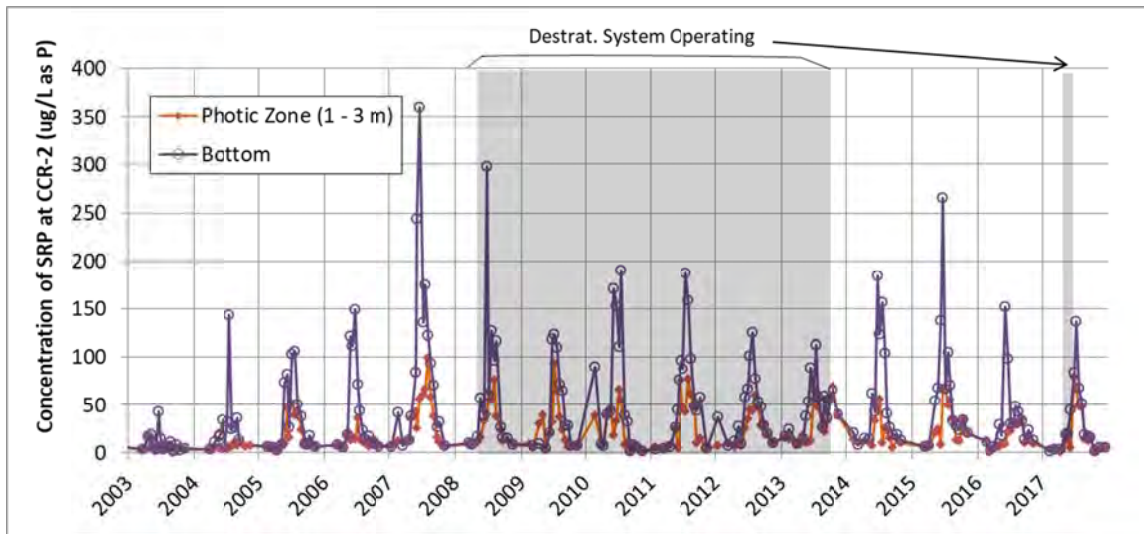


Figure 36. Observed of SRP Concentrations in the Photic Zone (1 – 3 m) and at the Bottom at CCR-2, 2003 - 2017

Patterns and ranges of nutrient concentrations do not show any indication of the intended effectiveness of the destratification system when comparing years with and without destratification system operation (Figure 34 through Figure 36). Likewise, closer inspection of the May through early June period of time (during which the destratification system appears to have some effect on thermal stratification) shows no clear effect on concentrations of ammonia (Figure 37 and Figure 38) or SRP (Figure 39 and Figure 40) at the bottom. This makes sense given the corresponding lack of clear effect on dissolved oxygen concentrations over the same period. Therefore, the data indicate that, while the destratification system appears to lessen thermal stratification in May and early June, there is no effect at that time or in the summer months on nutrient concentrations since the mixing is inadequate to bring enough oxygenated water to the deeper areas of the reservoir to overcome the water column and sediment oxygen demand.

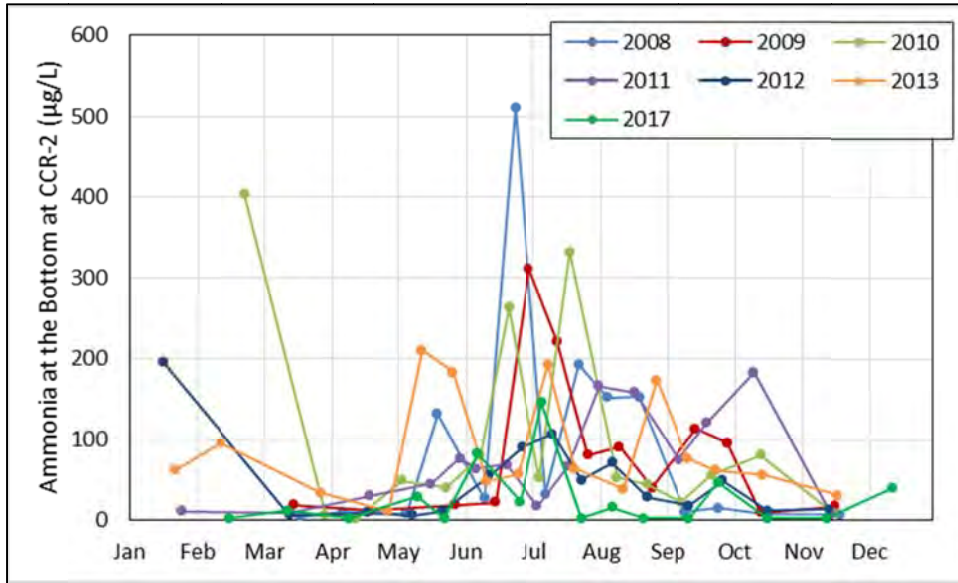


Figure 37. Bottom Ammonia Concentrations at CCR-2 for Years with Destratification System Operations; 2008 - 2013, 2017

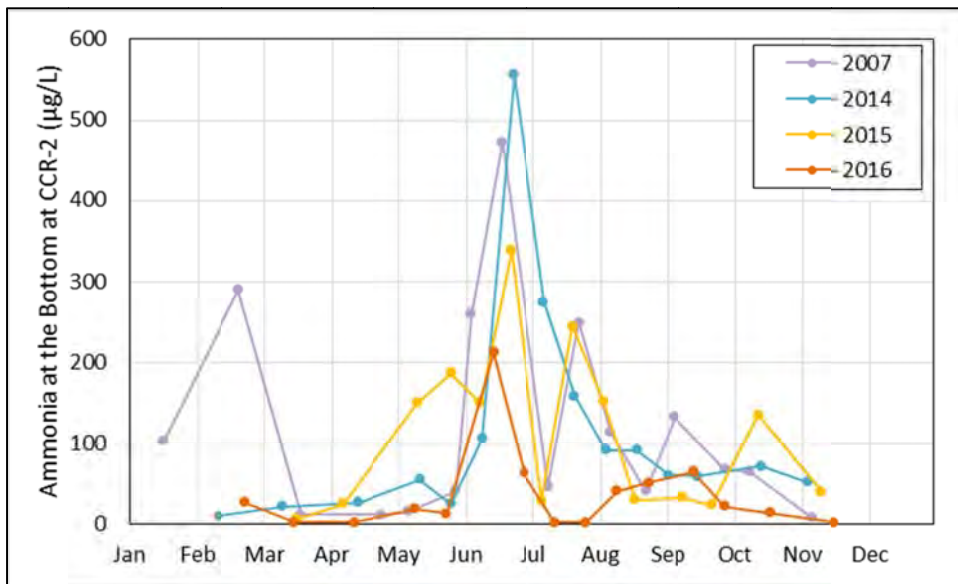


Figure 38. Bottom Ammonia Concentrations at CCR-2 for Years without Destratification System Operations; 2007, 2014 - 2016

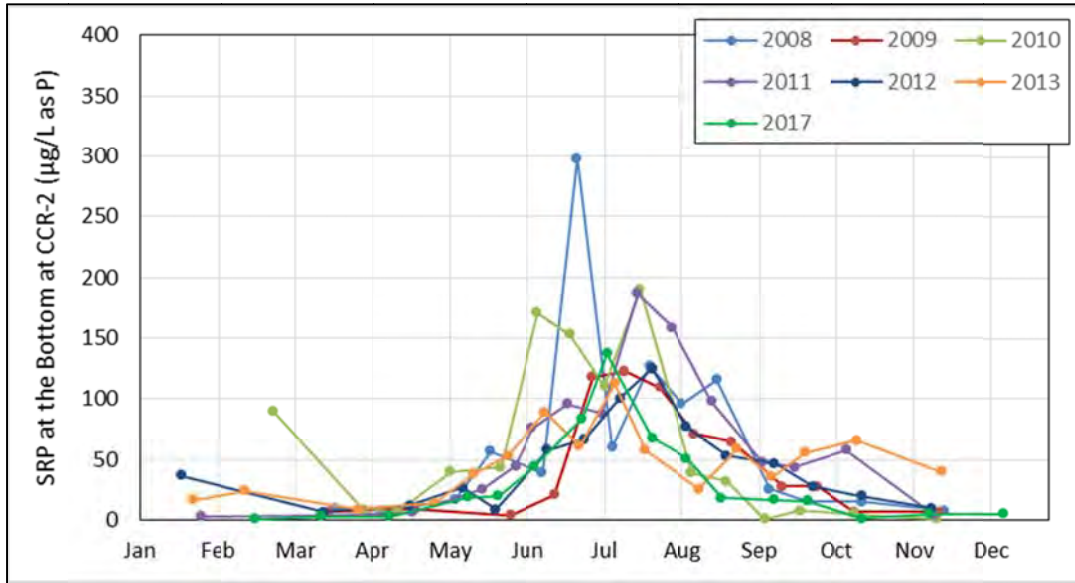


Figure 39. Bottom SRP Concentrations at CCR-2 for Years with Destratification System Operations; 2008 - 2013, 2017

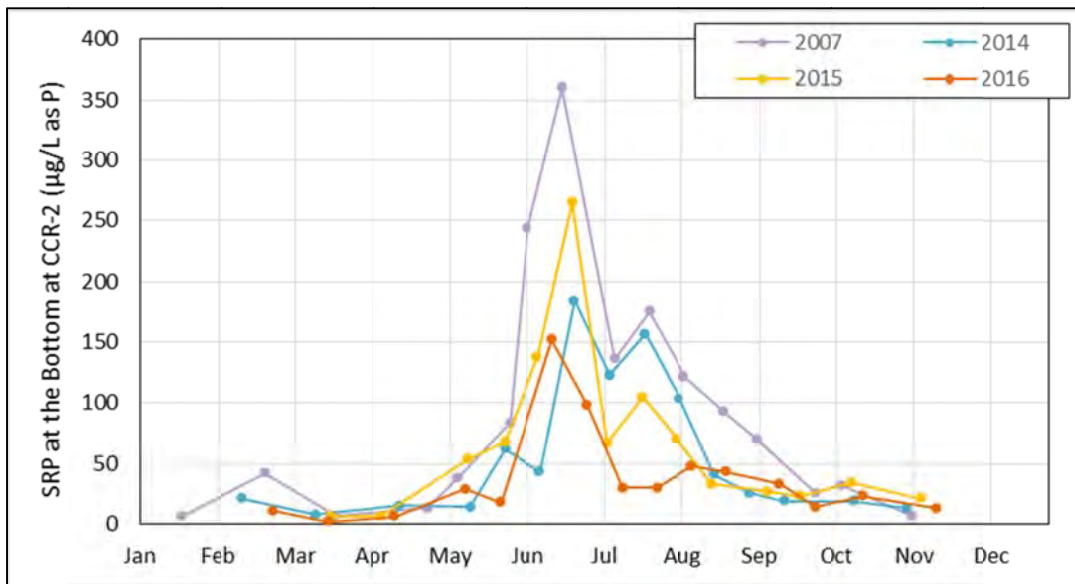


Figure 40. Bottom SRP Concentrations at CCR-2 for Years without Destratification System Operations; 2007, 2014 - 2016

2.4.4 Algal Growth

Algal growth, including cyanobacteria, is a key water-quality concern for Cherry Creek Reservoir. The following subsections present chlorophyll *a*, algal biovolume by species, and cyanobacteria data from 2014 through 2017, making comparisons to 2003 through 2013. The effect of the destratification system on cyanobacteria is also evaluated using the additional recent years of biovolume record while the destratification system was not operated.

2.4.4.1 Chlorophyll a

Chlorophyll *a* concentrations in the reservoir for 2014 through 2017 fell within ranges observed from 2003 through 2013 (Figure 41). Summertime peaks occur in late July or early August, near the timing of peak surface water temperatures. In the recent four years, the highest chlorophyll *a* concentrations in summer months were observed in 2014, which was a relatively dry year. The average summertime chlorophyll *a* concentrations were above the site-specific standard value (18 µg/L) in each of the recent four years except 2015 (Figure 42).

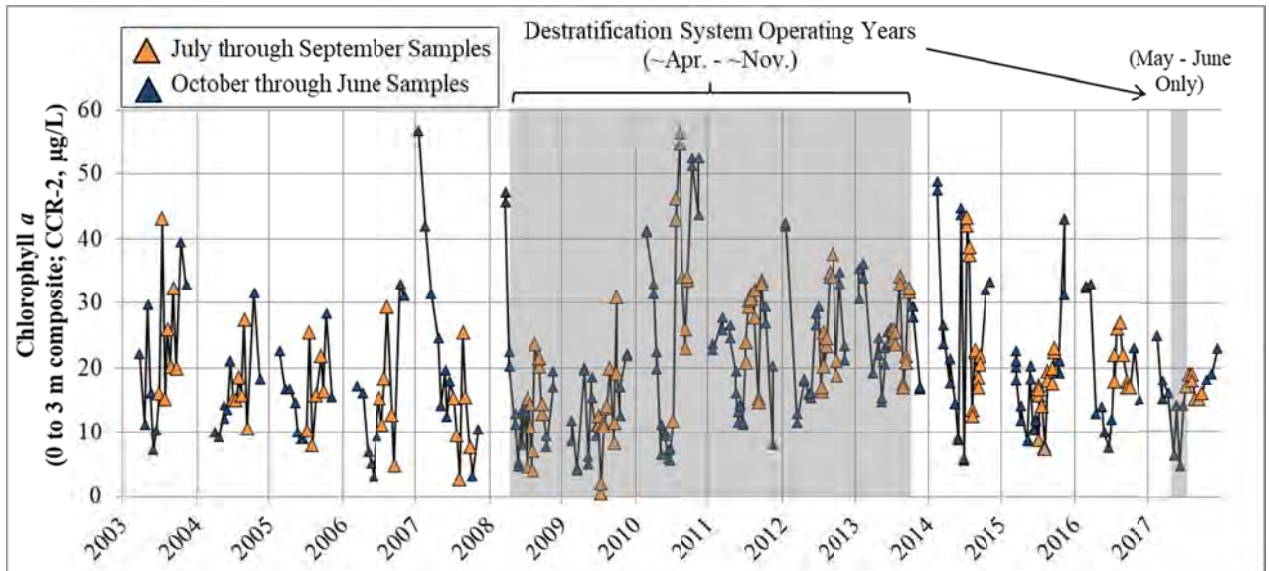


Figure 41. Chlorophyll *a* Concentrations at CCR-2, 2003 – 2017

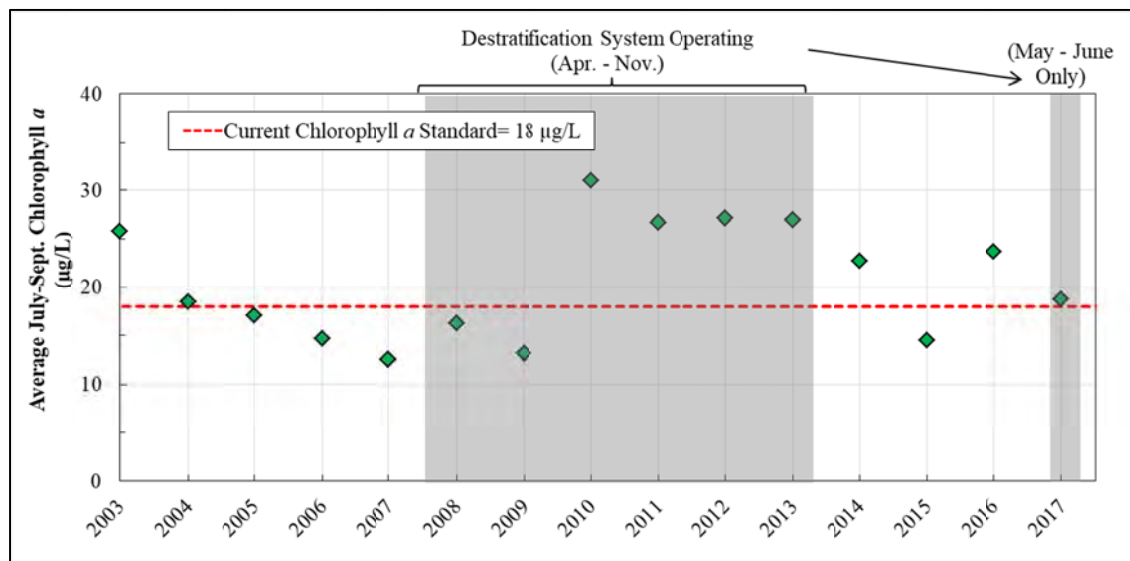


Figure 42. Average Summertime Chlorophyll *a* Concentrations in Cherry Creek Reservoir Compared the Site-Specific Standard Value, 2003 – 2017

The additional four years of record provide no indication that the July – September chlorophyll *a* concentrations are affected by operation of the destratification system (Figure 41 and Figure

42). There is, however, an apparent pattern of higher summertime chlorophyll *a* with lower residence time, and vice versa (Figure 43). High inflow/outflow volumes may play a role in affecting which algal species dominate, thereby affecting the resulting chlorophyll *a*. The relationship, however, is imperfect as a singular predictor (e.g., 2010), recognizing that many other factors (such as the occurrence of extended periods of stratification and surface water temperatures) also play an important role.

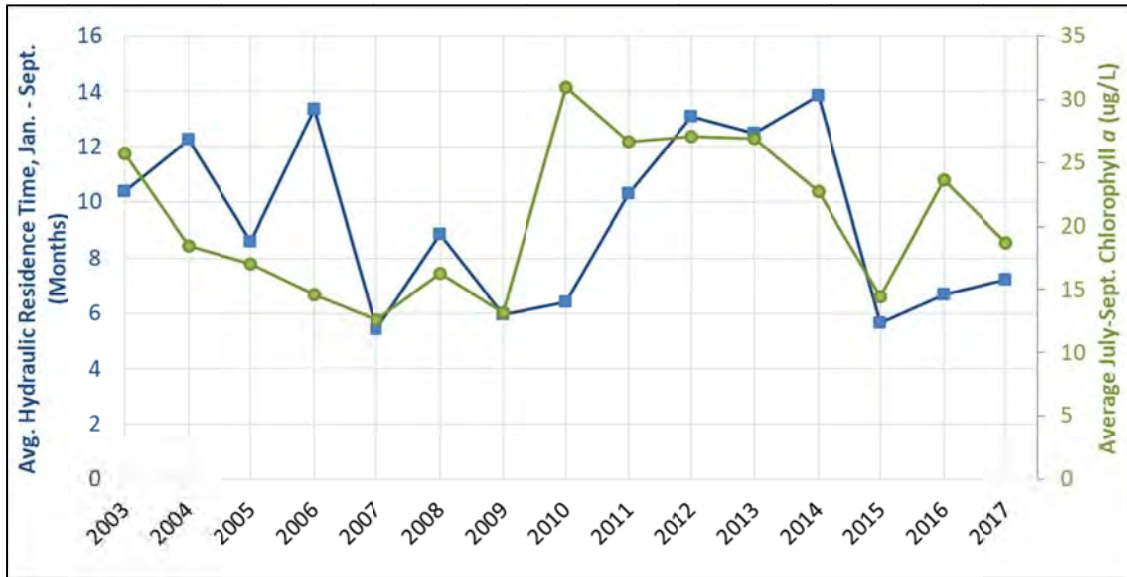


Figure 43. Average January - September Residence Time and Average Summertime (July – September) Chlorophyll *a*, 2003 - 2017

2.4.4.2 Algal Biovolume

While chlorophyll *a* concentrations for 2014 – 2017 agreed well with previously observed ranges and patterns, a higher range of total algal biovolume was seen in the recent years (Figure 44). There was a laboratory change from Aquatic Analysts to PhycoTech between the 2015 and 2016 sampling seasons, which could explain the jump in baseline biovolume; however, there is no definitive evidence that the biovolume data from the two labs are not comparable.

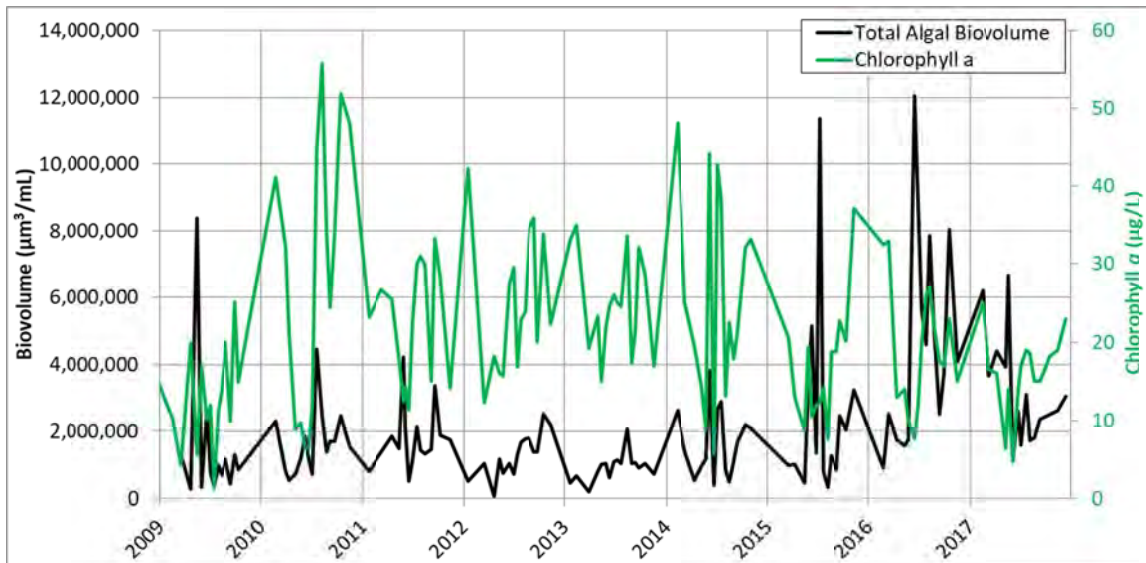


Figure 44. Total Algal Biovolume and Chlorophyll *a* Concentrations in the Photic Zone at CCR-2, 2009 – 2017 (No Biovolume Data Available before 2009)

The species-specific biovolume data indicate that the higher biovolume observations of 2015 – 2017 correspond primarily to major diatom (bacillariophyta) blooms and secondarily to chrysophyta (Figure 45). The diatoms identified in these samples (e.g., *Fragilaria crotonensis*) tend to be large with rapid growth and settling rates. A large fraction (~40 to 78%) of the mass of diatoms is silica (Sicko-Goad et al., 1984), and chrysophyta can develop silica scales. The other non-silicate algae in the reservoir are comprised primarily of organic (non-silicate) biomass. The high silica content of the blooms explains the high biovolume values which do not correspond to higher chlorophyll *a* or total organic carbon⁴ in the reservoir (Figure 46).

⁴ If the biovolume associated with the diatom blooms were assumed to have the same fraction of carbon as the non-silicate algal groups, the biovolume associated with the blooms would be expected to cause increased TOC concentrations on the order of 3 to 5 mg/L; however, that is not apparent in the observed dataset (Figure 46). Instead, TOC concentrations at the top of the reservoir are relatively low during the times of the higher biovolume observations. This further supports the assertion that the high biovolume values are indicative of a high fraction of silica.

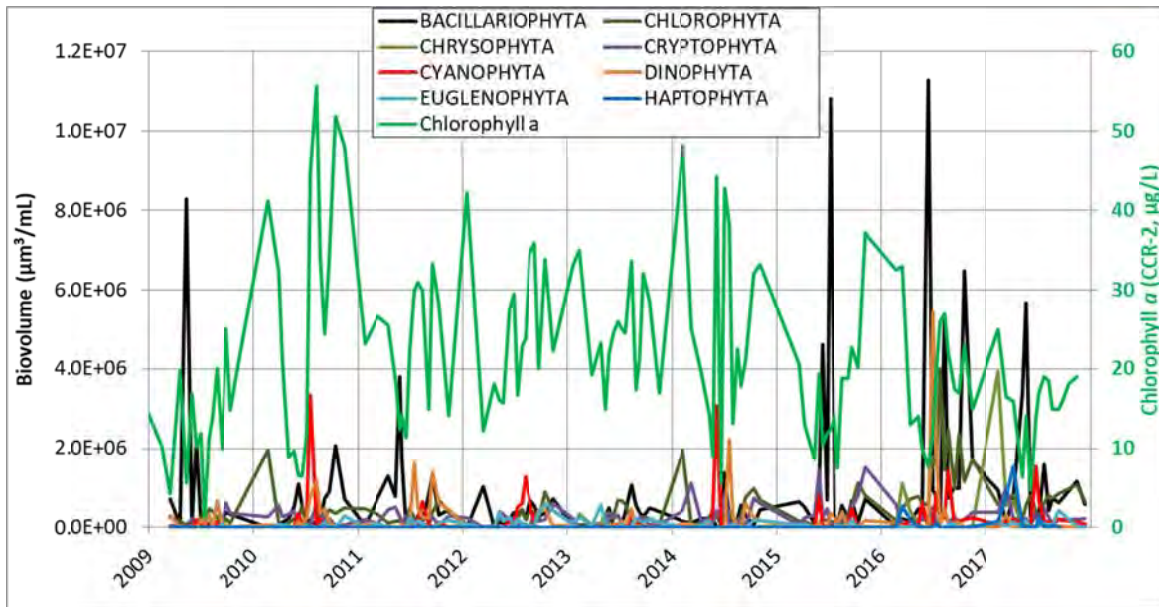


Figure 45. Chlorophyll *a* and Biovolume by Algal Type in the Photic Zone of Cherry Creek Reservoir, 2009 – 2017

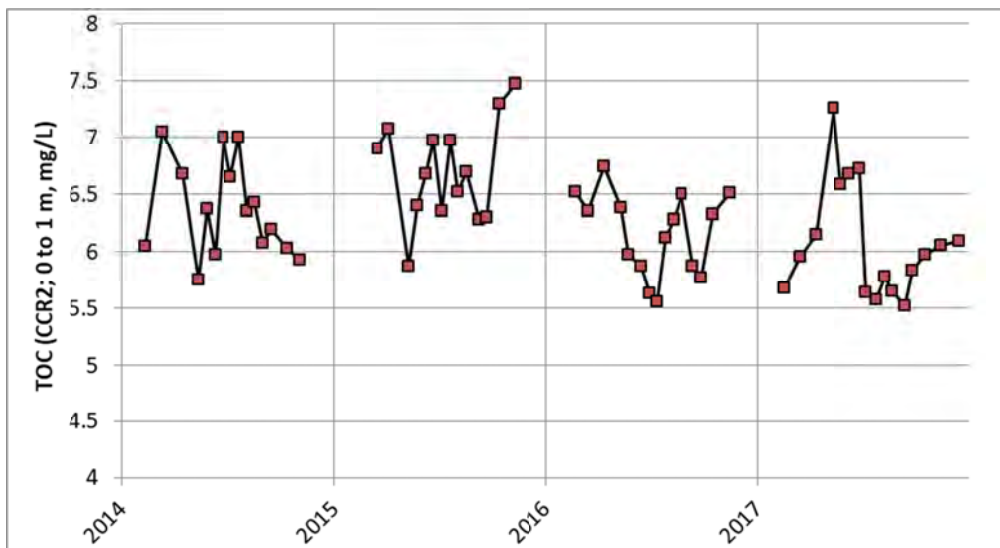


Figure 46. Total Organic Carbon Concentrations at the Top at CCR-2, 2014 - 2017 (Data Collection began in 2014)

The diatom blooms can be considered beneficial. Because they grow quickly and settle quickly, they can rapidly remove nutrients from the photic zone. In Cherry Creek Reservoir, they are often associated with times of lower chlorophyll *a* (Figure 45) and greater relative clarity, though lack of clarity data in 2016 makes this difficult to fully evaluate (Figure 47).

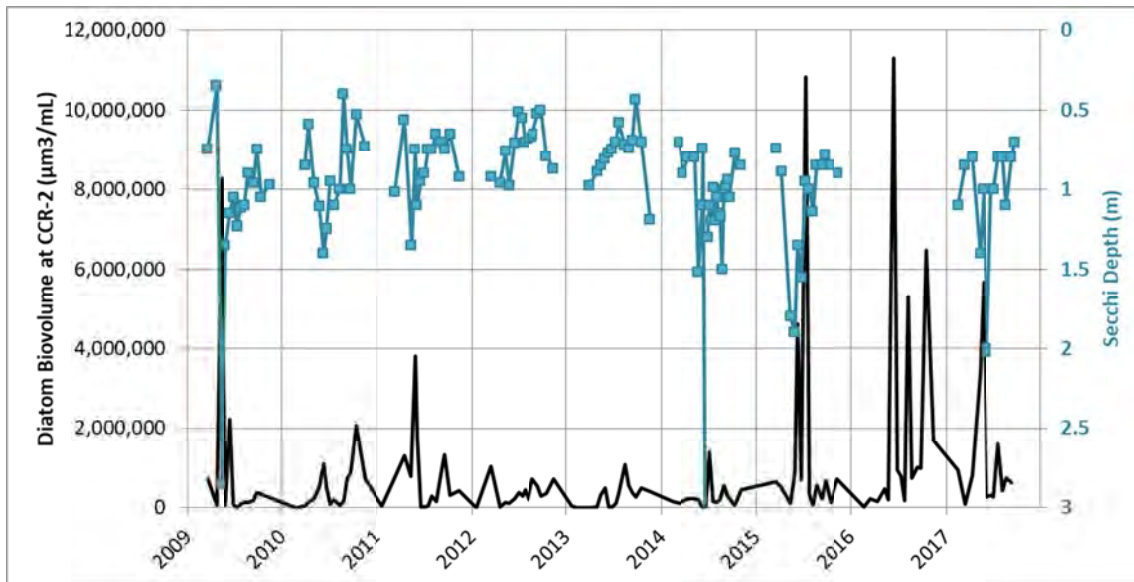


Figure 47. Secchi Depth and Diatom Biovolume in Cherry Creek Reservoir at CCR-2, 2009 - 2017 (Note: No Clarity Data Available from 2016)

It is not currently fully understood why diatom blooms were so dominant in 2009, 2015, 2016, and 2017; however, it may be related to inflows. The recorded years with major diatom blooms (2009, 2015, 2016, and 2016 [Figure 45]) are also years with low residence times (Figure 43) due to high inflow and outflow volumes. This could indicate loading of silica allowing for large blooms, though silica data are not collected in the reservoir to verify this. Limited historical silica data (a few samples from the early 1980's) do not suggest silica limitation in the reservoir; however, conditions may have changed, and/or there could be seasonal limitation. The high inflows could also lead to greater clarity, which would encourage diatom blooms.

Currently the water-quality model simulates diatoms as part of larger algal groups and not as a distinct algal group. To simulate diatoms as a distinct group, collection of inflow and in-reservoir dissolved and particulate silica data could be helpful. This would also require a subsequent recalibration to add the group and define settings to simulate the observed response timing. Such modifications to the model or the sampling program are not considered critical to meet the current objectives of the modeling effort. However, given the good (relative) water-quality conditions associated with diatoms, it may become advantageous in the future to improve the understanding what drives such blooms.

2.4.4.3 Cyanobacteria

Cyanobacteria are a particular concern for Cherry Creek Reservoir, given its high recreational value. There were notable cyanobacteria blooms in each of the recent four years (2014 – 2017; Figure 45). These blooms followed similar patterns to those identified in the previous data analysis (Hydos, 2017). Specifically, the cyanobacteria blooms correspond to high chlorophyll a concentrations (Figure 45). Further, cyanobacteria blooms in the warmest months of July and August tend to be dominantly *Aphanizomenon*, while those in the cooler months of May, June, or September, tend to be *Anabaena* (Figure 48). The dominant species that are observed at

Cherry Creek Reservoir are capable of fixing atmospheric nitrogen, and the blooms typically begin at times of low nitrogen-to-phosphorus ratios in the photic zone (Figure 49).

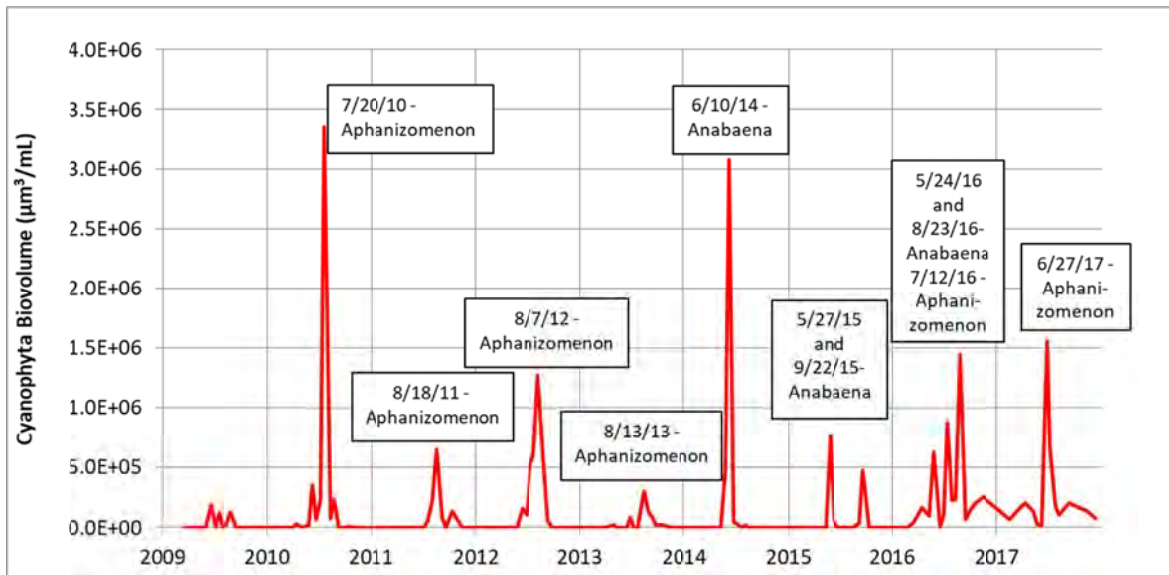


Figure 48. Dominant Cyanobacteria by Date during Major Blooms, 2009 – 2017

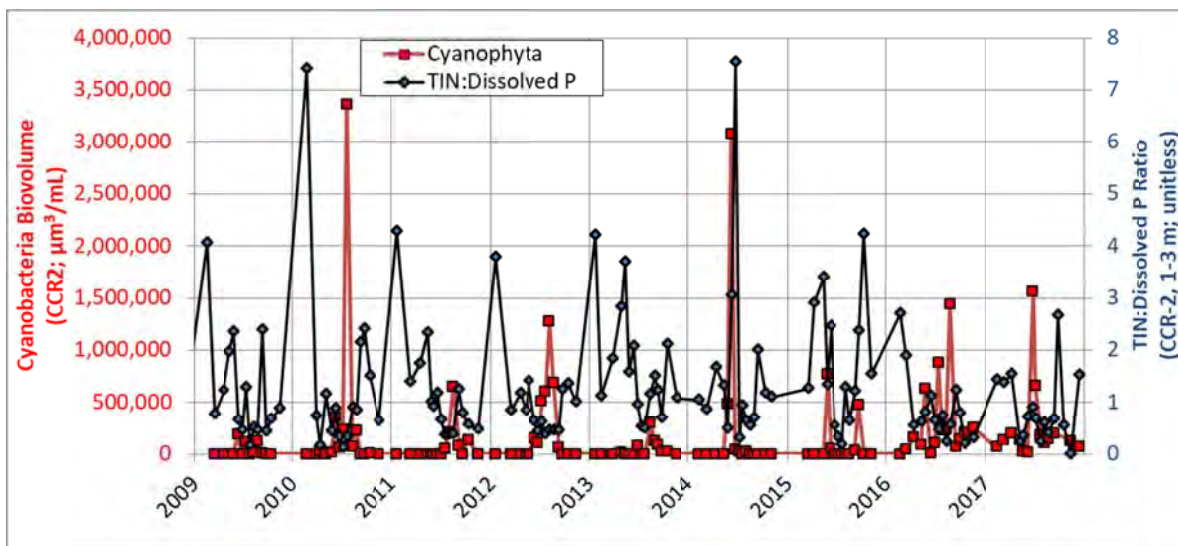


Figure 49. Cyanophyta Biovolume and the Nitrogen-to-Phosphorus Ratio in the Photic Zone, 2009 – 2017

While it is recognized that the current destratification system fails to reduce anaerobic internal loading by increasing dissolved oxygen at depth, there have been some varying statements over time about its effectiveness in reducing cyanobacteria. Even without decreasing internal nutrient loading, added mixing could potentially reduce cyanobacteria by disrupting their buoyancy advantage. The conceptual understanding presented with the 2003-2013 model calibration (Hydos, 2017) showed that there was no evidence to support statements that the current destratification system reduces the summertime cyanobacteria. However, it was also noted that, due to lack of biovolume data for years without destratification system operations, it

was difficult to definitely state that there was no effect. Data from 2014 – 2017 provide an opportunity to more fully evaluate this question.

Comparison of biovolume results during periods of record with and without destratification system operation suggests that the ranges of cyanobacteria bloom sizes are similar under both conditions (Figure 50). The cyanobacteria species patterns, however, show that there have been more cases of *Anabaena* blooms in years without destratification system operations (Figure 48). Based on this, the seasonality of cyanobacteria bloom occurrences was reviewed in greater detail. The data show that cyanobacteria blooms in May and early June only occurred in years when the destratification system was not operated (Figure 51 and Figure 52). This timing matches the noted timing of apparent effect on reducing thermal stratification (see Section 2.4.1). Therefore, while not definitive, the available data suggest that operation of the destratification system may help prevent/limit *Anabaena* bloom formation in May and early June.

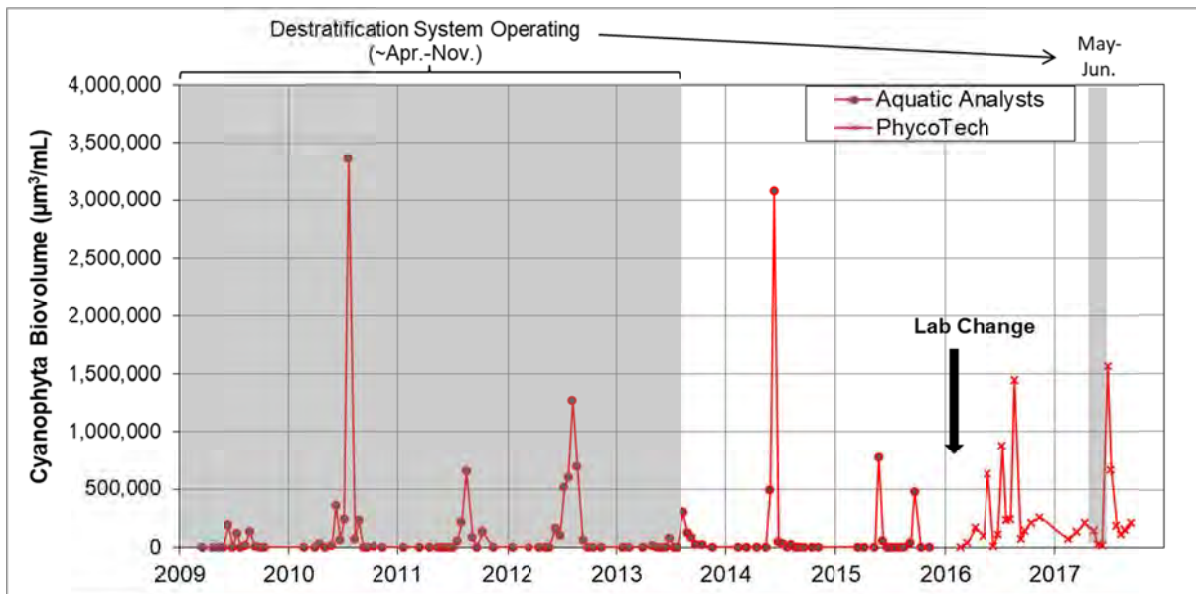


Figure 50. Cyanophyta Biovolume at CCR-2, 2009 - 2017

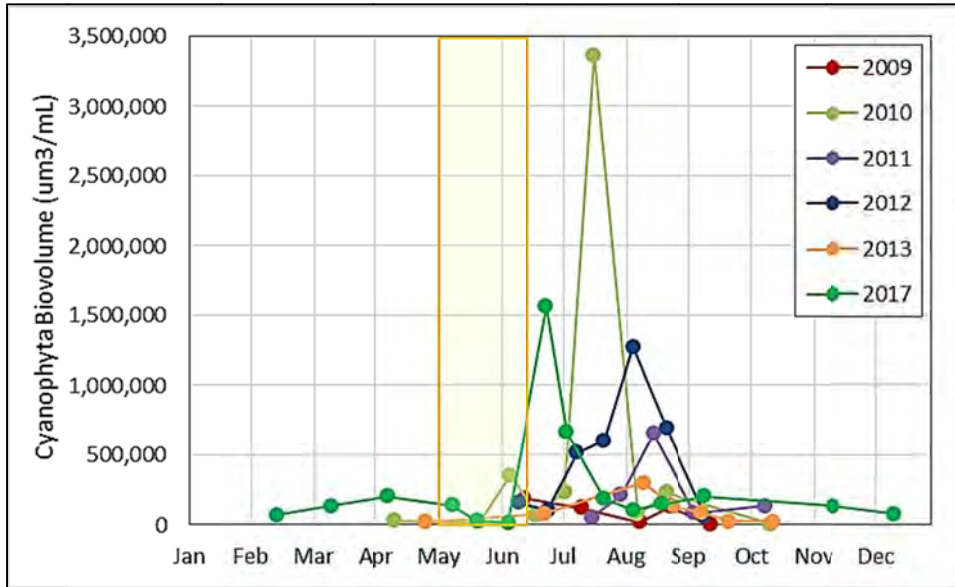


Figure 51. Cyanobacteria Biovolume at CCR-2 for Years with Destratification System Operations; 2008 – 2013, 2017 (Yellow Box Indicates May – Early June Period with Noted Mixing Effects on Temperature Attributed to the Destratification System)

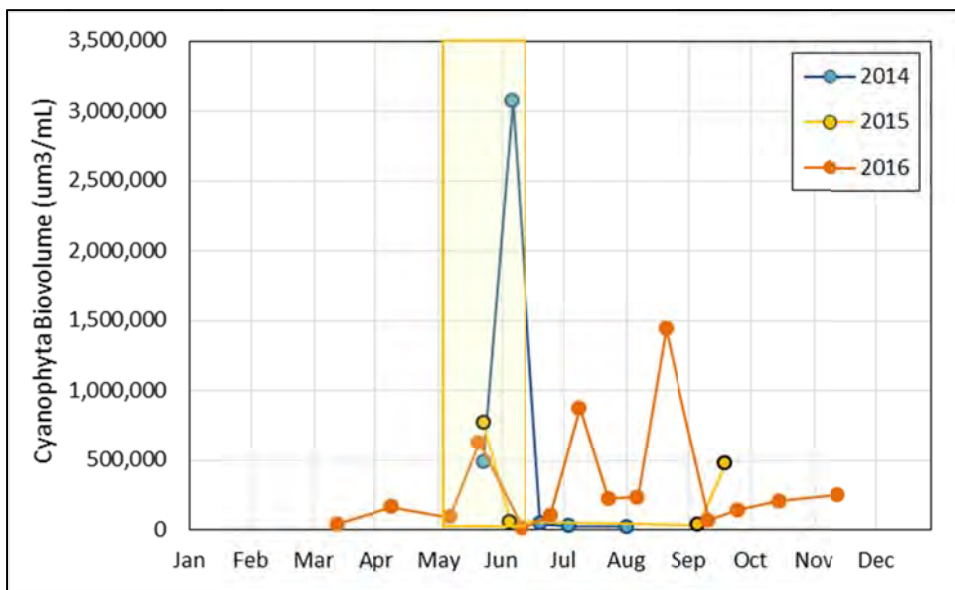


Figure 52. Cyanobacteria Biovolume at CCR-2 for Years without Destratification System Operations; 2007, 2014 - 2016 (Yellow Box Indicates May – Early June Period with Noted Mixing Effects on Temperature Attributed to the Destratification System)

3 Model Extension Results

The reservoir water-quality model, originally calibrated to observed data from 2003 through 2013, was updated to include 2014 through 2017. Inputs were developed from observed data following the approach documented in Hydros (2017). No model settings were adjusted for the extension simulation. Simulation results are summarized in the following subsections (3.1 through 3.5) for surface water elevation, water temperature, dissolved oxygen, nutrients, chlorophyll a , total algal biomass, and cyanobacteria biomass. Calibration statistics were also updated to include the extended simulation for comparison to quantitative calibration targets for the original model calibration (based on Wells, et al. [2008]).

While all calibration targets were met by the extended model, and the unadjusted model is considered adequate for application to the pending bubble plume analysis, a minor proposed refinement is presented in Section 3.6. This adjustment of model settings was tested to improve the simulated timing of *Anabaena* blooms.

3.1 Surface Water Elevation

As with the original calibration, the model matched observed surface water elevations well (Figure 53). The simulated mean absolute error (MAE) for the full extended simulation was well below the target MAE of ≤ 10 cm (Table 1).

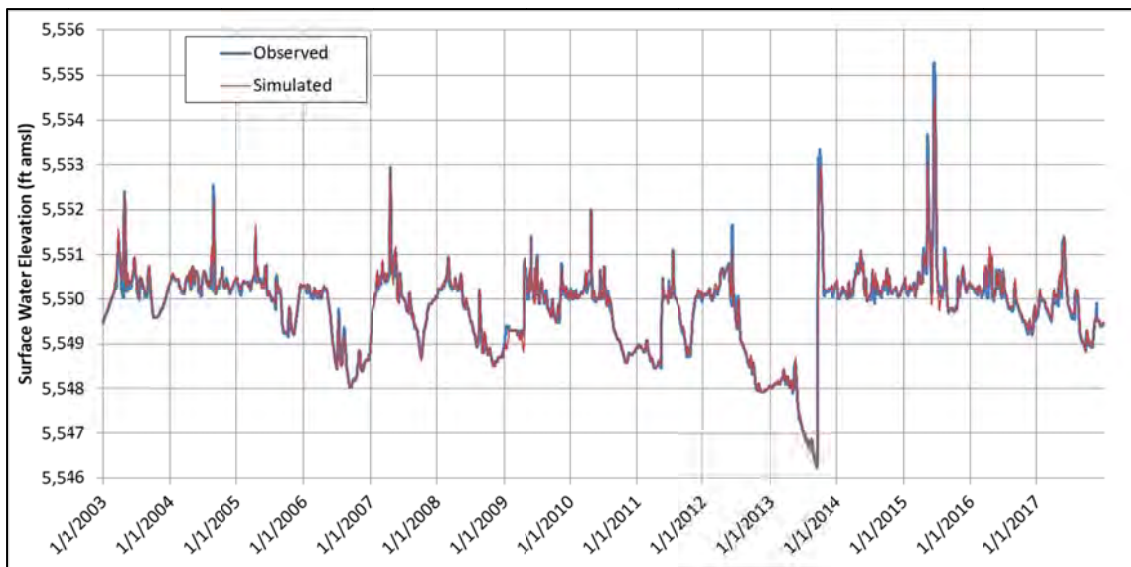


Figure 53. Comparison of Simulated and Observed Daily Water Levels, 2003-2017

Table 1. Summary Calibration Statistics for Surface Water Elevation

Metric	2003-2013	2014-2017	2003-2017
MAE (cm)	1.7	2.3	1.8
Calibration Target (cm)	MAE < 10	MAE < 10	MAE < 10

3.2 Temperature

The extended model continued to perform well in simulation of water temperature in the reservoir. The simulation reflected observed seasonal patterns and magnitudes at the top and bottom of the reservoir (Figure 54 and Figure 55) as well as vertical variations apparent in the profile data (e.g., Figure 56). The full set of simulated and observed temperature profiles from 2014 through 2017 for CCR-2 and CCR-3 is presented in Attachment A.

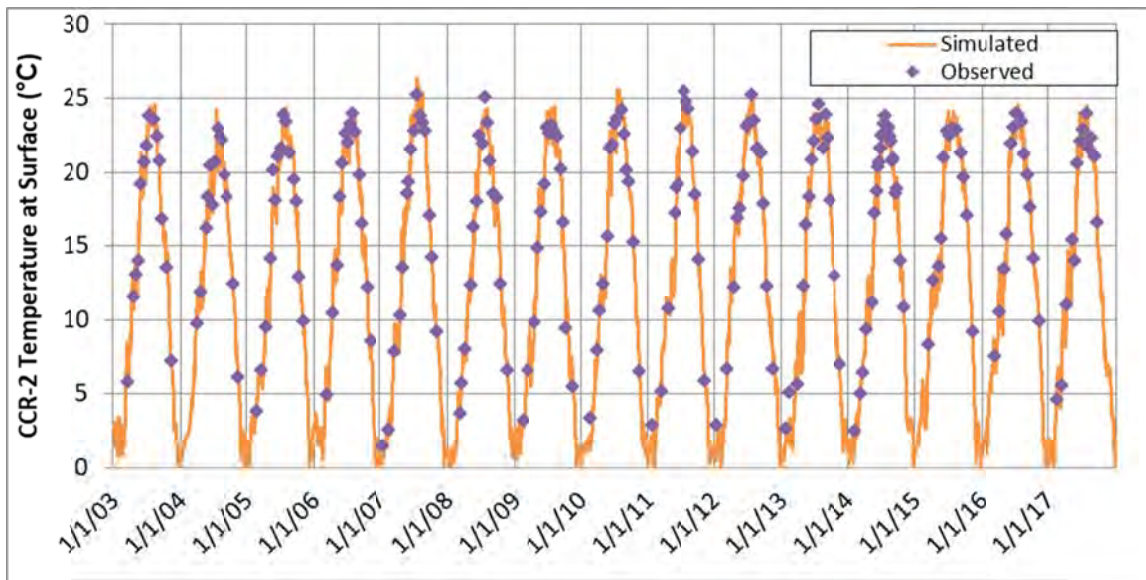


Figure 54. Simulated and Observed Temperature at the Top at CCR-2, 2003-2017

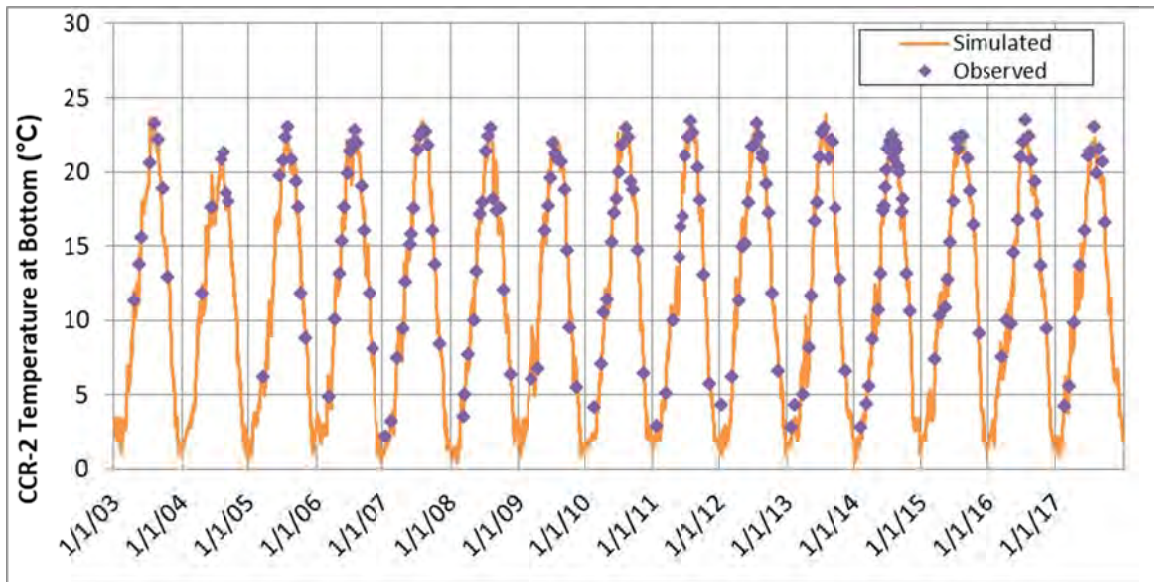


Figure 55. Simulated and Observed Temperature at the Bottom at CCR-2, 2003-2017

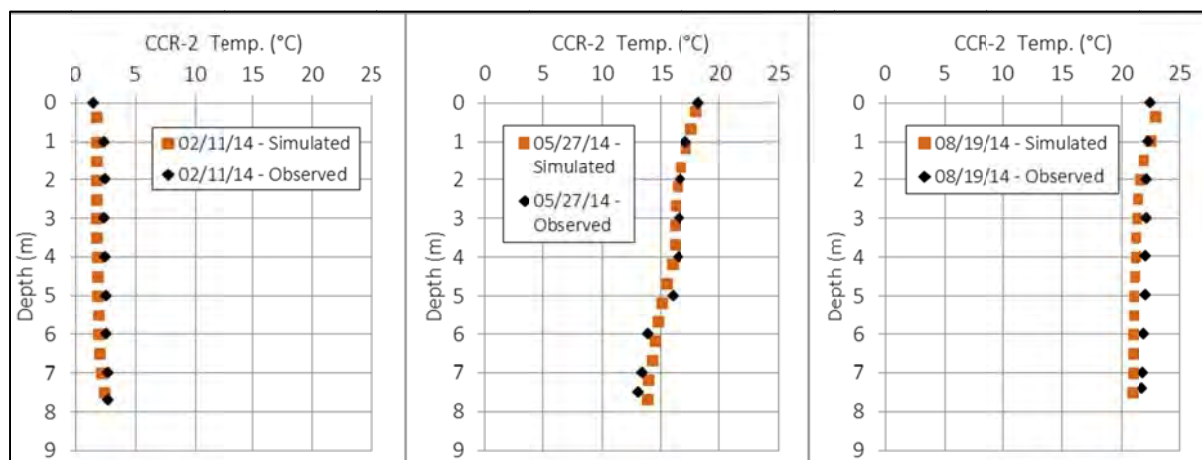


Figure 56. Example Calibration Profiles at CCR-2 from 2014

The simulated MAE for the full extended simulation met the calibration target of MAE < 1 °C, though the result was slightly higher (worse) than that for the 2003 – 2013 calibration period (Table 2). This difference is expected to reflect the added uncertainty associated with use of meteorological data collected farther from the reservoir for 2014 – 2017. The Authority’s in-process installation of an on-site meteorological station will be beneficial for future modeling.

Table 2. Summary Calibration Statistics for Temperature Profiles (All Locations)

Metric	2003-2013	2014-2017	2003-2017
MAE (°C)	0.6	0.7	0.6
Calibration Target (°C)	MAE ≤ 1	MAE ≤ 1	MAE ≤ 1

3.3 Dissolved Oxygen

The extended model simulation of dissolved oxygen continued to reflect observed seasonal patterns and ranges at the top and bottom of the reservoir (Figure 57 and Figure 58) as well as spatial variations in dissolved oxygen at the bottom (Figure 59). The full set of simulated and observed dissolved oxygen profiles from 2014 through 2017 for CCR-2 and CCR-3 is presented in Attachment B.

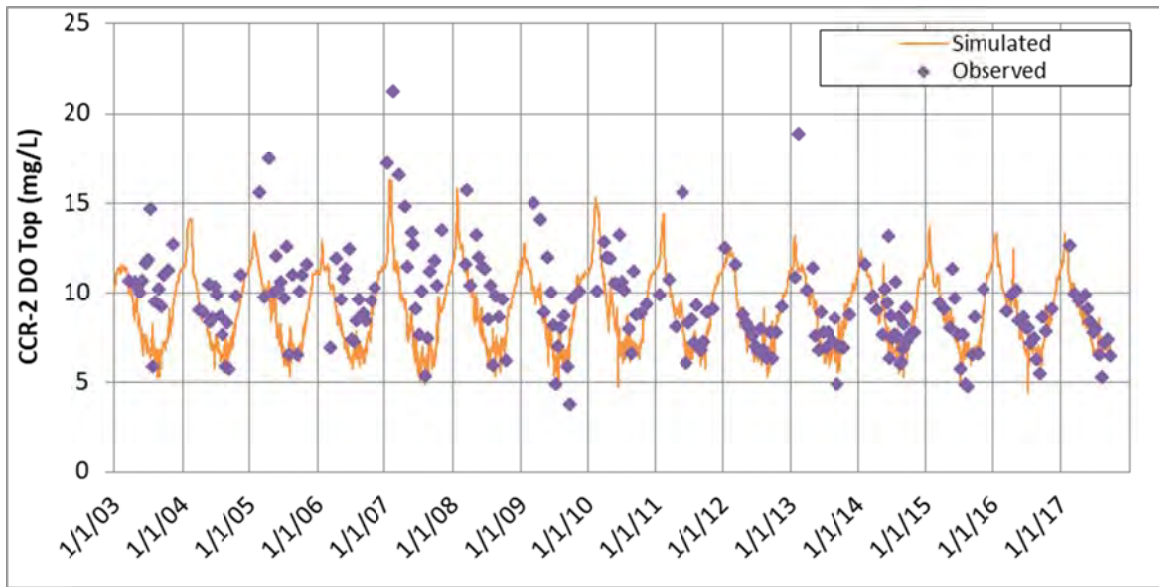


Figure 57. Simulated and Observed Dissolved Oxygen at the Top at CCR-2, 2003-2017

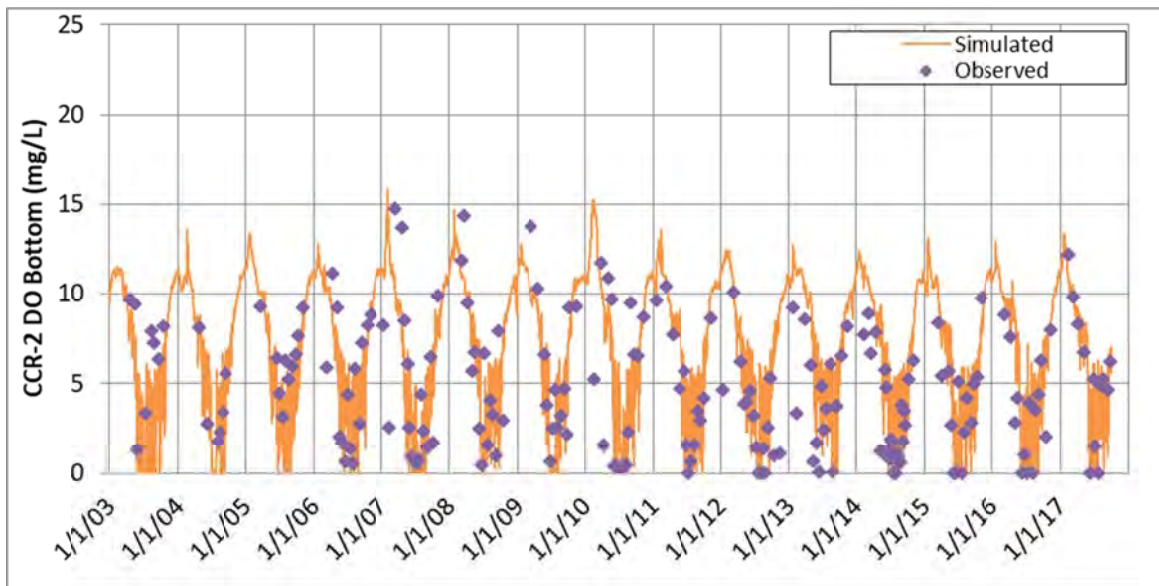


Figure 58. Simulated and Observed Dissolved Oxygen at the Bottom at CCR-2, 2003-2017

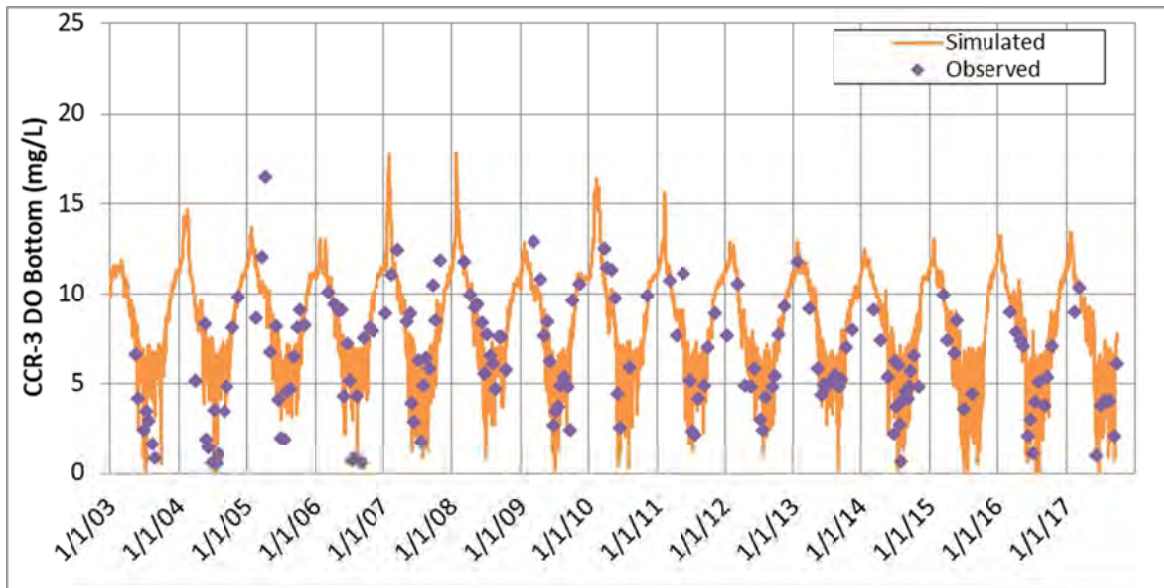


Figure 59. Simulated and Observed Dissolved Oxygen at the Bottom at CCR-3, 2003-2017

The extended simulation met the dissolved oxygen calibration target of MAE < 2 mg/L. The result for the extended period was slightly better (lower) than that for the 2003 – 2013 calibration period (Table 3). This may reflect improved data quality since 2010.

Table 3. Summary Calibration Statistics for Dissolved Oxygen Profiles (All Locations)

Metric	2003-2013	2014-2017	2003-2017
MAE (mg/L)	1.7	1.3	1.6
Calibration Target (mg/L)	MAE ≤ 2	MAE ≤ 2	MAE ≤ 2

The frequency of dissolved oxygen observation data continues to be a limitation on data interpretation and model assessment. As described in Hydros (2017), it is still recommended that continuous dissolved oxygen probes be installed at 1 m below the surface and at 0.5 m above the bottom of the reservoir at CCR-2. Alternatively, an in-reservoir buoy-based profiler could be placed in the reservoir for daily profile collection. These data would help determine how dynamic the actual dissolved oxygen response is in the deepest parts of the reservoir and provide a dataset to better evaluate effects of the current or an upgraded destratification system.

3.4 Nutrients

The extended model continued to reasonably simulate nutrients in response to the major processes of nutrient uptake, organic matter decay, and internal loading from the sediments. Simulated and observed results for the state-variable nutrients (SRP, nitrate+nitrite, and ammonia) are presented in Figure 60 through Figure 65.

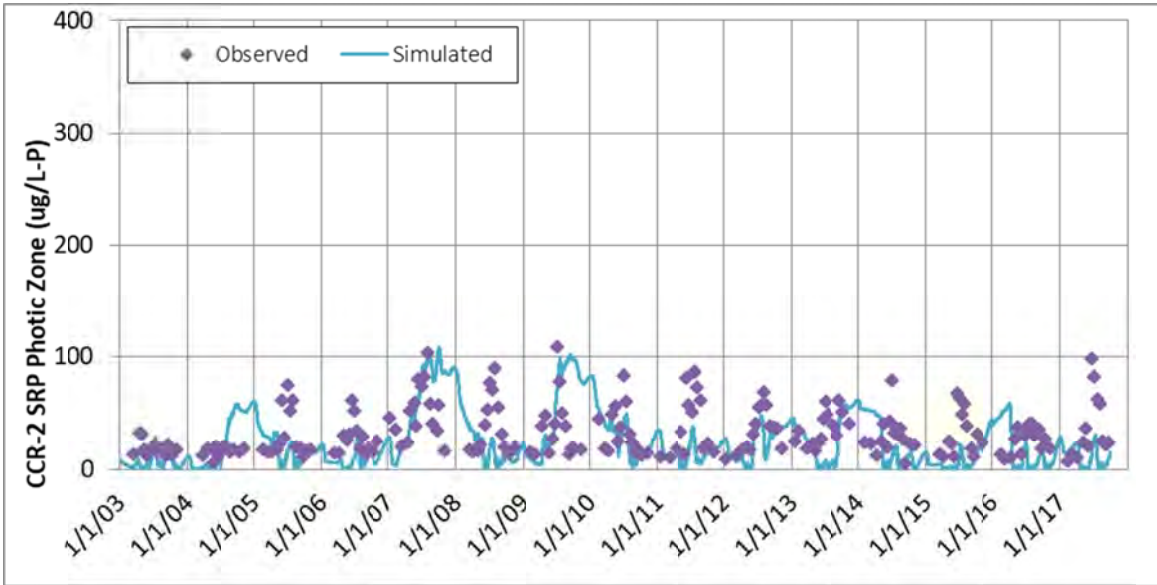


Figure 60. Simulated and Observed SRP at the Top at CCR-2, 2003-2017

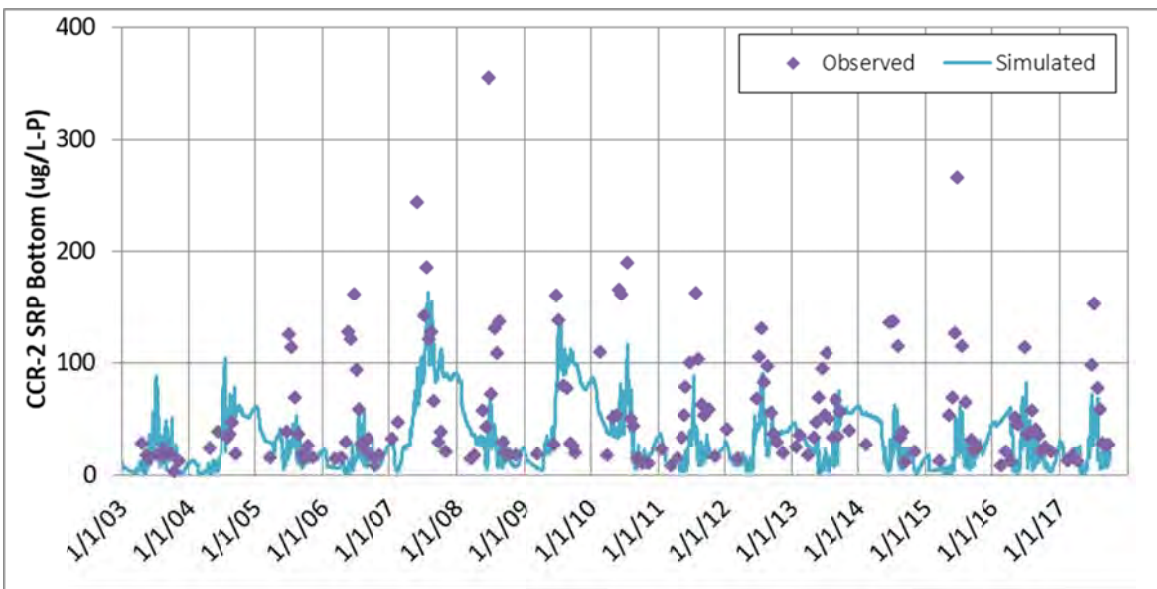


Figure 61. Simulated and Observed SRP at the Bottom at CCR-2, 2003-2017

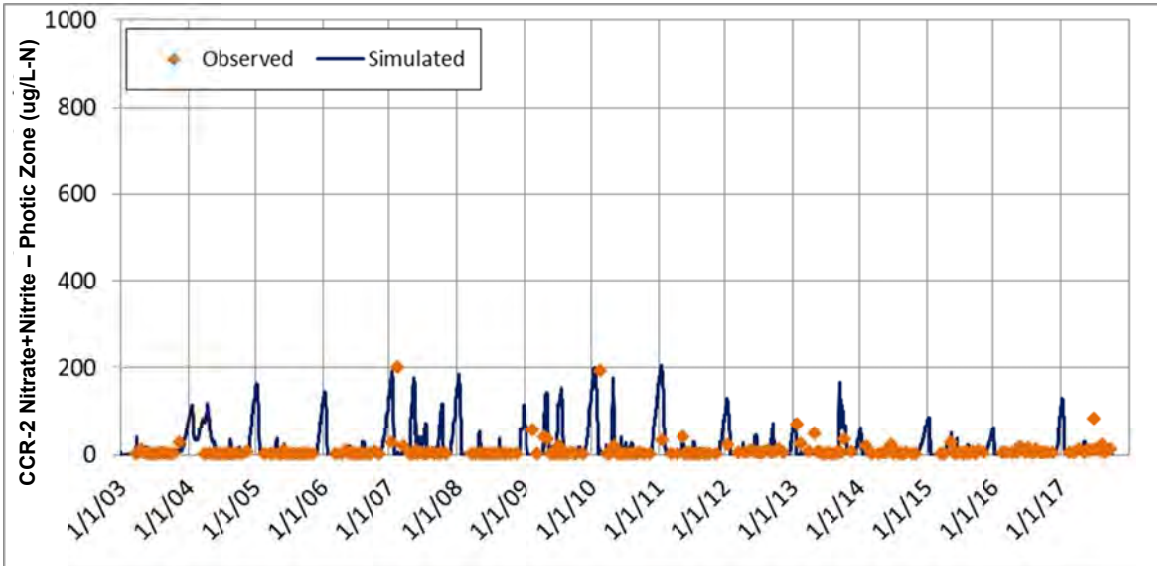


Figure 62. Simulated and Observed Nitrate+Nitrite at the Top at CCR-2, 2003-2017

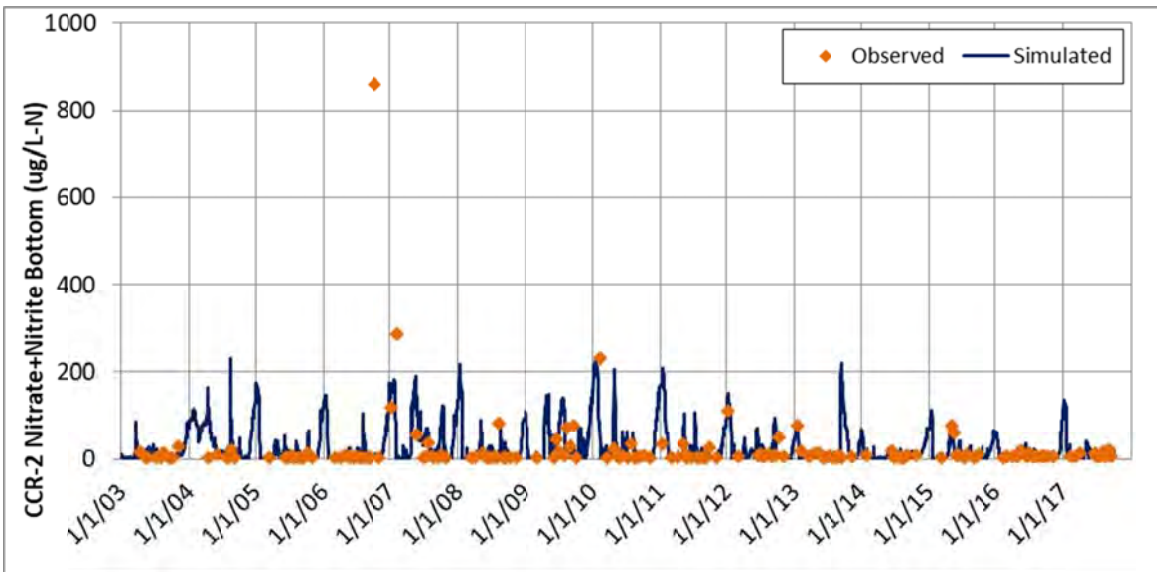


Figure 63. Simulated and Observed Nitrate+Nitrite at the Bottom at CCR-2, 2003-2017

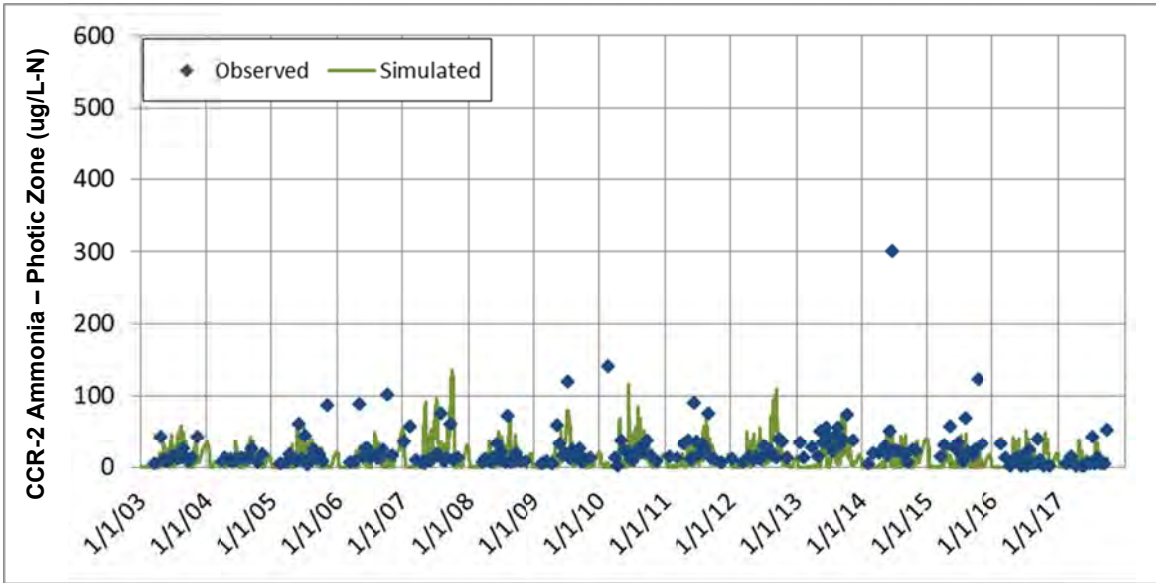


Figure 64. Simulated and Observed Ammonia at the Top at CCR-2, 2003-2017

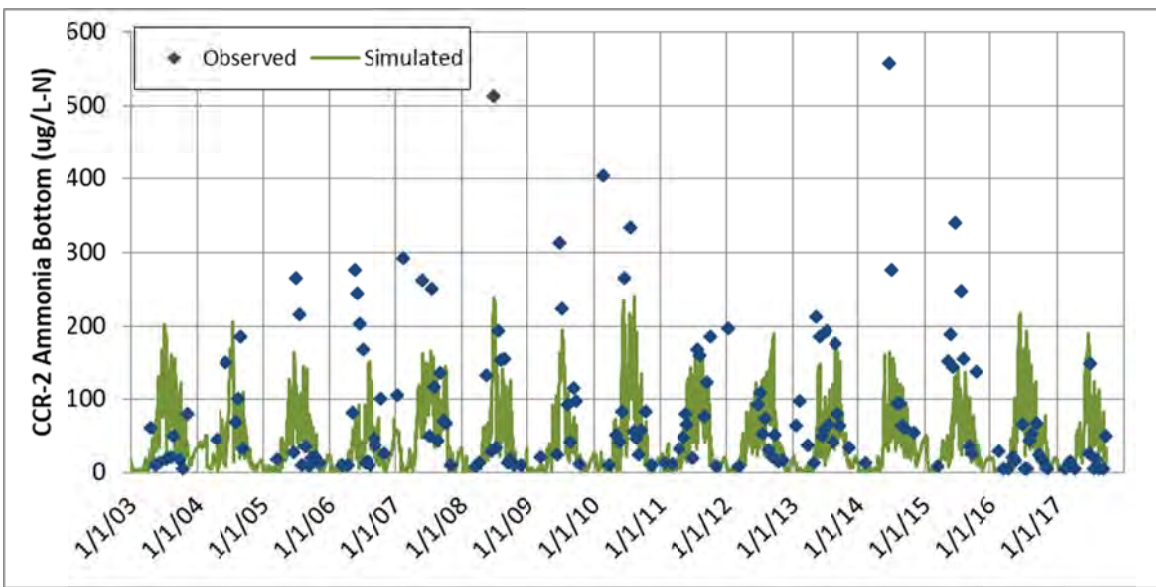


Figure 65. Simulated and Observed Ammonia at the Bottom at CCR-2, 2003-2017

The extended simulation met the nutrient calibration targets, with MAE results being less than 20% of the observed range. Statistical results for all three nutrients were comparable to the original 2003 -2013 calibration (Table 4).

Table 4. Summary Calibration Statistics for Nutrient Concentrations (All Locations)

Constituent	Calibration Target	2003-2013	2014-2017	2003-2017
	MAE as % of Obs. Range			
SRP	< 20%	7% (26 µg/L)	12% (31 µg/L)	8% (27 µg/L)
Nitrate+Nitrite	< 20%	3% (21 µg/L)	8% (7 µg/L)	2% (18 µg/L)
Ammonia	< 20%	6% (30 µg/L)	6% (34 µg/L)	5% (31 µg/L)

3.5 Chlorophyll a, Algae, and Cyanobacteria

The extended model reasonably simulated the general patterns and ranges of chlorophyll a concentrations in the reservoir for the added four years (Figure 66). Simulation of total algal biomass, however, does not agree as well (Figure 67). This is attributed to the large diatom blooms in 2015, 2016, and 2017, the mass of which includes a large fraction of silica, which is not simulated (discussed further in Section 2.4.4.2). It is expected that if the observed biomass could be adjusted to remove the silica fraction, it would better align with the simulated (non-silicate) organic biomass, given the historical match.

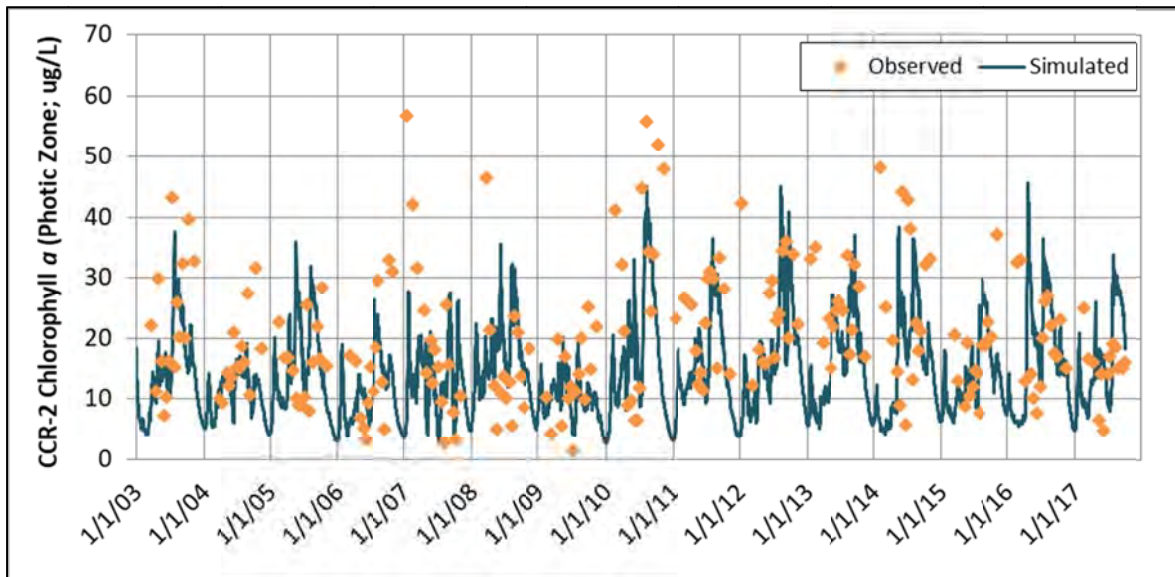


Figure 66. Simulated and Observed Chlorophyll a at CCR-2, 2003-2017

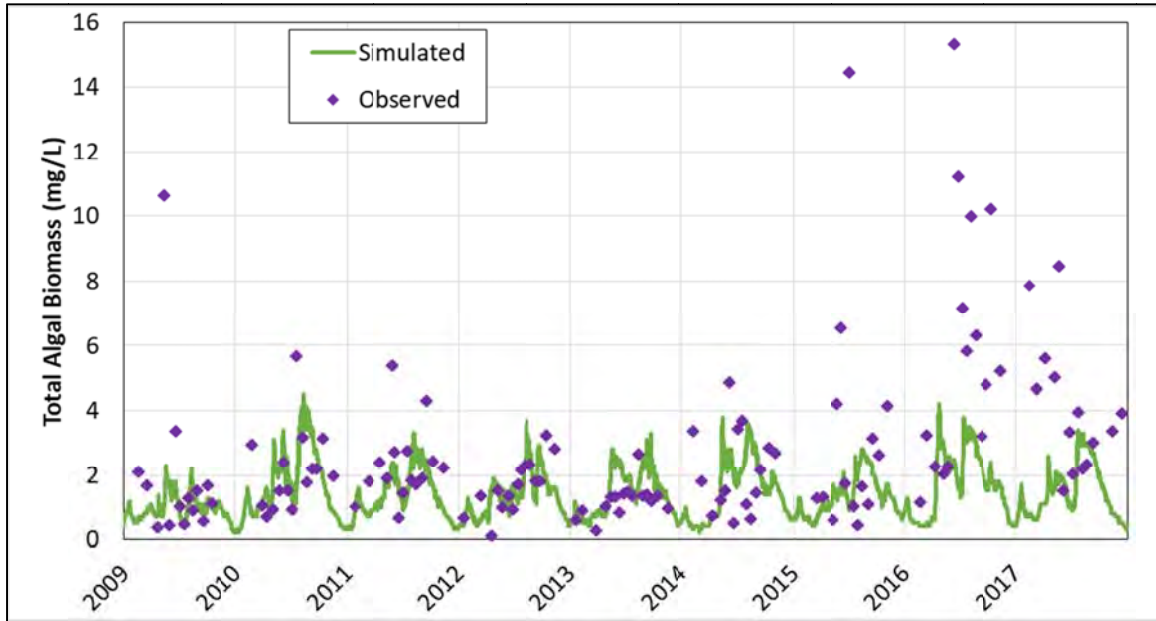


Figure 67. Simulated and Observed Total Algal Biomass, 2009-2017

The model continued to produce a reasonable simulation of the range and patterns of cyanobacteria biomass, particularly for *Aphanizomenon* (Figure 68). The occurrence of observed *Anabaena* blooms in the recent years indicates that the simulated timing of these blooms (purple lines) could be improved, though it is not critical to the summertime chlorophyll *a* since the *Anabaena* tend to bloom outside of the July through September period. To address this, a proposed refinement to the model settings is presented in the following Section (3.6).

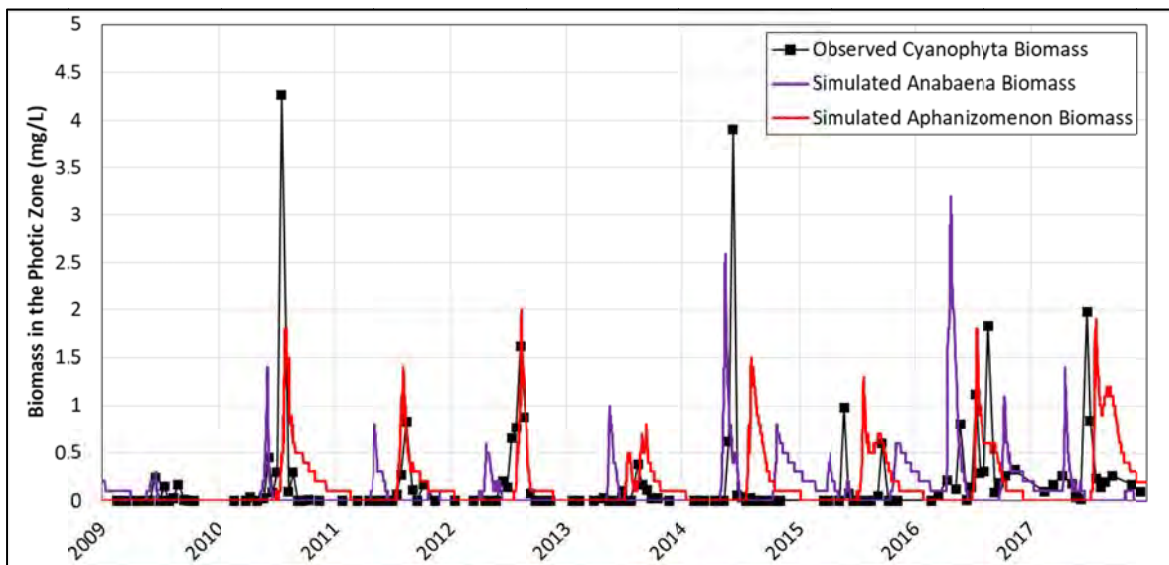


Figure 68. Simulated and Observed Cyanophyta Biomass, 2009 – 2017

The extended model met the target calibration statistics for chlorophyll *a* (Table 5) and showed continued good simulation of average summertime chlorophyll *a* (Figure 69 and Table 6).

Table 5. Summary Calibration Statistics for Chlorophyll *a* (All Locations)

Metric	2003-2013	2014-2017	2003-2017
MAE (µg/L)	8.9	9.6	8.8
MAE as % of Obs. Range	15%	16%	14%
Calibration Target (MAE as % of Obs. Range)	≤ 20%	≤ 20%	≤ 20%

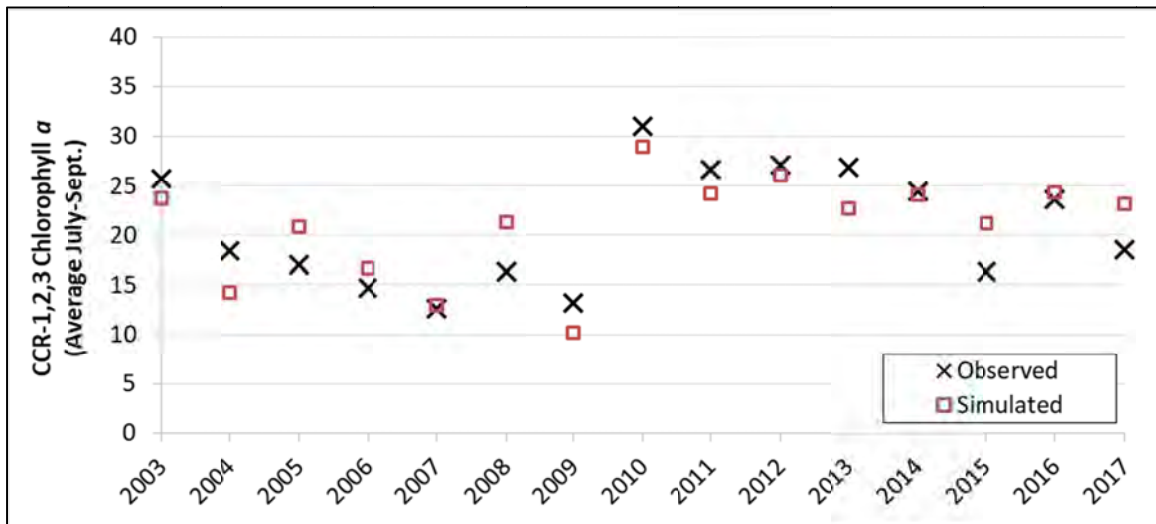


Figure 69. Simulated and Observed Summertime Average Chlorophyll *a*, µg/L, 2003 - 2017

Table 6. Summary Calibration Statistics for July – September Average Chlorophyll *a*

Metric	2003-2013	2014-2017	2003-2017
MAE (µg/L)	2.8 µg/L	2.6 µg/L	2.7 µg/L

3.6 Recommended Model Refinement

Though the model is considered adequate “as-is” for application to the in-progress bubble plume modeling effort, a minor refinement is suggested to improve simulation of the timing of *Anabaena* blooms. There were no major *Anabaena* blooms in the original calibration 2009 – 2013 biovolume dataset to support calibration of temperature settings associated with that algal group. The unadjusted model performed reasonably well with this group (Figure 68); however, a few model setting adjustments were tested to determine whether the simulation could be improved in terms of the timing of the blooms. All values were adjusted within recommended ranges for settings per Cole and Wells (2017). Specifically, the following adjustments were made for the proposed refinement:

- The second of four algal temperature rate coefficients for the *Anabaena* algal group was changed from 12 °C to 16.2 °C;
- The growth rate for that algal group was changed from 2.8/day to 2.2/day, and the mortality rate was changed from 0.16/day to 0.12/day; and
- The settling rate for particulate organic matter was changed from 0.05 m/day to the default value of 0.1 m/day.

The resulting simulation still meets all calibration target criteria (with nearly identical statistics), but the timing for the cyanobacteria biomass is improved, particularly for *Anabaena* (purple lines; Figure 70 compared to Figure 68). For example, the large spring *Anabaena* bloom in 2014 was observed to peak on June 10, 2014, and the original calibration predicted that peak to occur 3.5 weeks too early (on May 16), while the adjusted model predicts the peak on May 31, 10 days before the observed peak and between the observed peak and the previous observation. Similarly, the 2016 spring *Anabaena* bloom was observed to peak on May 17, and the refinement improved the simulated timing difference from 3 weeks early to 7 days late (and between the peak observation data and the next observation). Additionally, the proposed refinement improved the MAE for average summertime chlorophyll *a* improved slightly for full period (2003 – 2017) from 2.7 µg/L to 2.5 µg/L (Figure 71).

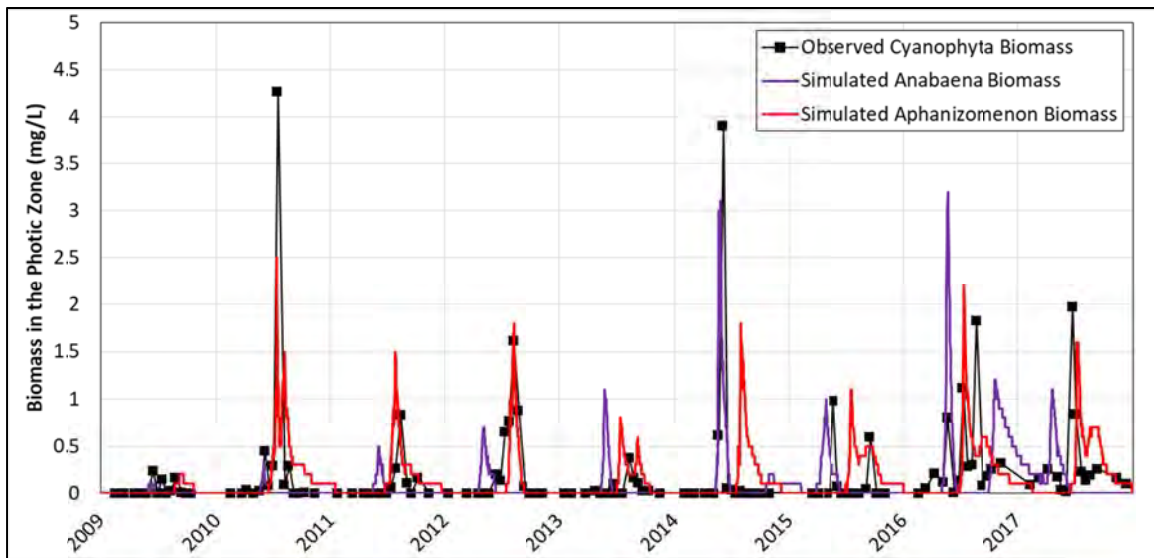


Figure 70. Simulated and Observed Cyanophyta Biomass for Proposed Calibration Refinement Run, 2009 - 2017

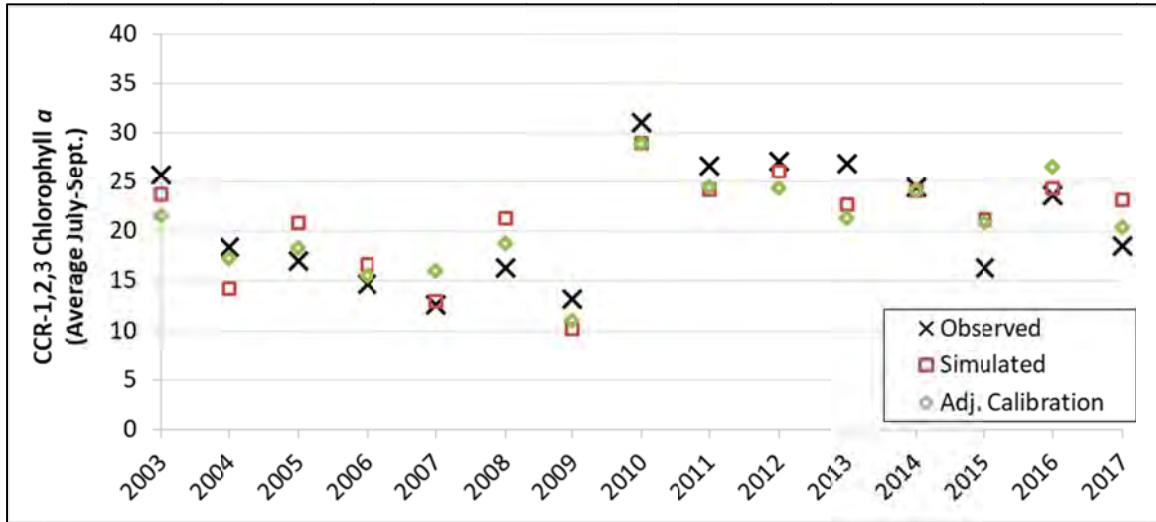


Figure 71. Simulated and Observed Summertime Average Chlorophyll *a* for Unadjusted Simulation and Proposed Calibration Refinement Run, µg/L, 2003 - 2017

Other future model refinements could include recalibration to add a distinct algal group for diatoms to better capture their distinguishing characteristics of growth rate, settling rate, and silica content. However, the model performs reasonably well in simulation of the primary calibration target (summertime chlorophyll *a*) without such a refinement. Further, such a refinement would require collection of dissolved and total silica on the inflows and in-reservoir. Addition of a diatom algal group is not considered critical at this time for the current modeling objectives; however, given the good (relative) water-quality conditions associated with diatoms, it may become advantageous in the future to improve the understanding what drives these blooms.

4 Water-Quality Response Overview, 2014-2017

In addition to updating the model with observed data from 2014 through 2017, which included an analysis of the observed data, the Authority requested a discussion of the key drivers of water-quality response (particularly summer average chlorophyll *a* and cyanobacteria blooms) on a year-by-year basis. The following discussions for each year present a summary of the main factors thought to be responsible for the observed algal response, relying upon the detailed data analysis and graphics presented in Section 2.

4.1 2014

2014 was a relatively low-flow year (Figure 9) with cooler than average peak air and water temperatures (Figure 12 and Figure 24). The destratification system was not operated during the year. The chlorophyll *a* standard value (18 ug/L as a July – September average) was not met in 2014 (22.7 ug/L; Figure 69). Additionally, there was a large cyanobacteria bloom that peaked on June 10, 2014 (Figure 48).

Thermal stratification set up from mid-May to early June as well as from late July to mid-August, with additional periods of weak stratification throughout the summer (Figure 27).

Correspondingly, hypoxic to anoxic conditions were observed at the bottom at CCR-2 in May and from late June through August.

The relative isolation of the epilimnion during the stratification from mid-May to early June is expected to have contributed to a reduction in the nitrogen-to-phosphorus ratio in the photic zone (Figure 49). The low nitrogen-to-phosphorus ratio likely gave an advantage to the nitrogen-fixing cyanobacteria that tend to bloom in spring water temperatures in the reservoir (*Anabaena*). The resulting bloom peaked on June 10. Rising ammonia concentrations due to the mixing (destratification) that occurred ~June 7 – 9 may have caused the cyanobacteria to lose their advantage. On the sampling event following the crash of the bloom (June 24) elevated ammonia concentrations were observed at the top and bottom of the reservoir (Figure 34 and Figure 35) due to decay of the algal biomass. This spike in ammonia supports the occurrence of nitrogen fixation since it cannot be fully explained by inflow loading or internal loading. It is not certain whether operation of the destratification system could have prevented or minimized the June 10 *Anabaena* bloom, but analysis of the full observed record suggests it is possible (see Section 2.4.4.3).

Through the summer months of July through September, there were no major cyanobacteria blooms, possibly due to below average peak water temperatures. In spite of the lack of cyanobacteria blooms in these months, the site-specific chlorophyll *a* standard was not met. Though external loading was relatively low throughout the summer (due to low inflow volumes), there were periods of weak stratification and internal loading of nutrients. While the standard was not met, the average chlorophyll *a* was lower than that of the previous four years when the destratification system was operated. This may be due overall to the cooler water temperatures.

4.2 2015

Inflows were very high in 2015, particularly in May and June, resulting in a low annual residence time (Figure 3 and Figure 10). Water temperatures at the surface were above average in June, but average to below average in July and August (Figure 24). The destratification system was not operated during the year. 2015 was the only year among the four being evaluated that met the chlorophyll *a* standard value (18 ug/L as a July – September average), with a result of 14.5 ug/L (Figure 69). There were no major summer cyanobacteria blooms, but there were *Anabaena* blooms mid-May and late September (Figure 48).

There was an extended period of thermal stratification in 2015, from late May into July (Figure 27). This temperature differential was due in large part to underflow by the cooler inflowing water. While there were periodic occurrences of anoxia at the bottom, there was not an extended period of anoxia matching the extended thermal stratification (Figure 33). This may reflect the influx of oxygenated water (i.e., from the underflow).

While the nitrogen-to-phosphorus ratio dropped in the photic zone in the summer, there were no major *Aphanizomenon* blooms. This may reflect the fact that peak temperatures in the photic zone did not reach values seen in other years with major *Aphanizomenon* blooms. Additionally, conditions were apparently good for diatoms to bloom. There were major diatom blooms in June and July at times of relatively high clarity (Figure 47). These major blooms corresponded to high algal biovolume, but low chlorophyll *a*. The drivers of the diatom blooms are not completely understood but could be related to inflow loading of silica in this high inflow year, though this is speculation in the absence of recent silica data. As discussed in Section 2.4.4.2, diatoms tend to bloom in Cherry Creek Reservoir in high inflow years.

4.3 2016

2016 was also a high inflow year, with the highest flows from April through June and a low annual residence time (Figure 3 and Figure 10). Water temperatures at the surface were above average in June and July and below average in the second half of August (Figure 24). The destratification system was not operated during the year. With an average summertime chlorophyll *a* of 23.7 ug/L (Figure 69), the site-specific standard value (18 ug/L) was not met. There were also three major cyanobacteria blooms between May and August (Figure 48).

Thermal stratification was observed in the reservoir in early May as well as over an extended period including June and part of July (Figure 27). Anoxic or hypoxic conditions were observed at CCR-2 during much of the June to early July period of stratification. Anoxia was also observed at the bottom at CCR-2 in mid-August when the reservoir was not significantly stratified (< 1 °C temperature difference from top to bottom). The occurrence of anoxia or hypoxia at the bottom at times of very weak stratification is indicative of the strong sediment oxygen demand of the system, capable of creating an oxygen gradient even with a limited density gradient.

Each of the three major cyanobacteria blooms was preceded by a decrease in the nitrogen-to-phosphorus ratio in the photic zone (Figure 49). Algal uptake can be effective at decreasing the nitrogen-to-phosphorus ratio in this system with surplus phosphorus, particularly during times of stratification which partially isolate the epilimnion. The type of cyanobacteria that dominated during each of the three 2016 blooms corresponded to the surface water temperature at the time (*Anabaena* in the cooler May temperatures and the unseasonably cool late August, and *Aphanizomenon* in the warmest part of the summer), matching typical patterns seen for the reservoir (Section 2.4.4.3).

While 2016 had the highest average summertime chlorophyll *a* concentrations of the recent four years (2014-2017), due in part to multiple cyanobacteria blooms, the average in this hot year might have been higher if not for the occurrence of major diatom blooms (Figure 44). The diatom blooms peaked a few weeks after each major cyanobacteria bloom. As seen in other years, the diatom blooms had high algal biovolumes but low relative chlorophyll *a* (Figure 44), bringing down the summertime average. As noted in the discussion for 2015 and Section 2.4.4.2, diatoms tend to bloom in Cherry Creek Reservoir in high inflow years, and this may indicate inflow of silica, though this is speculation in the absence of recent silica data.

There is no indication that the destratification system would have helped prevent the summertime *Aphanizomenon* bloom; however, the data evaluation (see Section 2.4.4.3) suggests that it may have been able to minimize the May *Anabaena* bloom. By extension, if the thermal resistance to mixing was adequately low in late August due to cooler temperatures, the destratification system may have provided beneficial mixing at that time also to disrupt the late-August *Anabaena* bloom.

4.4 2017

Similar to 2016, 2017 was a wet year with a relatively low annual residence time (Figure 9 and Figure 10). High inflows occurred mid-March to mid-June, with other notable inflow events in August and October (Figure 3). Water temperatures at the surface were above average in the first half of June and below average in the first half of August (Figure 26) in response to a storm event and cooler air temperatures. The average summertime chlorophyll *a* was 18.7 ug/L (Figure 69), just failing to meet the site-specific standard value (18 ug/L). There was one major cyanobacteria bloom in late June/early July (Figure 48). The destratification system was operated in May and June.

Anoxia at the bottom at CCR-2 was observed in two samples, one from mid-June and one from mid-July (Figure 32), while thermal stratification was largely limited to the first half of June, with some variable weak stratification in July and August. The occurrence of anoxia or hypoxia at the bottom at times of very weak stratification is indicative of the strong sediment oxygen demand of the system, capable of creating an oxygen gradient even with limited vertical density differential.

There was a major diatom bloom in May of 2016 (Figure 45). This event followed the noted patterns seen in previous years for major diatom blooms. The bloom was associated with high inflows and exhibited high biovolume but low chlorophyll *a* (Figure 45) at a time of relatively high clarity (Figure 47). While consistent patterns are noted, additional understanding is needed regarding the specific cause(s) of major diatom blooms in the reservoir.

There were no major cyanobacteria blooms in May and early June of 2017 as seen in 2014 through 2016 (Figure 48). Based on analysis of the observed data (see Sections 2.4.1 and 2.4.4.3), this may be attributable to mixing induced by the destratification system in those months with lower thermal resistance to mixing.

The late June/early July cyanobacteria bloom was predominantly *Aphanizomenon*, characteristic of cyanobacteria blooms at warmer temperatures. The bloom occurred at a time of low nitrogen-to-phosphorus ratio in the photic zone (Figure 49), which likely gave the nitrogen-fixing species an advantage. Above average inflows in August, providing inorganic nitrogen and cooling the temperature at the surface, may be responsible for preventing major cyanobacteria blooms in August. Based on all available data for years with and without destratification system operations, there is no indication that the current destratification system would have helped to prevent or minimize the summertime *Aphanizomenon* bloom in July of 2017 or had any other notable effect on the July - September chlorophyll *a*.

5 Summary of Findings and Recommendations

At the request of the Authority, Hydros conducted a detailed evaluation of the observed data from 2014 through 2017 and updated the existing reservoir water-quality model to include those years of record. The following summarizes key findings and recommendations generated from that effort.

Key Findings:

- **Beneficial effects of the destratification system in May and early June:** The data indicated that there are some limited seasonal beneficial effects of the existing destratification system in May and early June.
 - Comparison of thermistor data from years with and without destratification system operations indicates that the current system can reduce thermal stratification in May and early June, when the thermal resistance to mixing is lower.
 - The data do not show a corresponding increase in dissolved oxygen or decrease in internal nutrient loading at the bottom at that time, suggesting that the mixing effect is inadequate to overcome gradients from the sediment and water column oxygen demand.
 - Data suggest that the mixing may effectively limit cyanobacteria blooms in May and early June. This effect is likely due to disruption of buoyancy effects, given no apparent effects on nutrients.
 - There is no change to previous findings regarding lack of effectiveness of the current destratification system on the July through September concentrations of dissolved oxygen, nutrients, or chlorophyll *a*.
- **Diatom blooms are associated with better (relative) water quality:** Data from 2015 through 2017 include observations of major diatom blooms in the reservoir that appear to have notable effects on water quality.
 - Diatom blooms tend to be associated with high algal biovolume but low chlorophyll *a* concentrations in Cherry Creek Reservoir.
 - The observed diatom blooms appear to be associated with high inflow volumes and correspondingly low residence times.
 - Diatoms appear to be associated with times of greater clarity in the reservoir. The greater clarity may be a condition associated with the high inflows that encourages diatom growth and/or it may be attributable to the fact that diatoms tend to grow rapidly and settle rapidly.
 - Given the good (relative) associated water quality, a greater understanding of what drives diatom blooms could be useful for management in the future.
- **Model extension met calibration targets:** The extended reservoir water-quality model successfully met all calibration targets for the added four years (2014 – 2017) as well as for the full 15 year simulation (2003 – 2017).

- **Minor model setting refinements were tested:** While the existing model is considered adequate for application to the bubble plume modeling effort, a model refinement was developed and tested to improve the simulation of cyanobacteria bloom timing.
 - Observed data from 2014 through 2017 included major *Anabaena* blooms not seen in the period of biovolume record available for the initial calibration. This provided an opportunity to calibrate the model those blooms.
 - The model refinement consists of adjustments to model settings related to the *Anabaena* growth, mortality, and temperature rate constants, as well as the particulate organic matter settling rate.
 - The refinement to settings produced an improved simulation of cyanobacteria bloom timing with no adverse effect to the rest of the calibration.
 - It is recommended that the refinement be adopted for use with the bubble plume modeling.

Recommendations:

- **Install continuous dissolved oxygen probe in the reservoir:** Installation of a continuous dissolved oxygen probes at CCR-2 (at 1 m from the top and 0.5 m from the bottom) or a daily automated profiler system is recommended to improve the understanding of oxygen dynamics at the bottom of the reservoir.
- **Test smaller filter sizes for SRP:** Analysis of SRP using additional smaller filter sizes is recommended as a first step to evaluate the potential significance of colloidal phosphorus for Cherry Creek Reservoir. This should include at least one average to wet year of sampling at CC-10 and CCR-2. SRP should be analyzed from samples filtered with 0.2 μm and 0.02 μm filtered samples (or 0.02 μm at a minimum if funding is limited) in addition to the already-measured 0.45 μm -filtered samples.
 - There are indications (though no definitive evidence) that the SRP data may overestimate the bioavailable phosphorus in Cherry Creek Reservoir due to the presence of colloidal phosphorus. This is significant given the emphasis on managing phosphorus inflows to the reservoir to control algal growth. Costly efforts to reduce phosphorus that do not target the bioavailable fraction of phosphorus will not produce the desired results of reduced algal and cyanobacterial growth in the reservoir.
 - If the finer filter analyses indicate significant colloidal phosphorus, further characterization can be conducted on subsequent samples to determine the bioavailable fraction. That information can be used to support appropriately-targeted management of inflow water quality to control algal/cyanobacterial growth in the reservoir.
- **Collect dissolved and particulate silica samples:** If the Authority is interested in improving the understanding of the drivers of beneficial diatom blooms and simulation of diatoms as a distinct algal group, dissolved and particulate silica should be added to the analyte lists of CC-10, CT-2, and CCR-2. This is considered a lower priority recommendation since it is not critical to current model objectives.

6 References

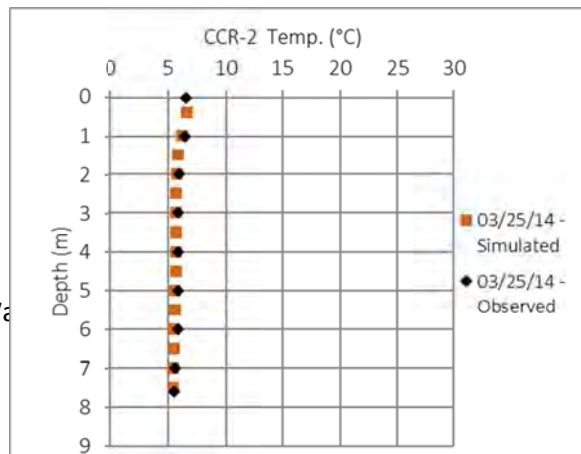
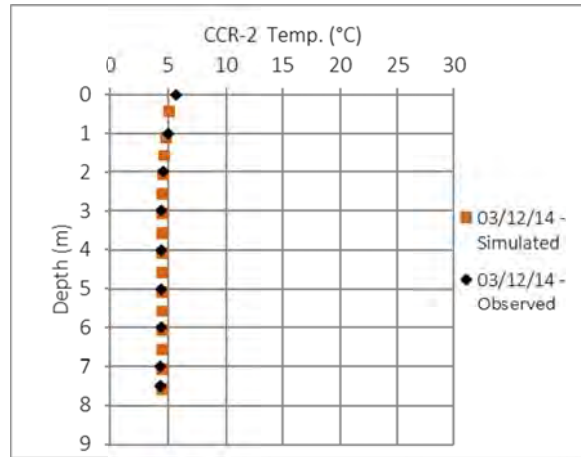
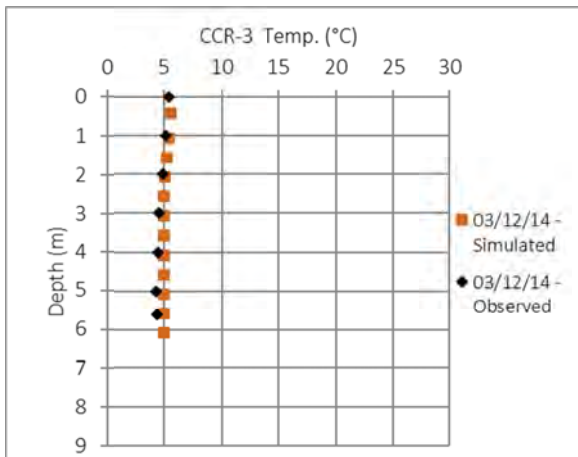
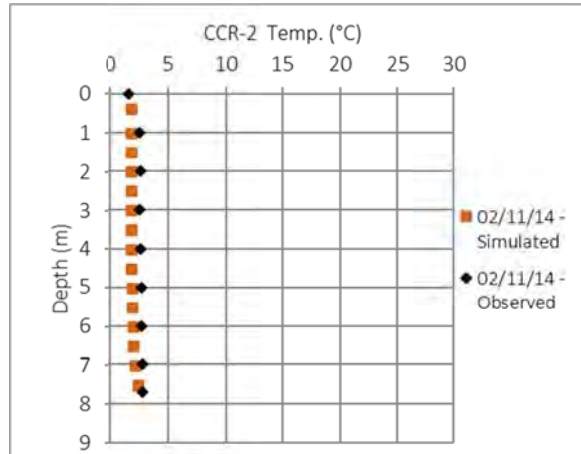
- AMEC Earth and Environmental Inc., Alex Horne Associates, Hydrosphere Resource Consultants Inc. 2005. Feasibility Report – Cherry Creek Reservoir destratification. AMEC document 5371009031. Submitted to Cherry Creek Basin Water Quality Authority. December 5, 2005.
- Andreas, A. and S. Wilcox. 2011. Solar Technology Acceleration Center (SolarTAC). Aurora, Colorado (Data); NREL Report No. DA-5500-56491.
<https://midcdmz.nrel.gov/apps/go2url.pl?site=STAC>
- Cole, T.M. and S.A. Wells. 2017. CE-QUAL-W2: A Two-Dimensional, Laterally Averaged, Hydrodynamic and Water Quality Model, Version 4.1. User Manual. Department of Civil and Environmental Engineering. Portland State University.
- Eckholm, P., Jouttijarvi, T., Priha, M., Rita, H., and H. Nurmesniemi. 2007. Determining Algal-Available Phosphorus in Pulp and Paper Mill Effluents: Algal Assays vs Routine Phosphorus Analyses. *Environmental Pollution*; Volume 145; Issue 3; Pages 715-722.
- Hudson, J.J., Taylor, W.D., and D.W. Schindler. 2000. Phosphate Concentrations in Lakes. *Nature*; Volume 406(6791); Pages 54-56.
- Hydos (Hydos Consulting Inc.). 2014. Cherry Creek Reservoir Water-Quality Modeling Project: Data Analysis (Task 1). Technical Memorandum prepared for the Cherry Creek Basin Water Quality Authority. August 4, 2014.
- Hydos. 2017. Cherry Creek Reservoir Water-Quality Model Documentation. Prepared by: Hawley C., J.M. Boyer, and B. Johnson. Prepared for the Cherry Creek Basin Water Quality Authority. April 5, 2017.
- JCHA (John C. Halapaska and Associates). 2007. West Cherry Creek Background Phosphorus Report. Report to Cherry Creek Water Quality Authority, Dated June 6, 2007.
- Kretzschmar, R., Borkovec, M., Grolimund, D. and M. Elimelech. 1999. Mobile Subsurface Colloids and their Role in Contaminant Transport. *Advances in Agronomy*. Volume 66; Pages 121-193.
- Li, B. and M.T. Brett. 2013. The Influence of Dissolved Phosphorus Molecular Form on Recalcitrance and Bioavailability. *Environmental Pollution* Volume 182; Pages 37-44.
- Li, B. and M.T. Brett. 2015. The Relationship between Operational and Bioavailable Phosphorus Fractions in Effluents for Advanced Nutrient Removal Systems. *International Journal of Environmental Science and Technology*; 12; Pages 3317-3328.

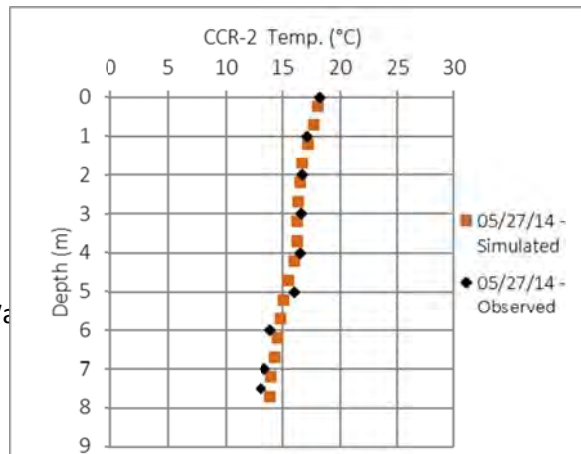
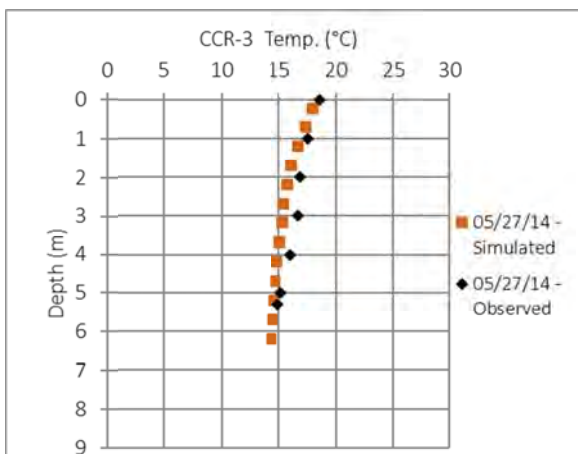
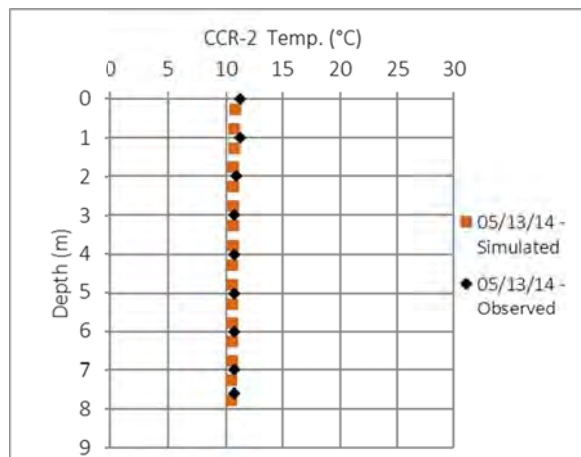
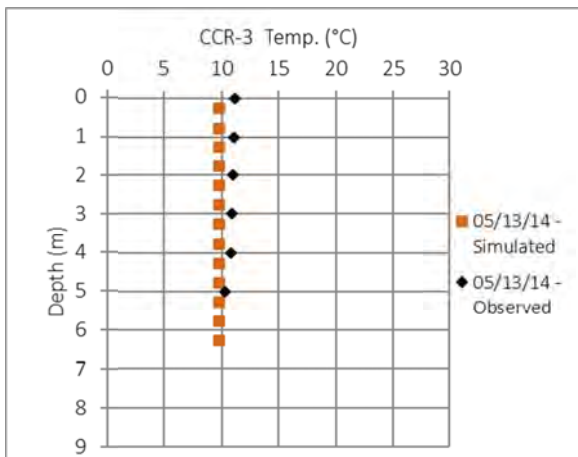
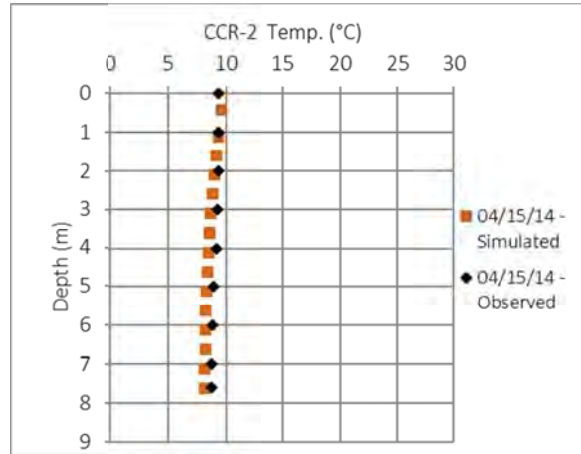
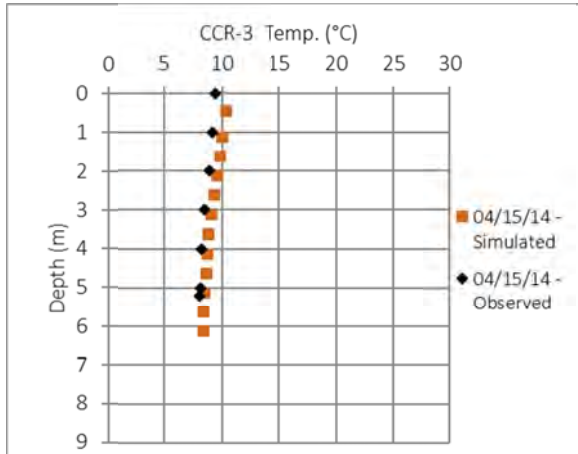
Sicko-Goad, L., C. Schelske, and E. Stoermer. 1984. Estimation of Intra-Cellular Carbon and Silica Content of Diatoms from Natural Assemblages Using Morphometric Techniques. *Limnology and Oceanography*. Volume 26 (6); Pages 1170-1178.

Twinch, A.J. and C.M. Breen. 1982. A Comparison of Nutrient Availability Measured by Chemical Analysis and Calculated from Bioassay Yields. *Hydrobiologia* Volume 93; Issue3; Pages 247-255.

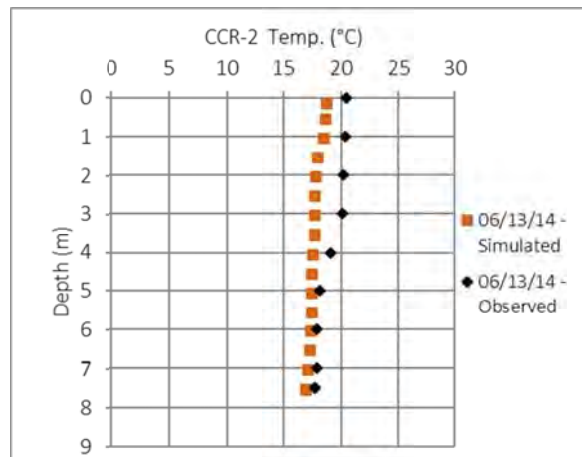
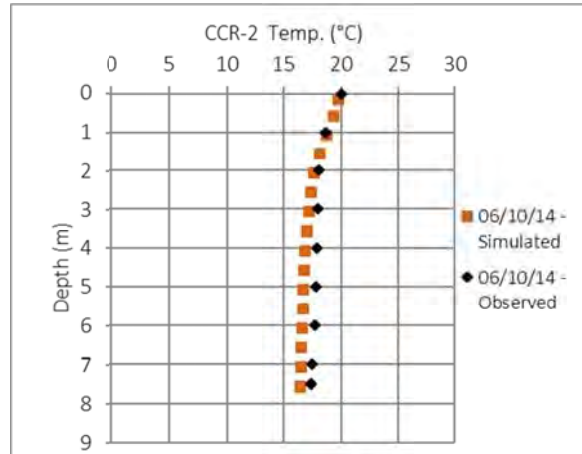
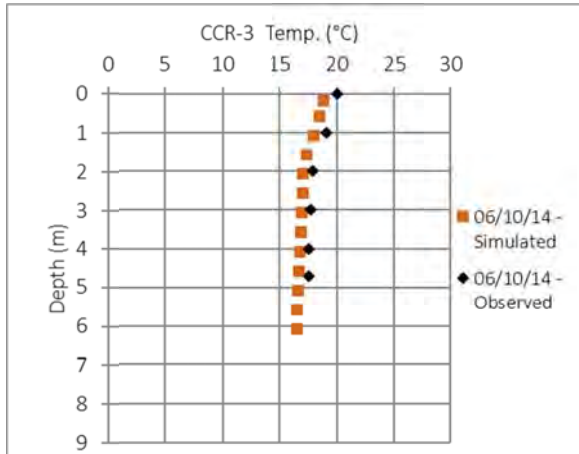
Wells, S.A., V.I. Wells, and C.J. Berger. 2008. Water Quality and Hydrodynamic Modeling of Tenkiller Reservoir. Expert Report prepared for the State of Oklahoma. Case No. 05-CU-329-GKF-SAJ. May 2008.

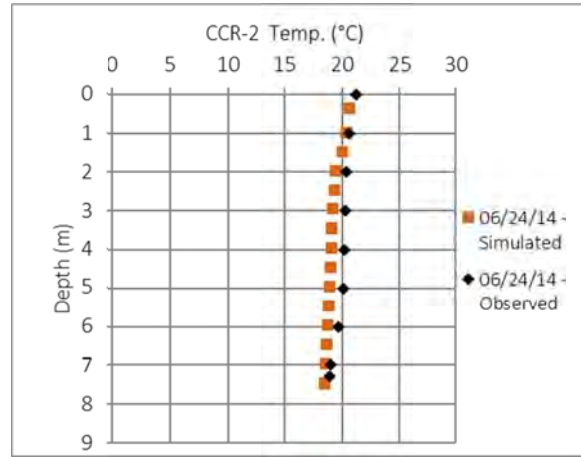
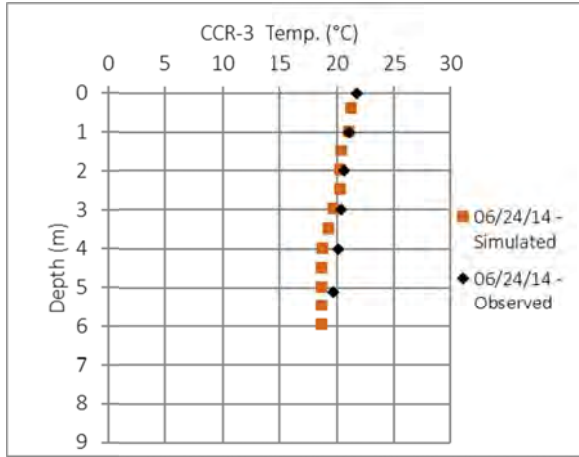
Attachment A: Observed and Simulated Temperature Results, 2014-2017

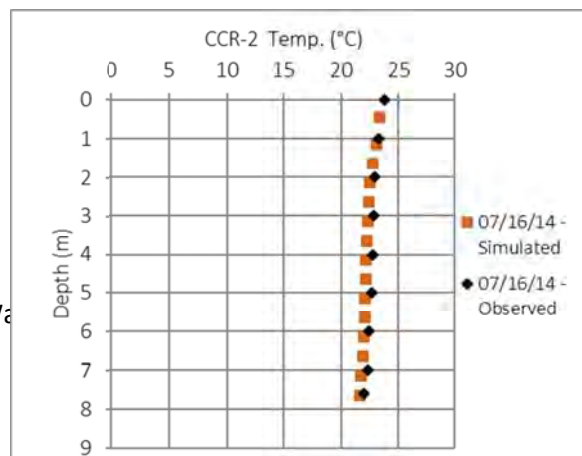
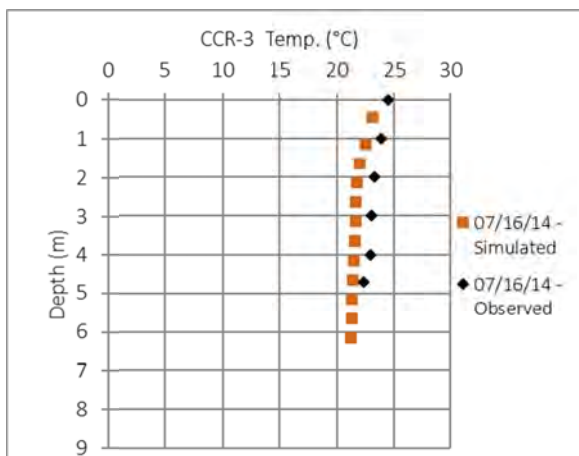
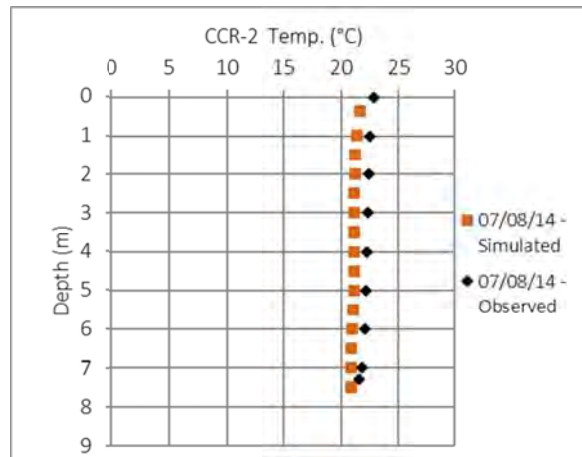
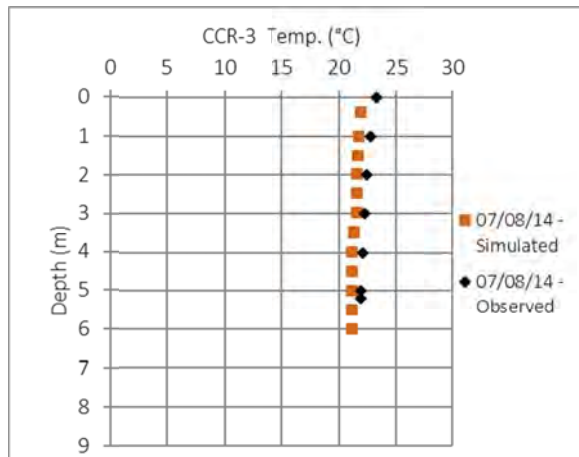
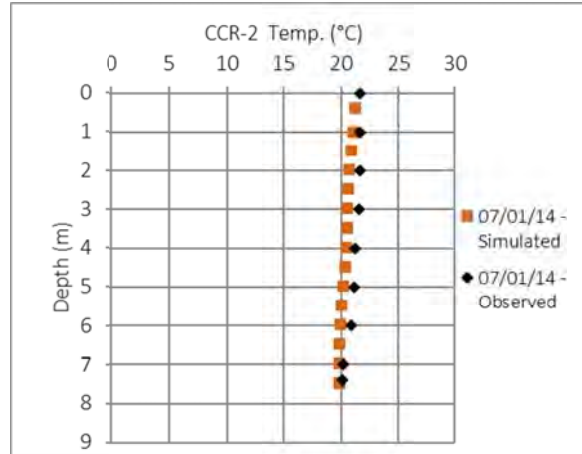
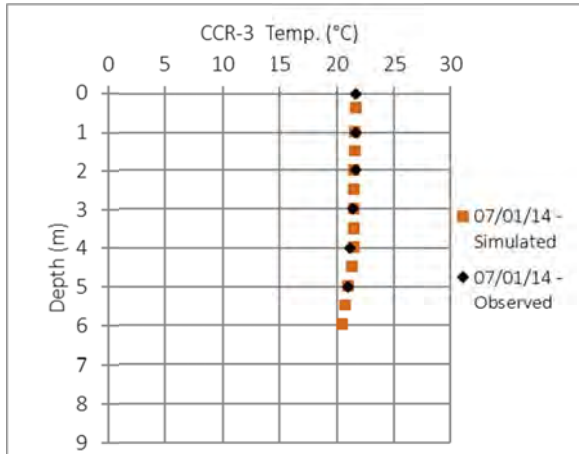




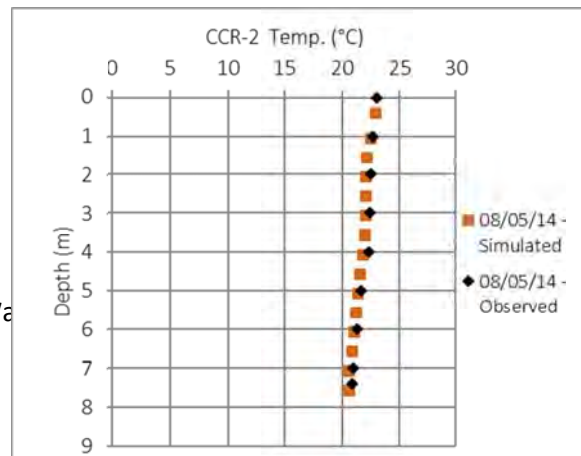
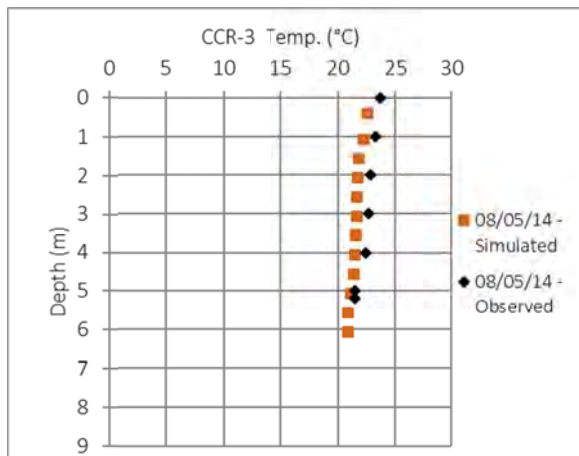
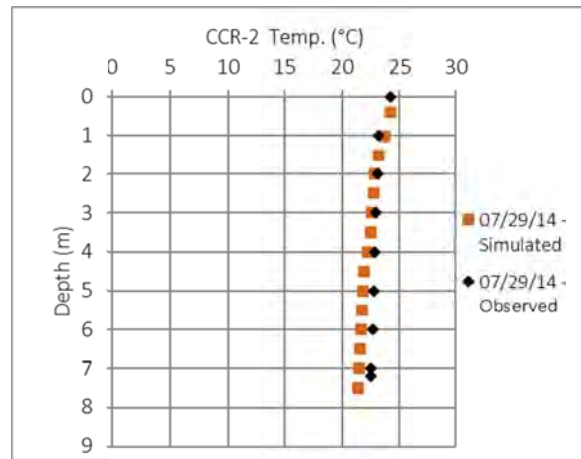
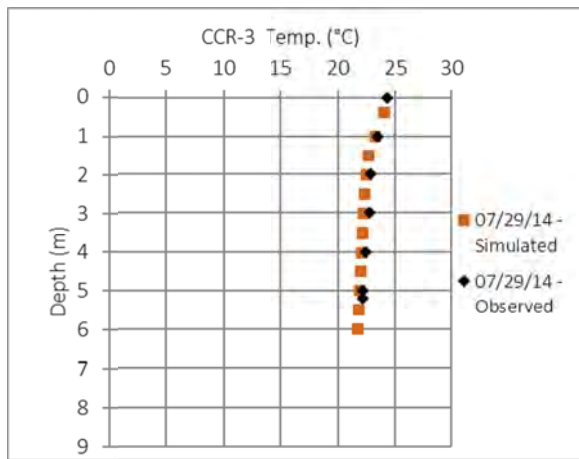
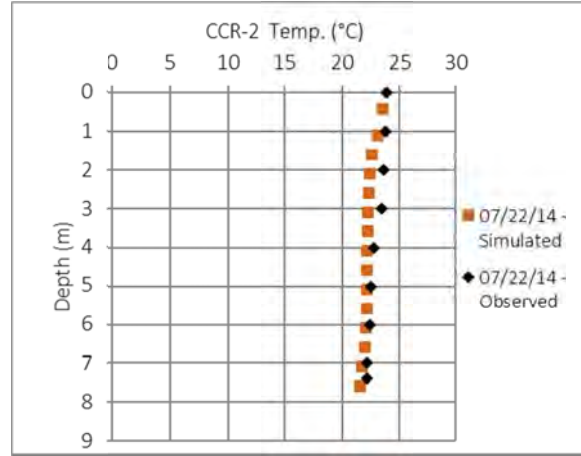
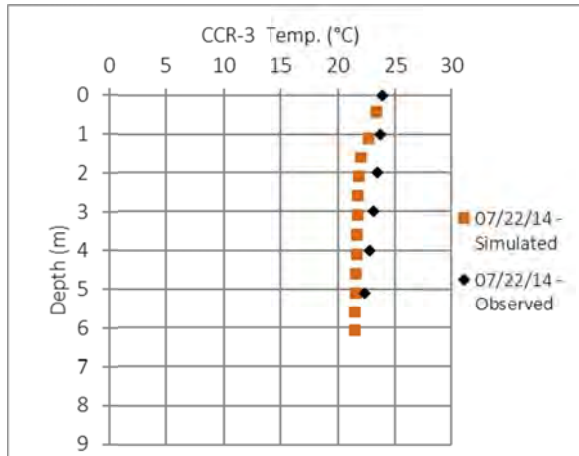
3 Wa



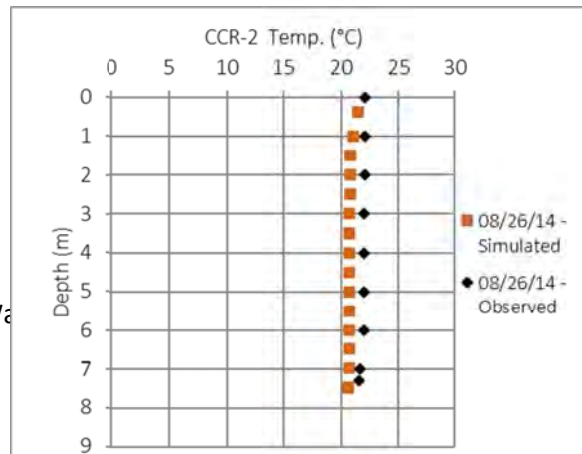
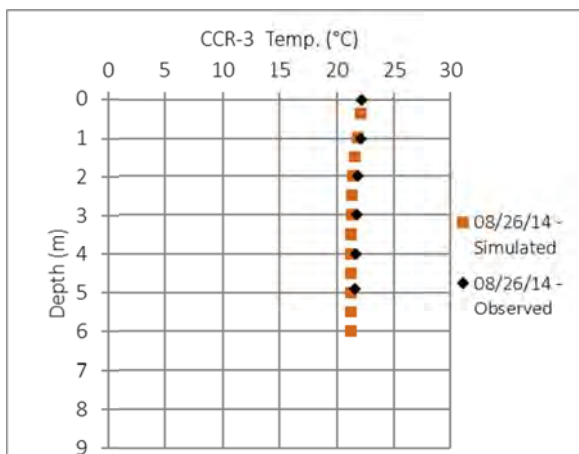
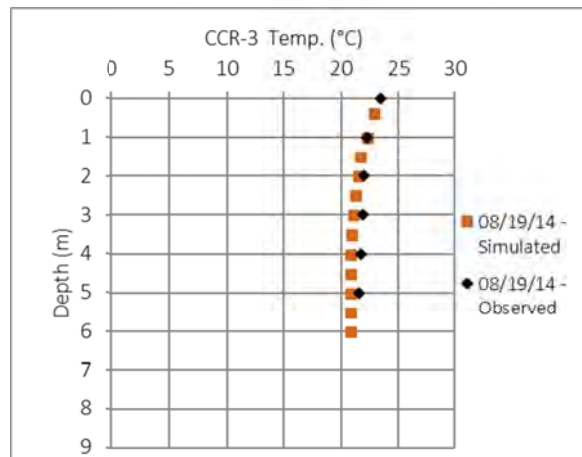
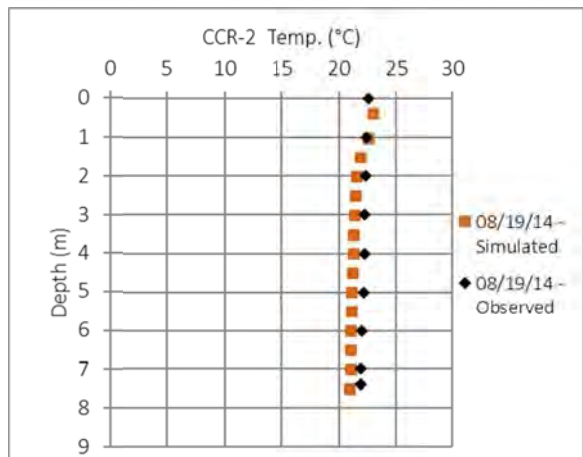
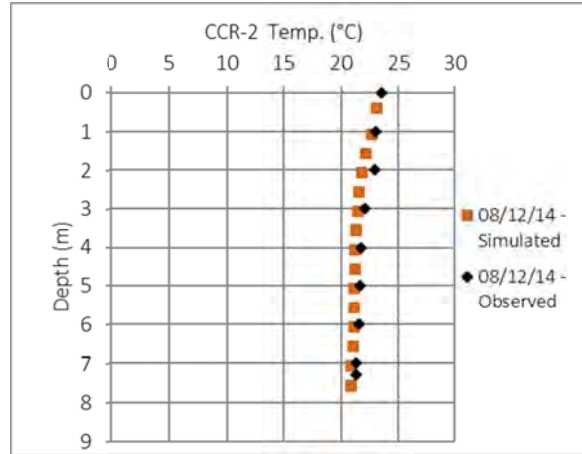
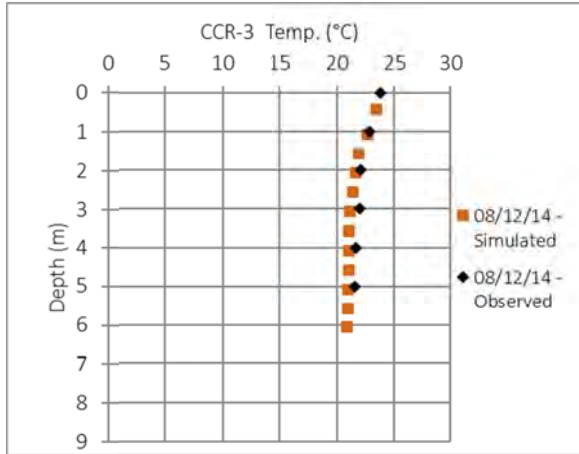




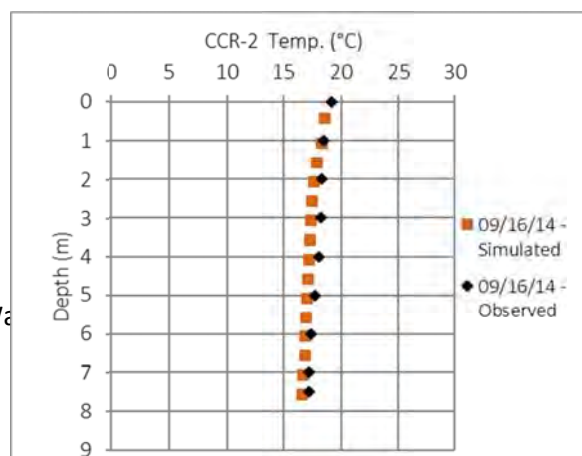
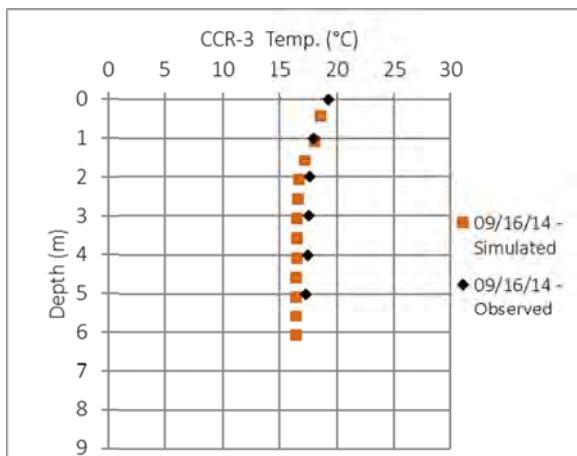
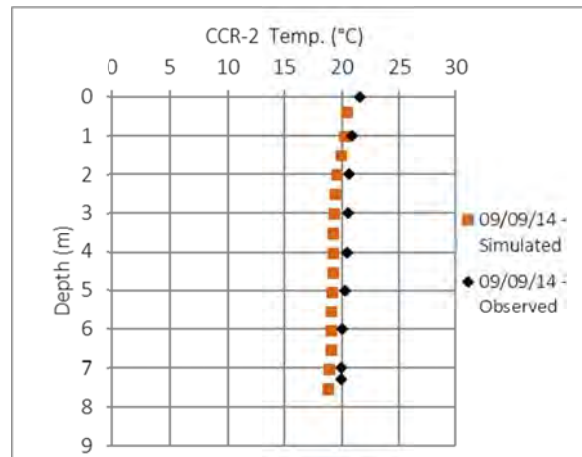
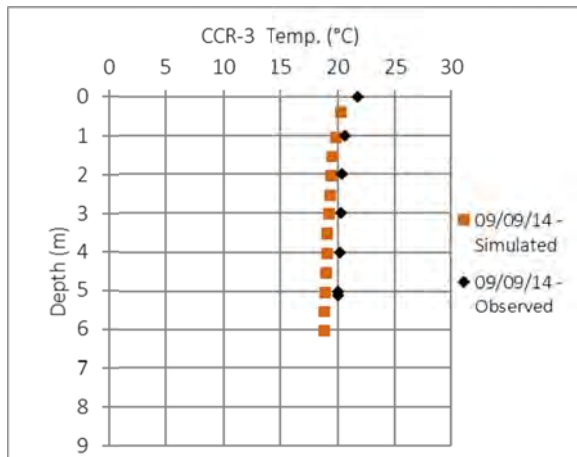
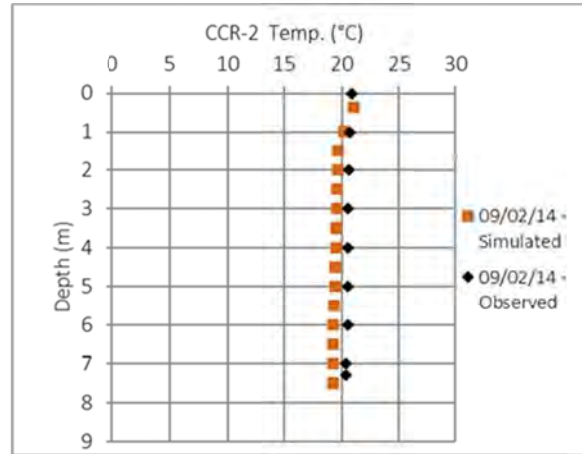
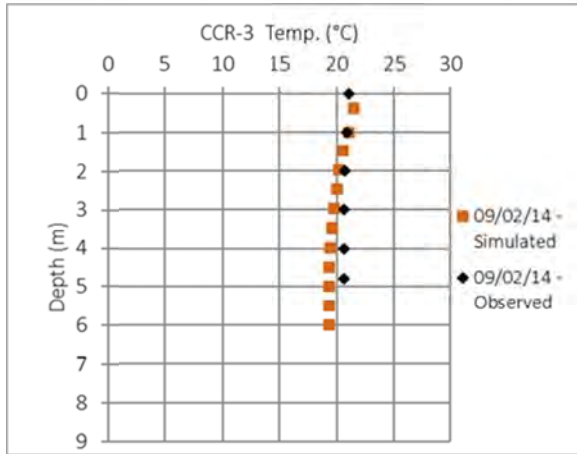
3 Wa



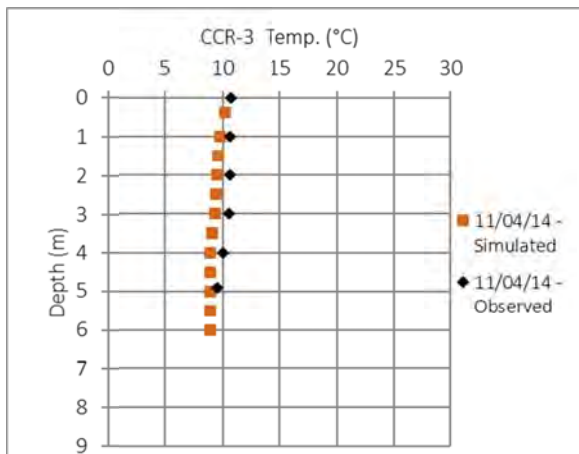
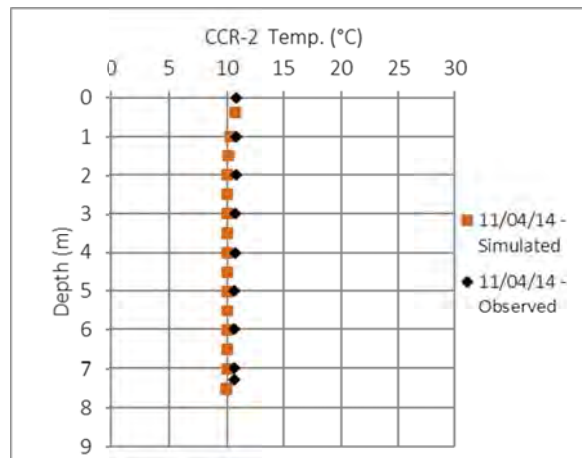
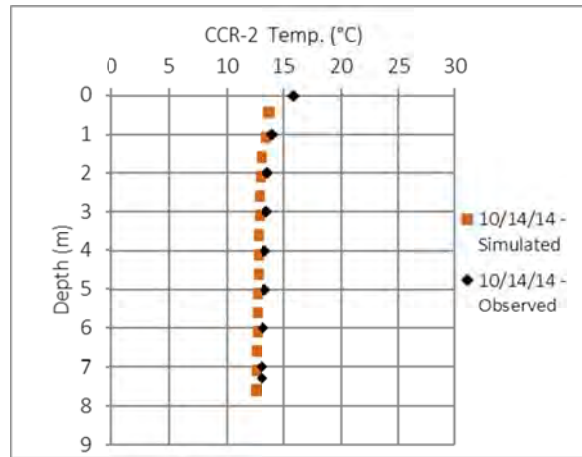
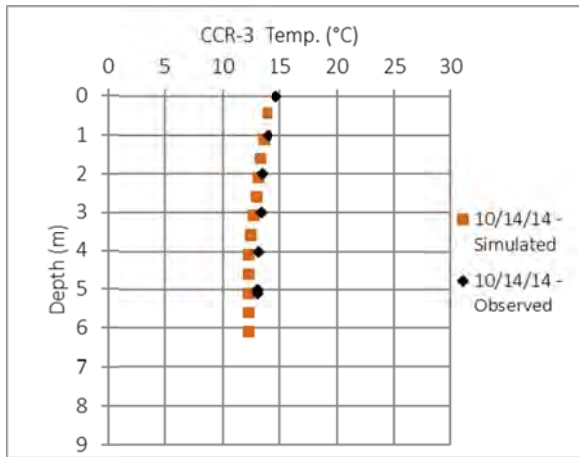
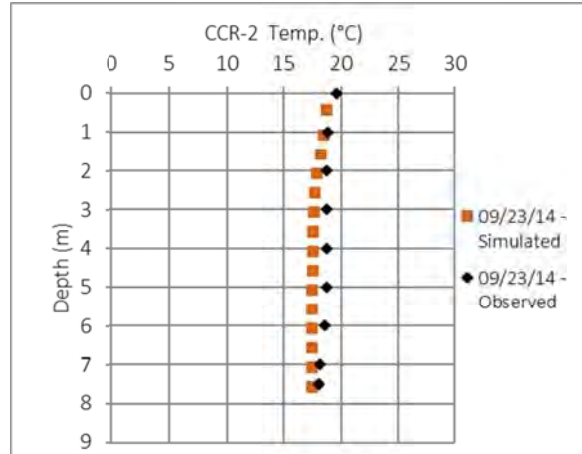
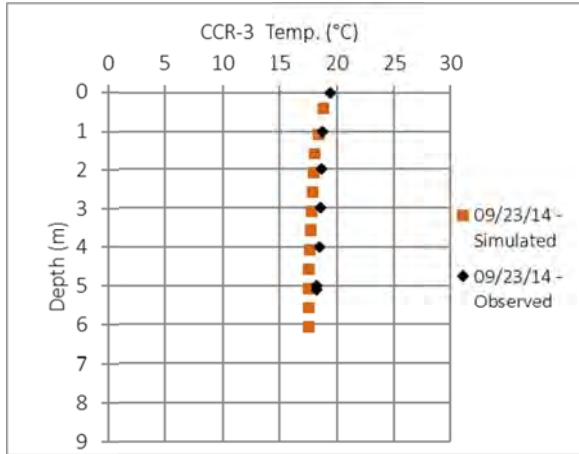
Water

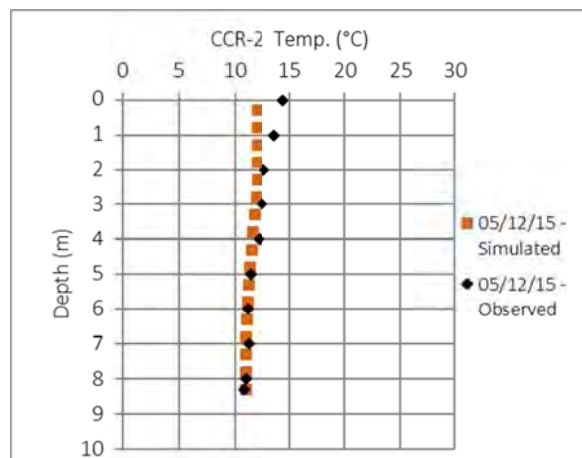
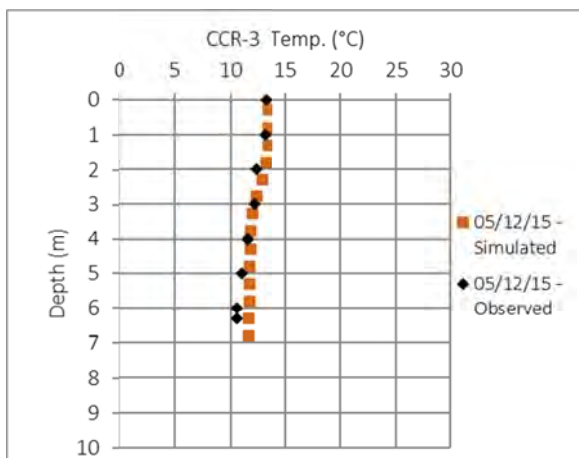
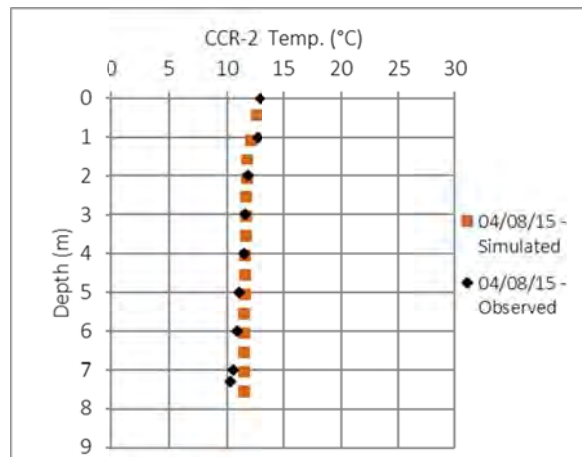
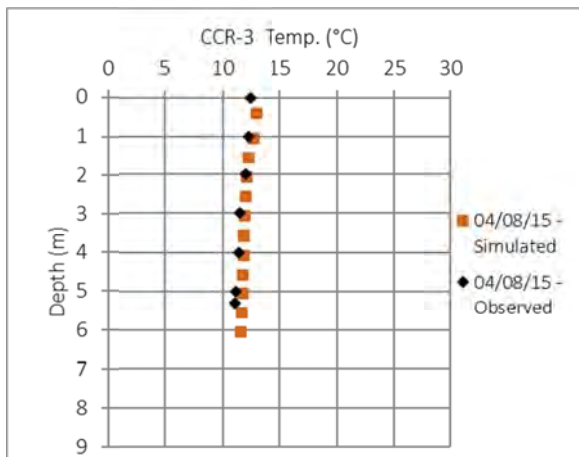
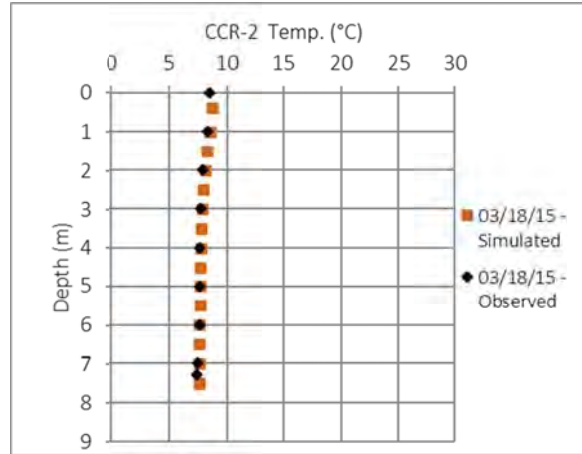
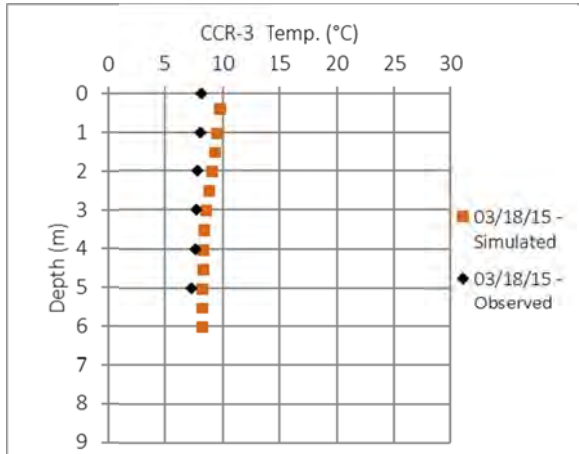


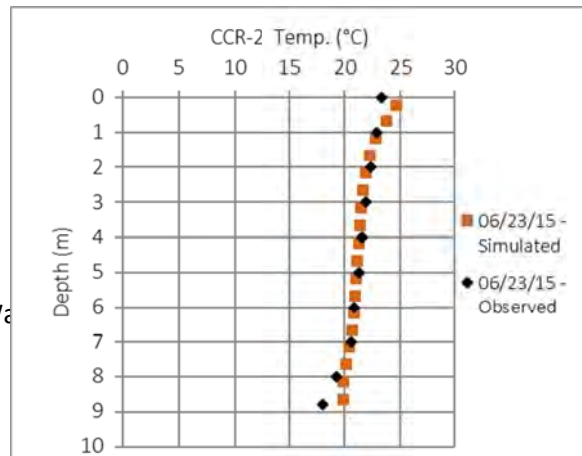
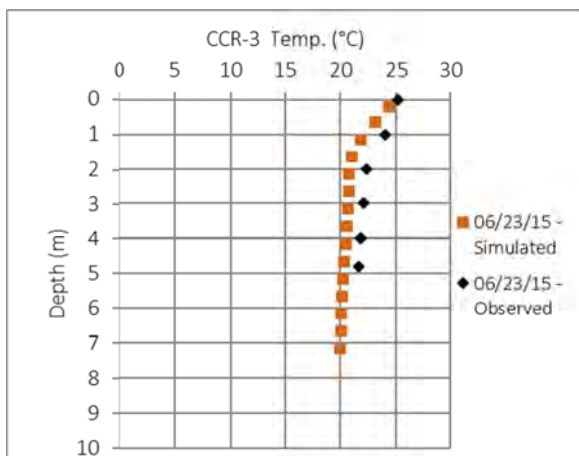
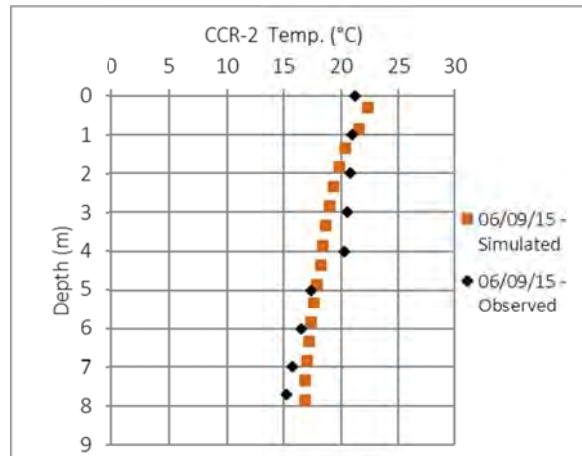
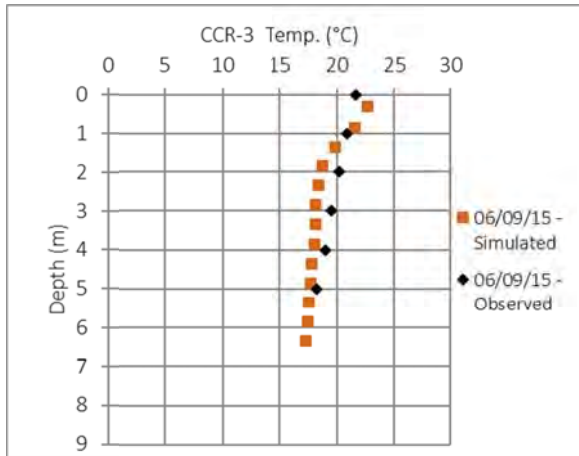
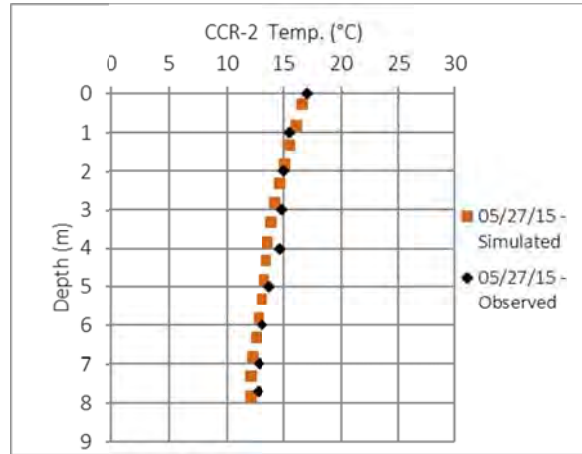
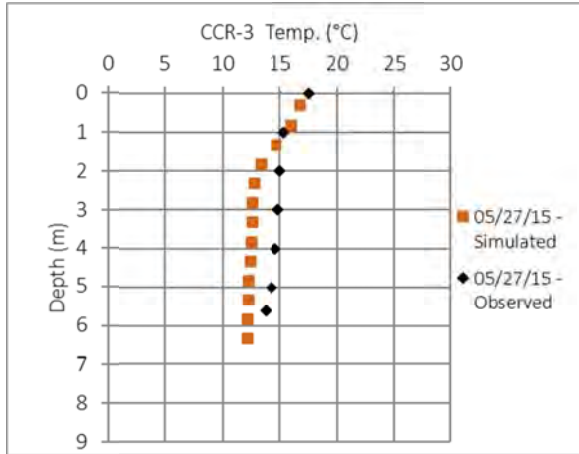
3 Wa



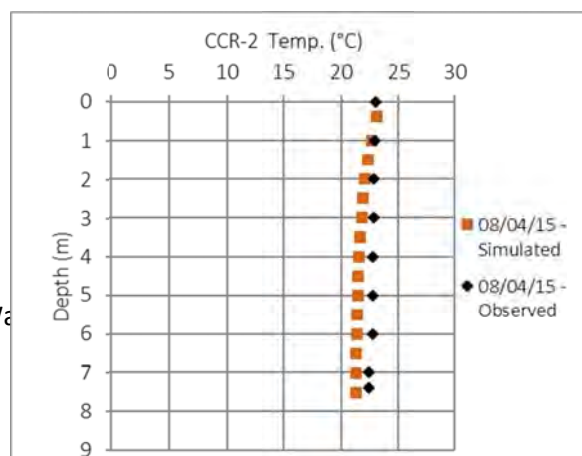
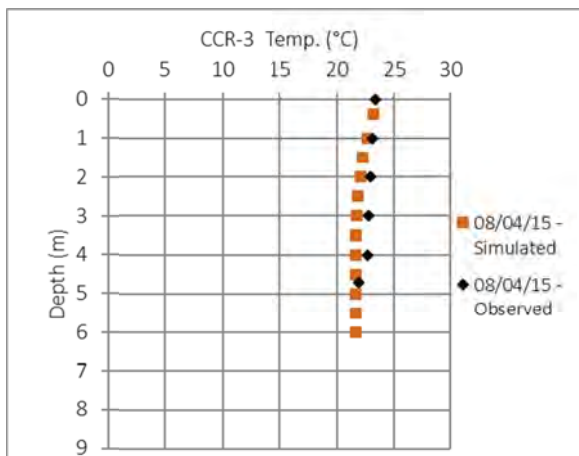
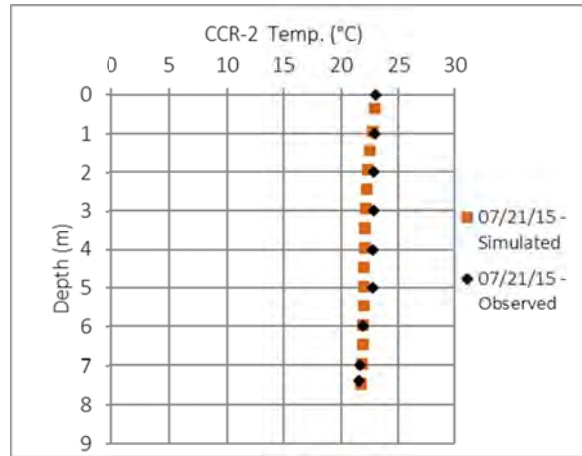
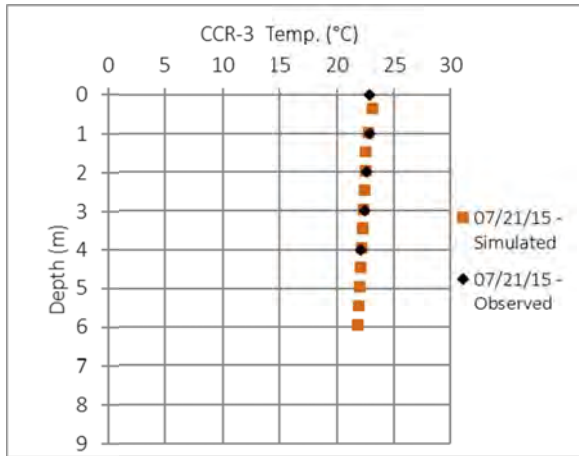
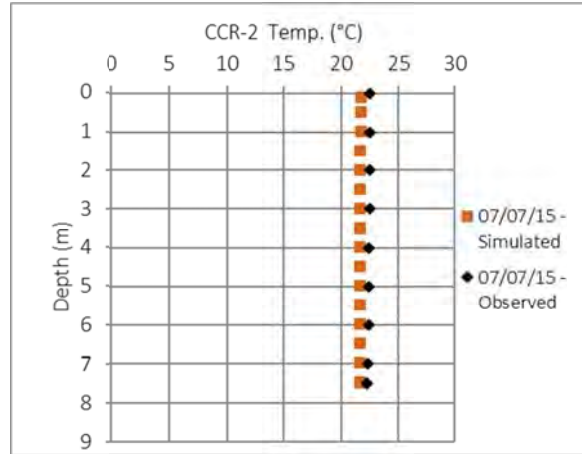
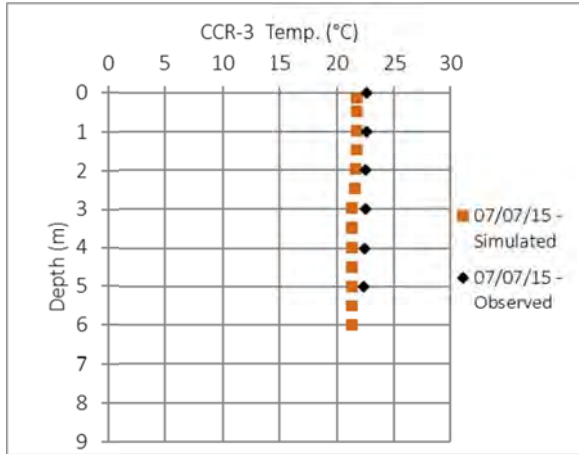
3 Wa



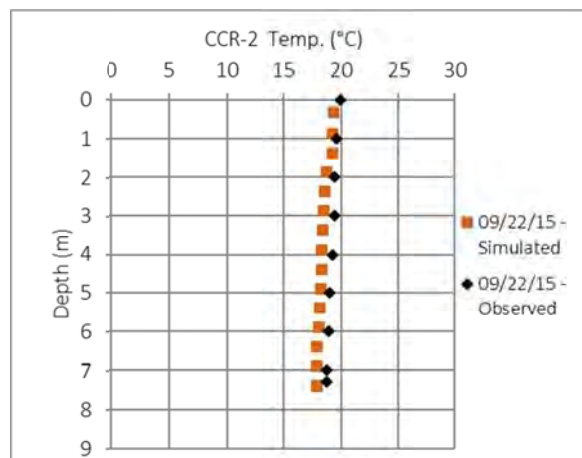
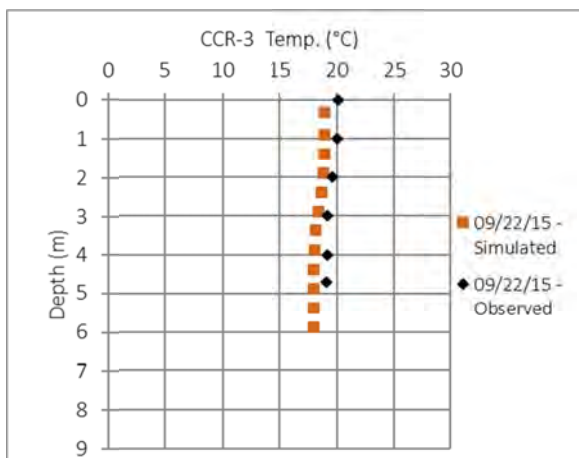
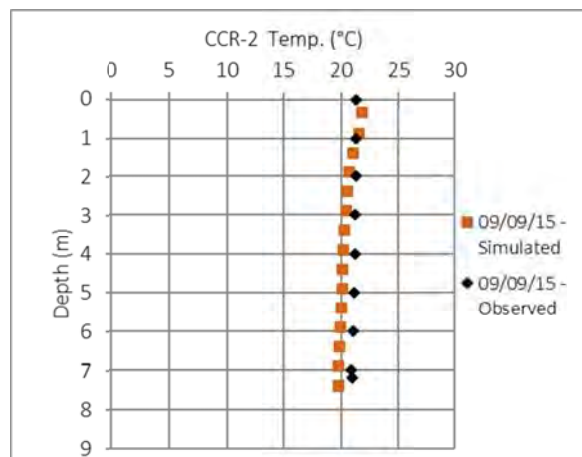
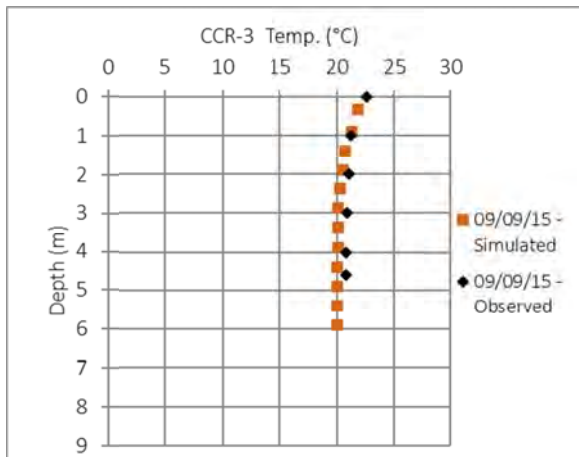
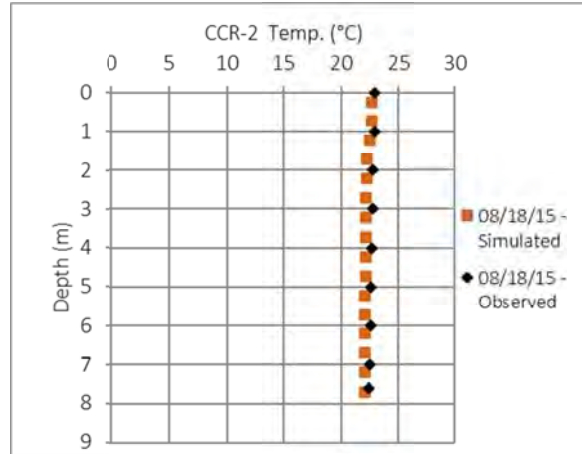
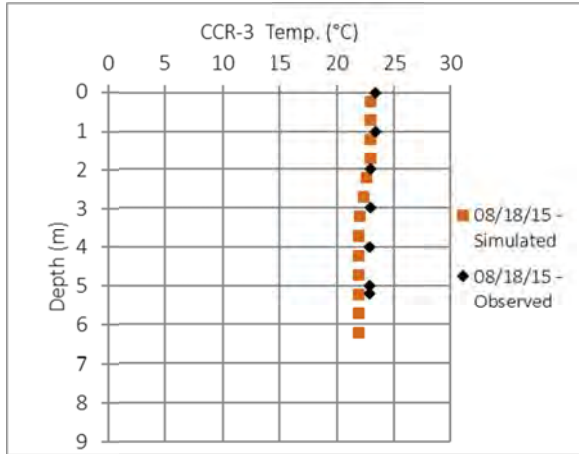


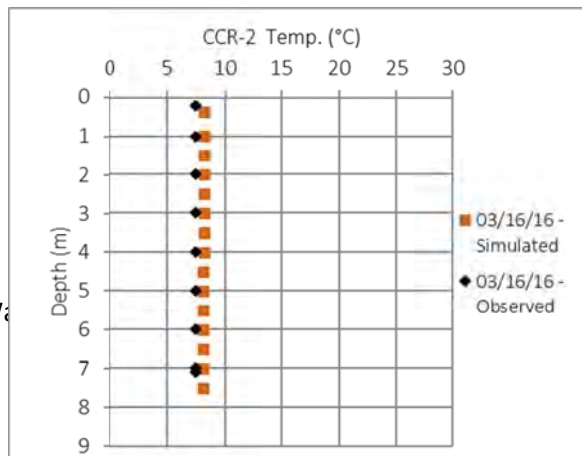
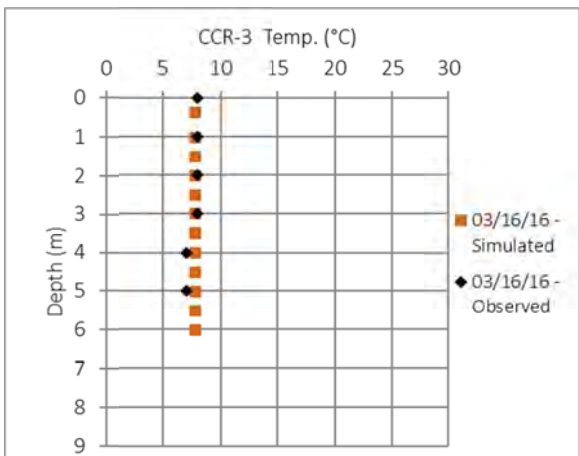
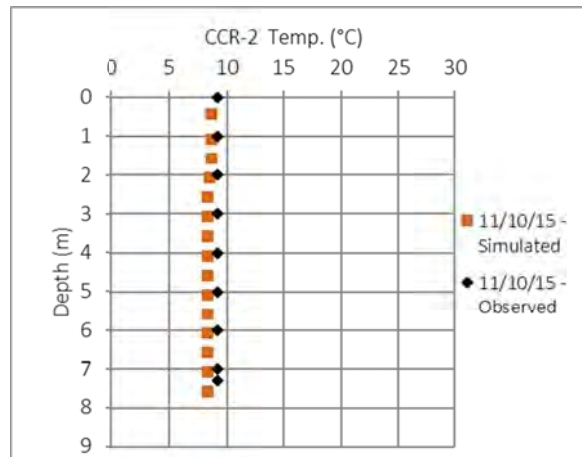
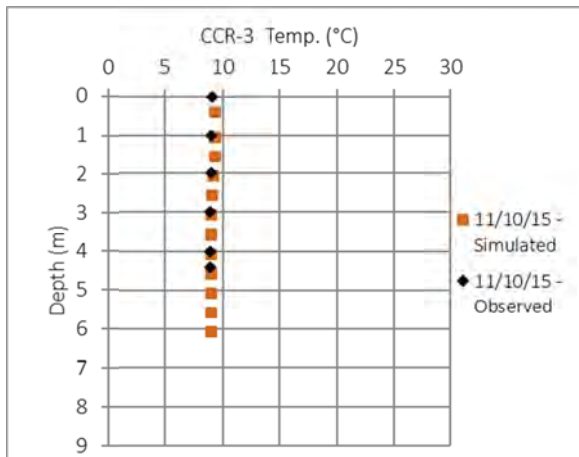
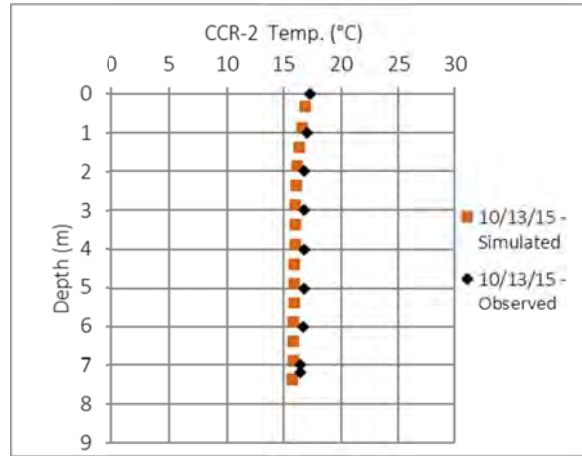
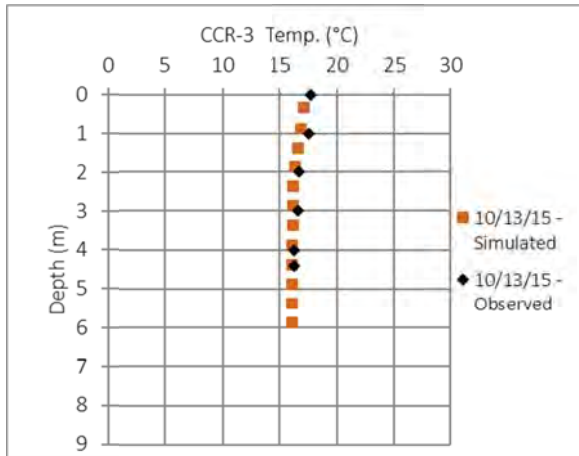


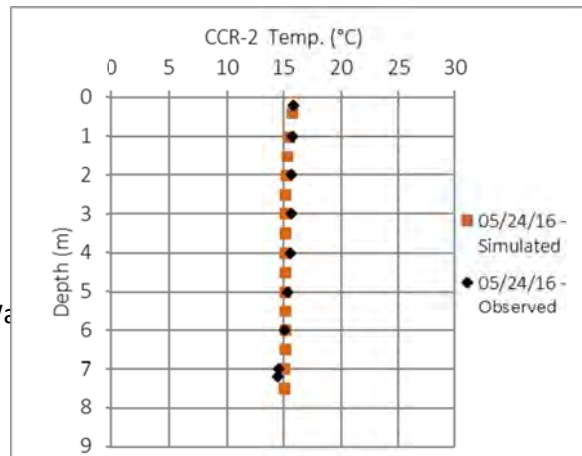
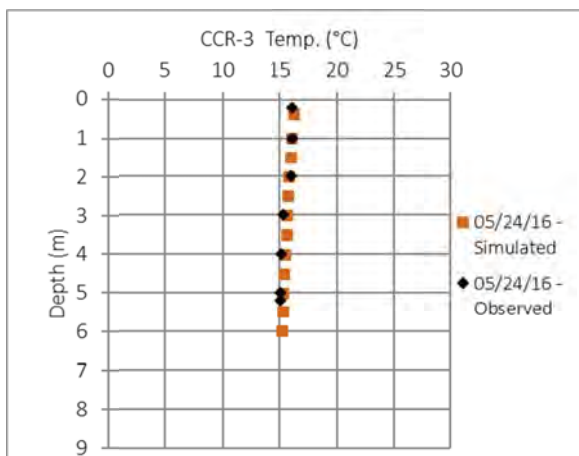
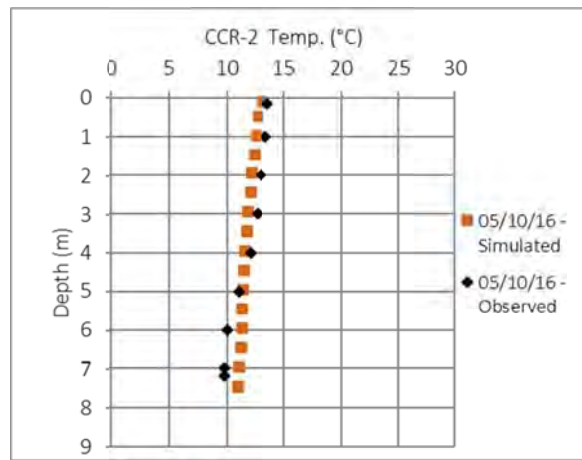
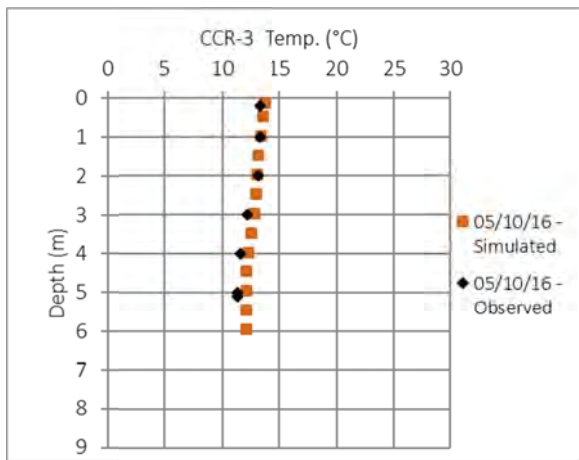
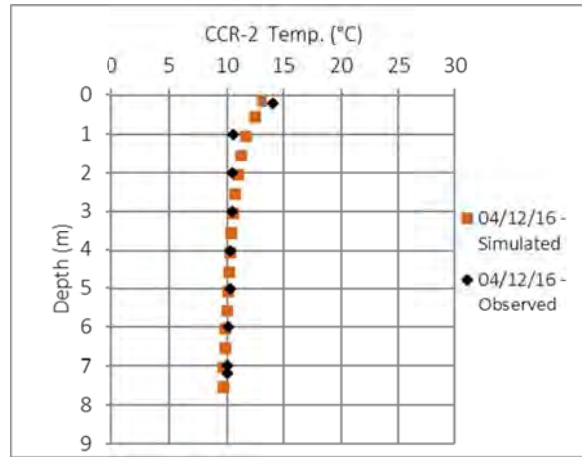
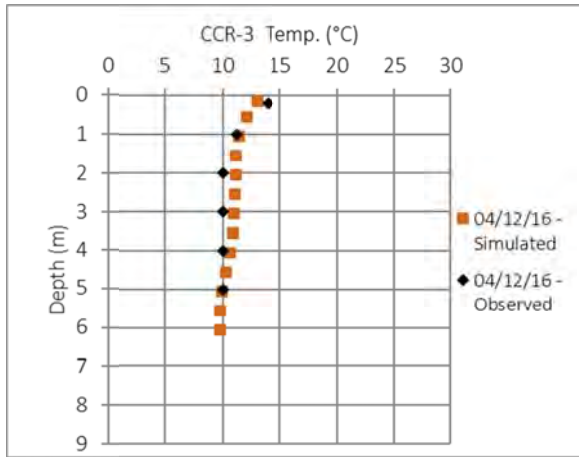
3 Wa



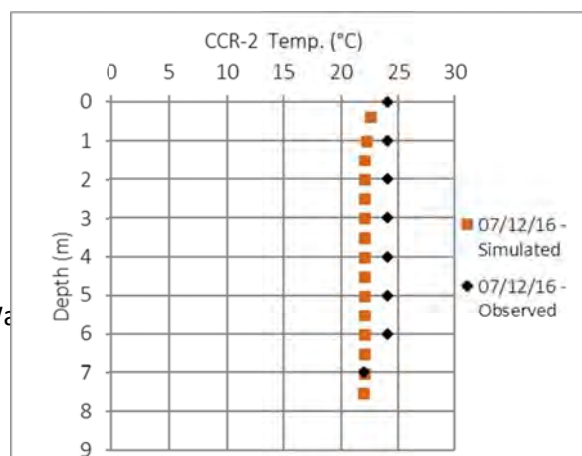
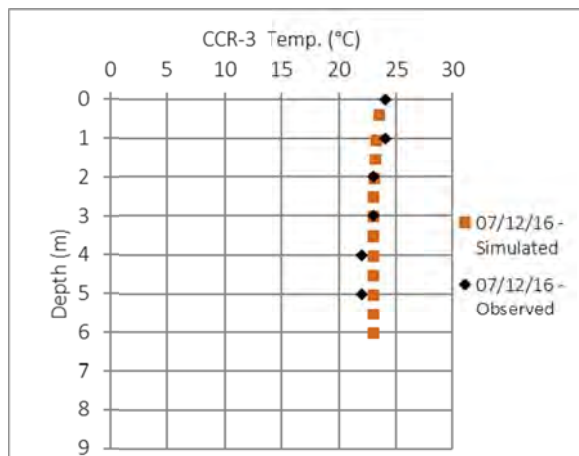
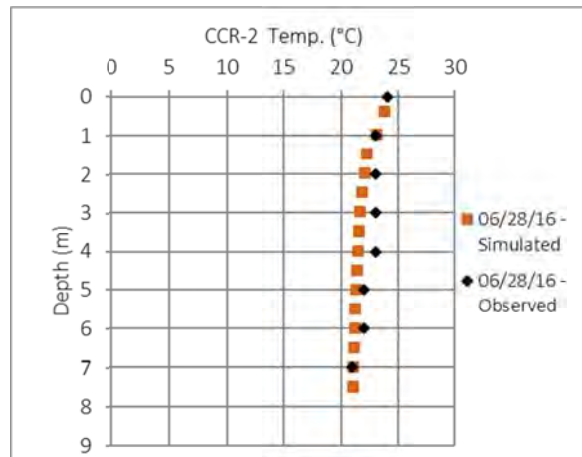
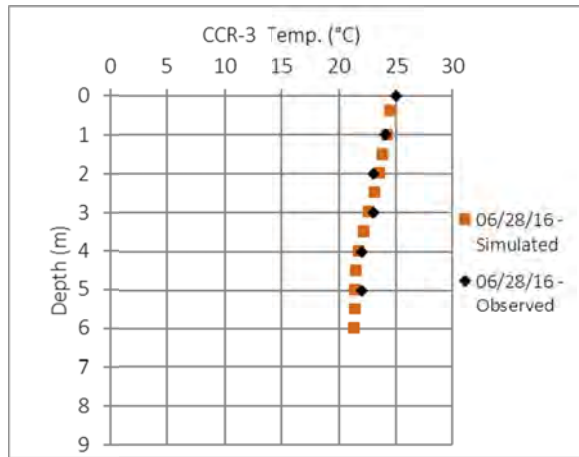
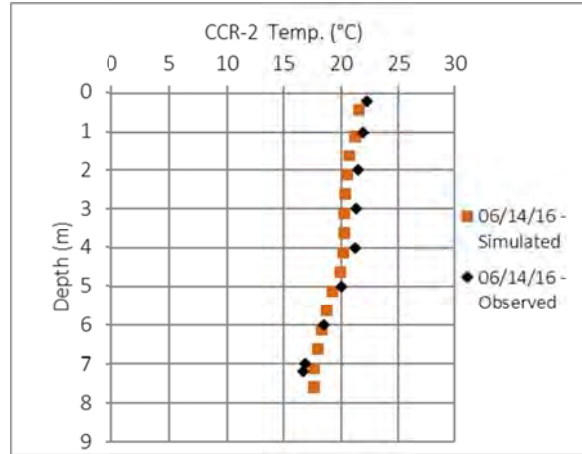
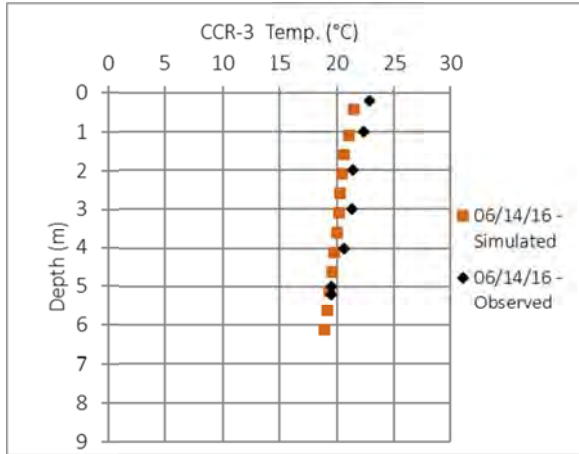
3 Wa

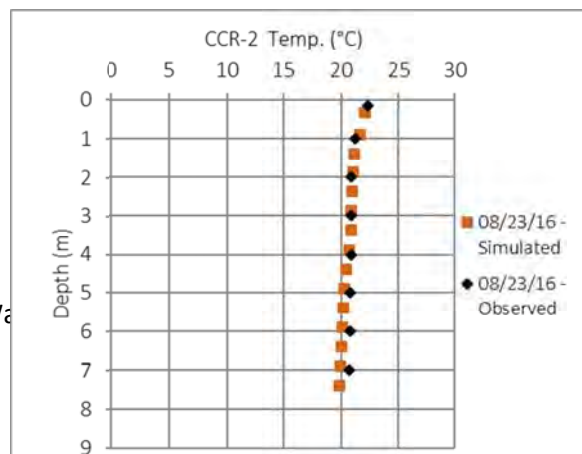
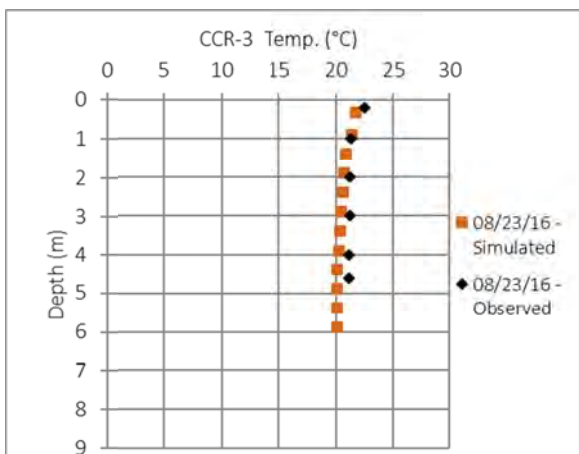
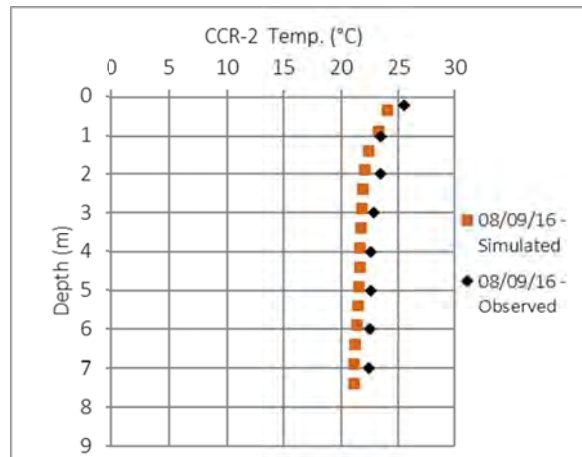
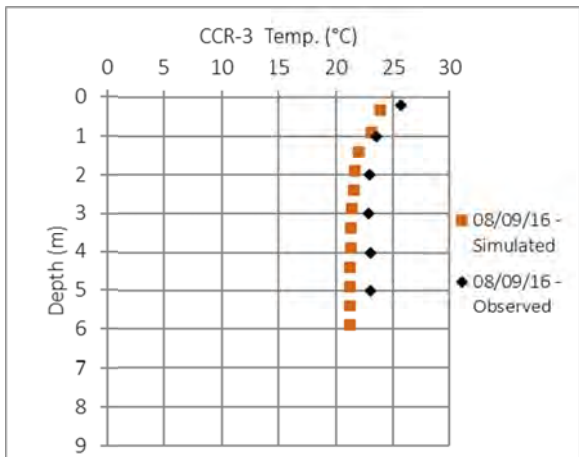
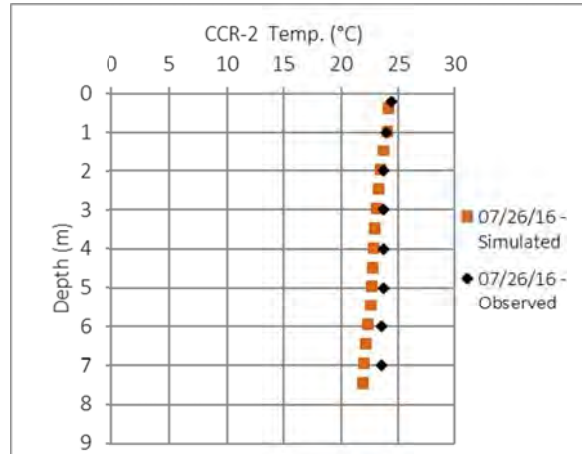
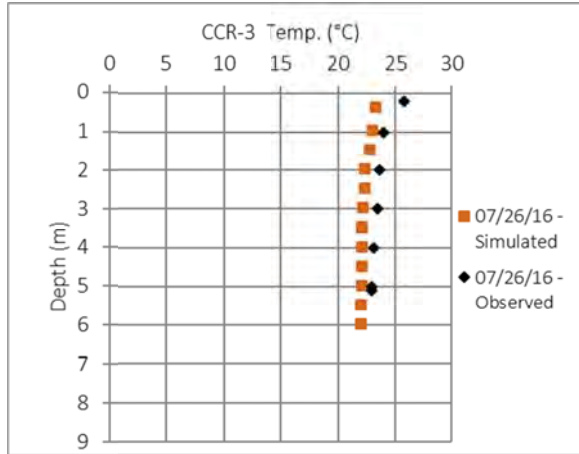




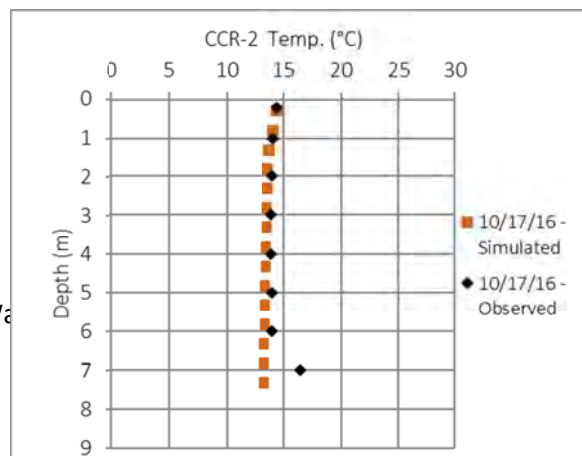
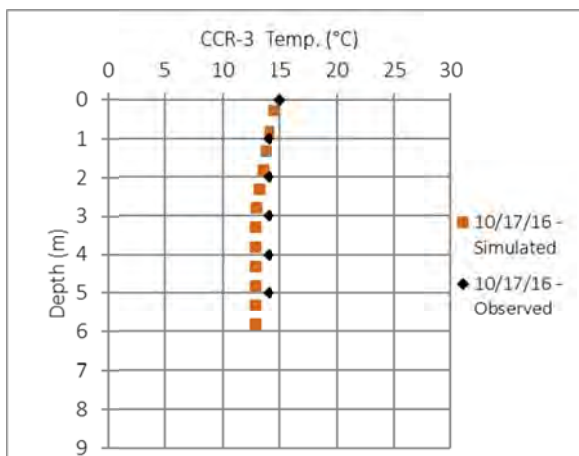
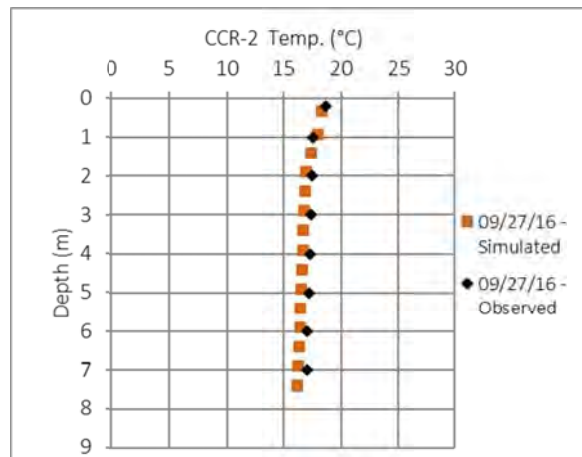
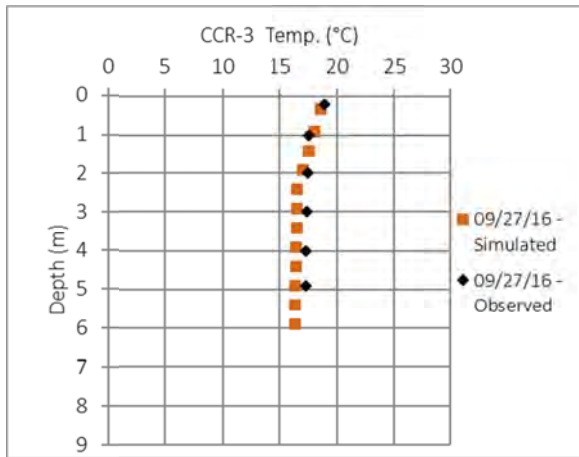
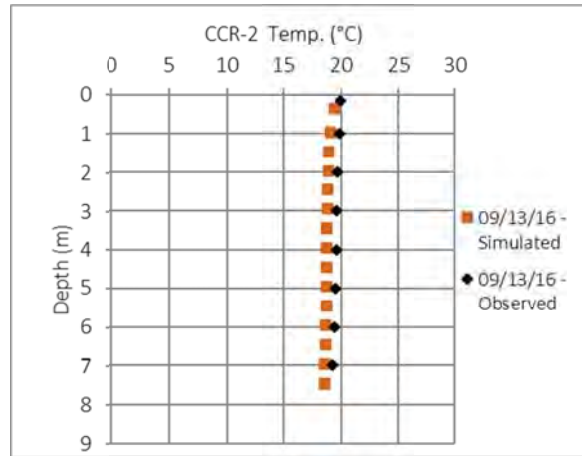
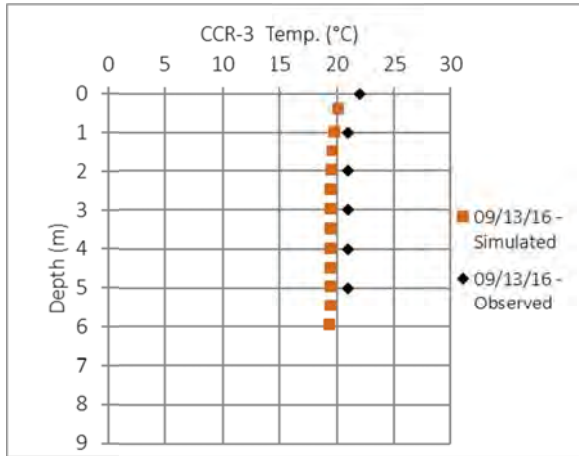


3 Wa

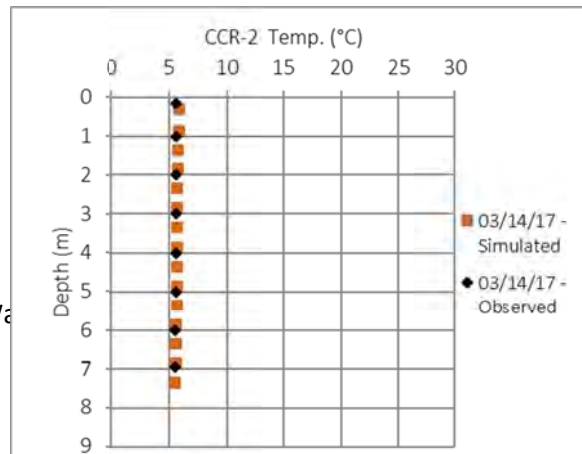
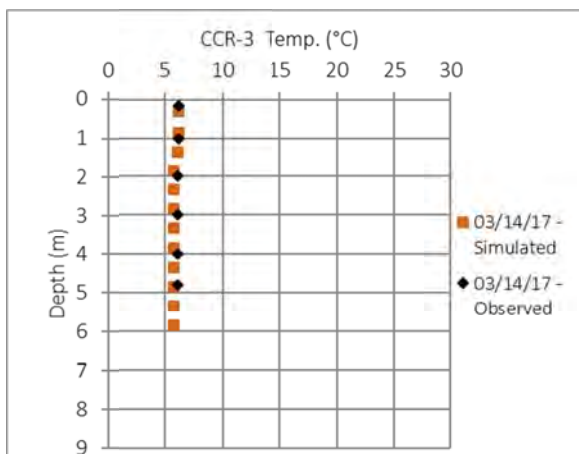
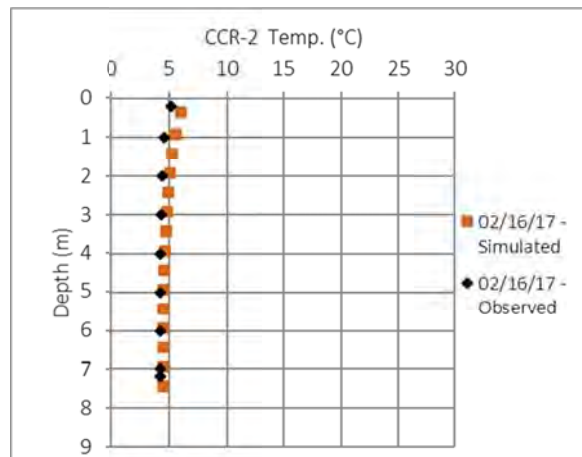
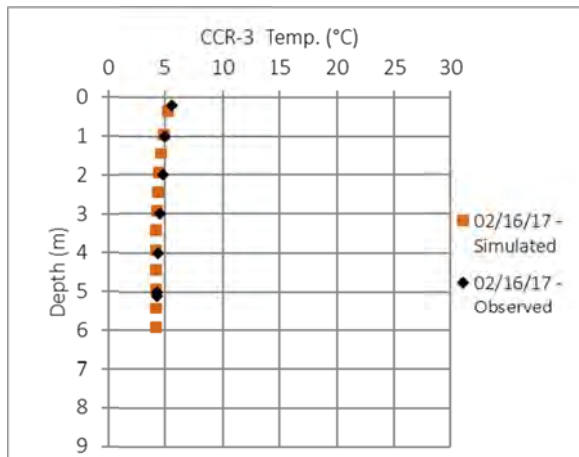
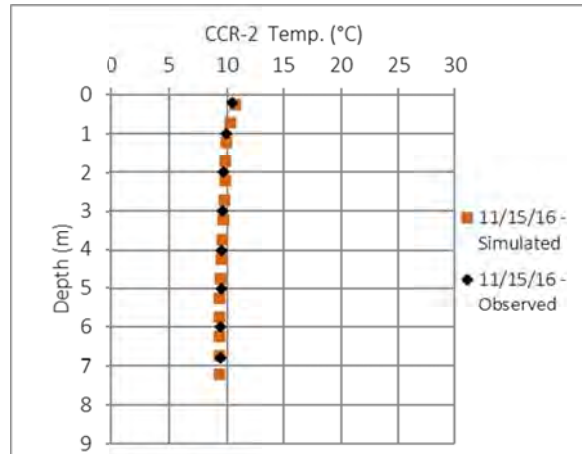
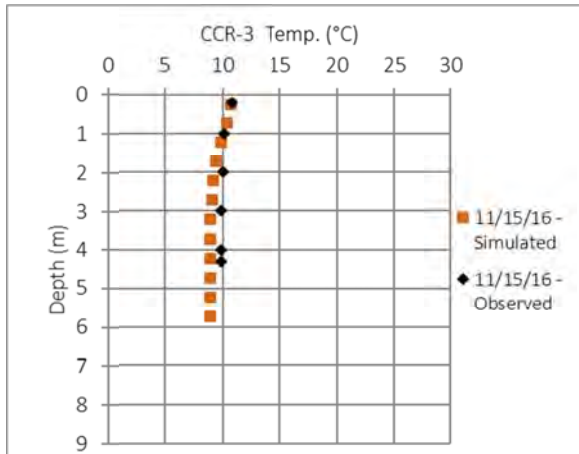




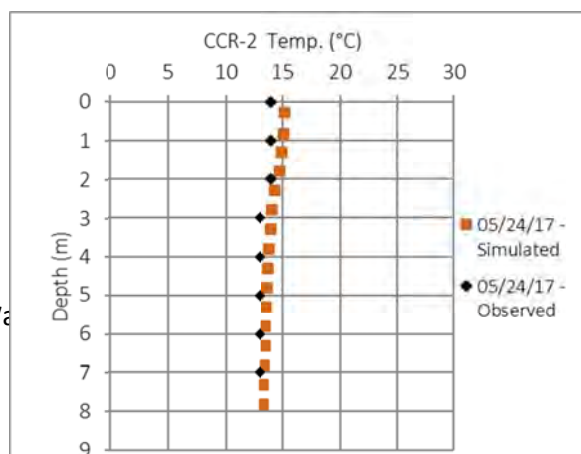
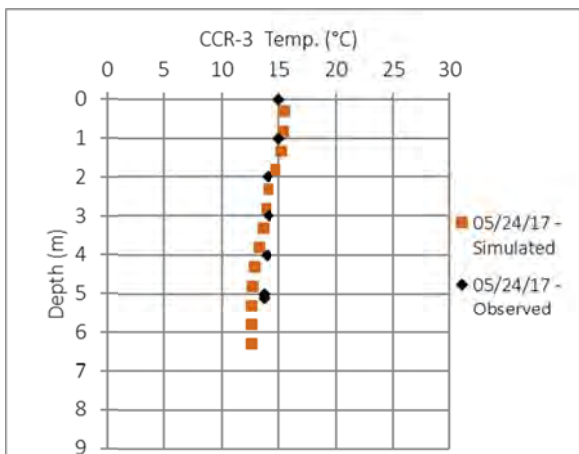
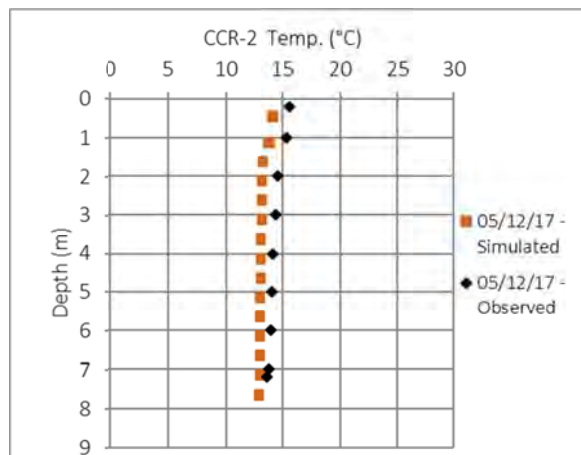
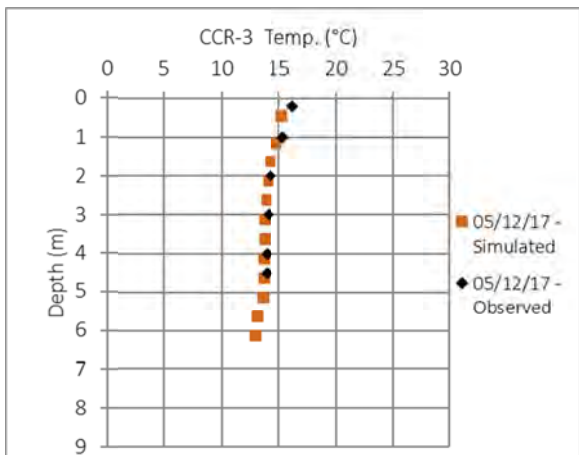
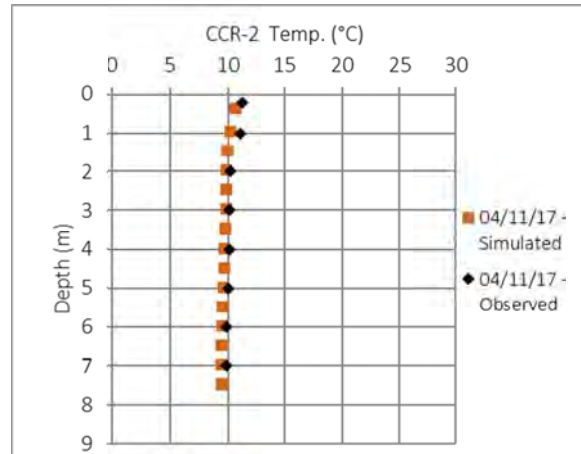
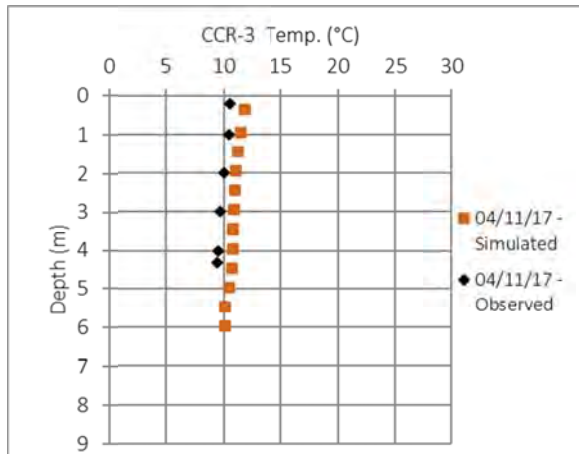
3 Wa



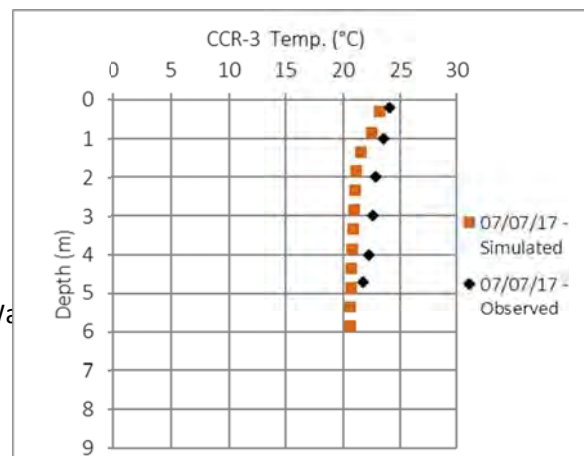
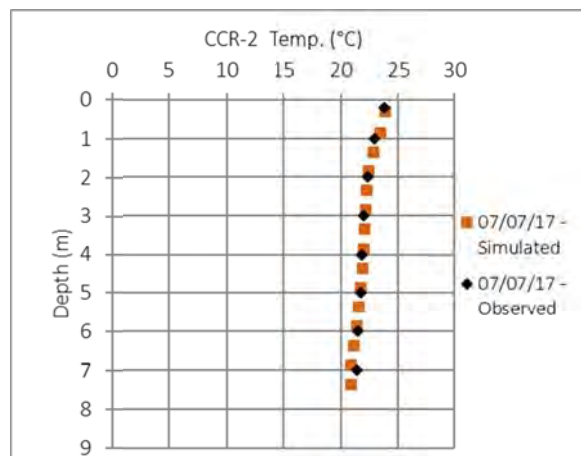
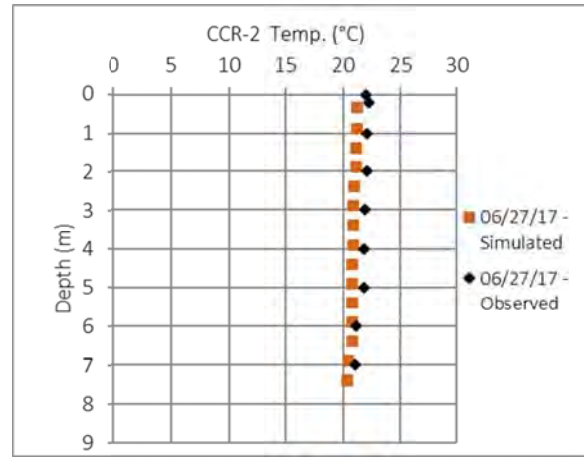
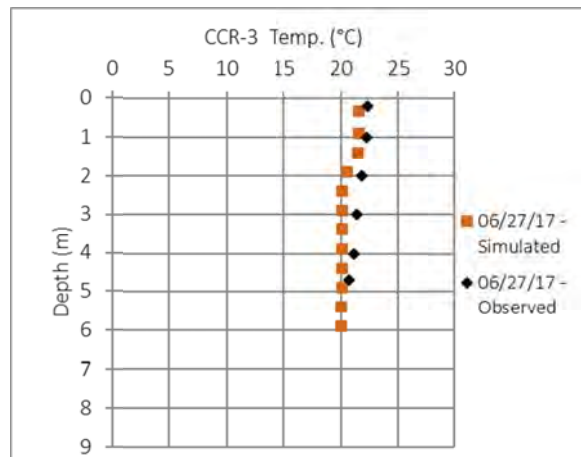
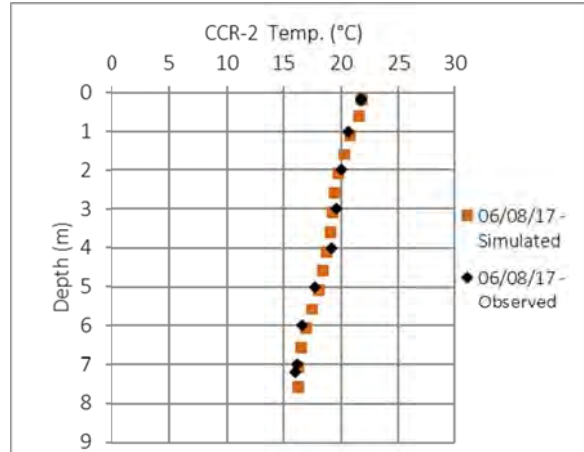
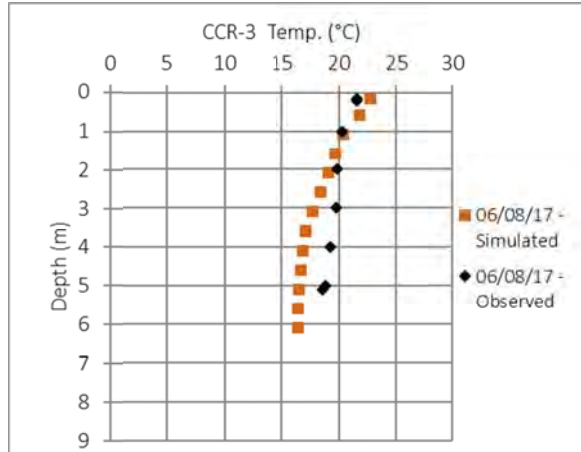
3 Wa



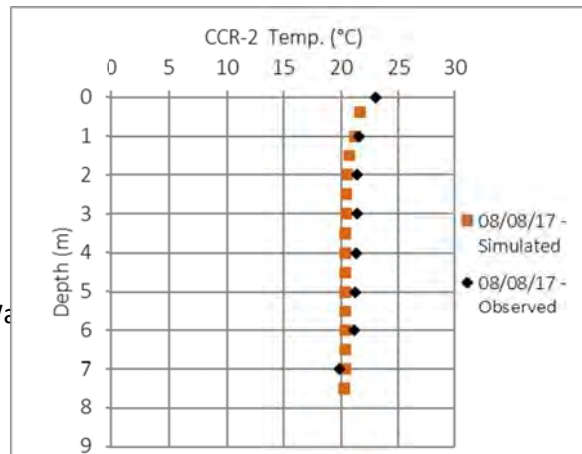
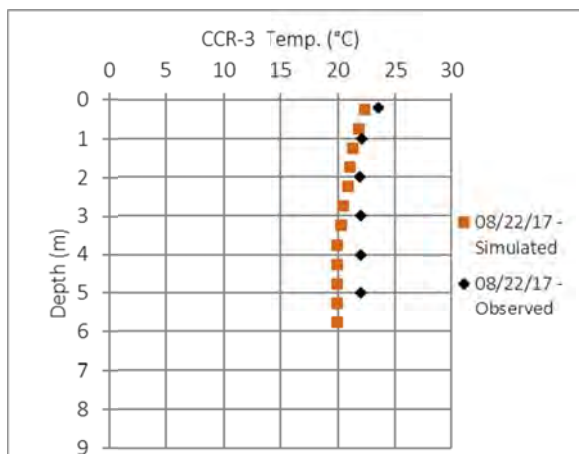
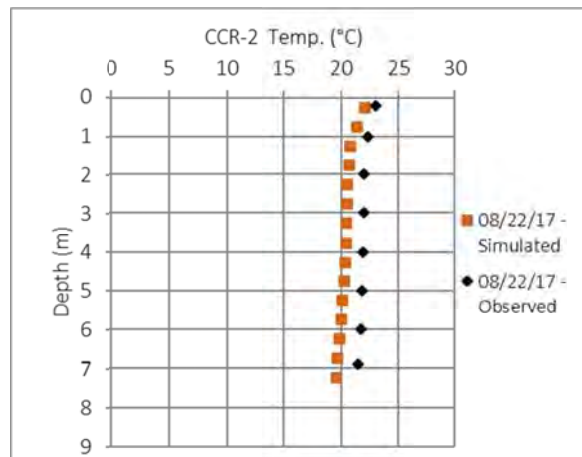
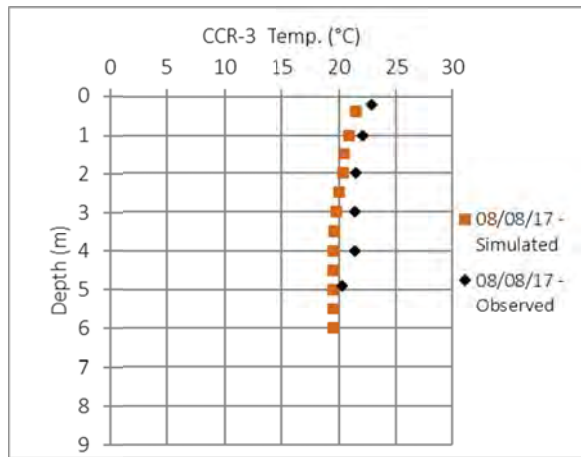
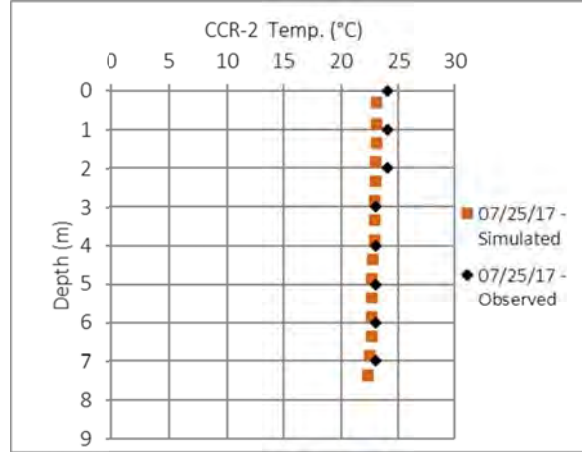
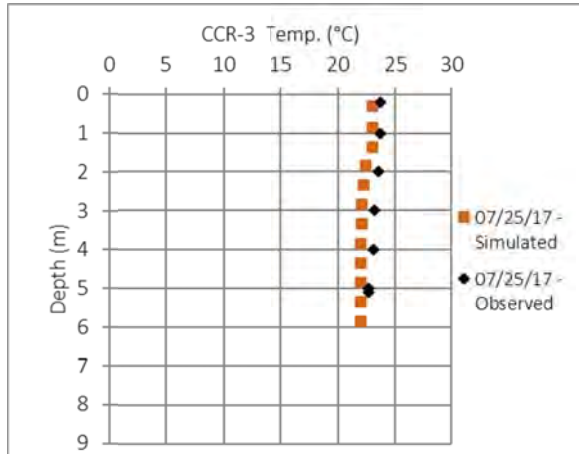
3 Wa



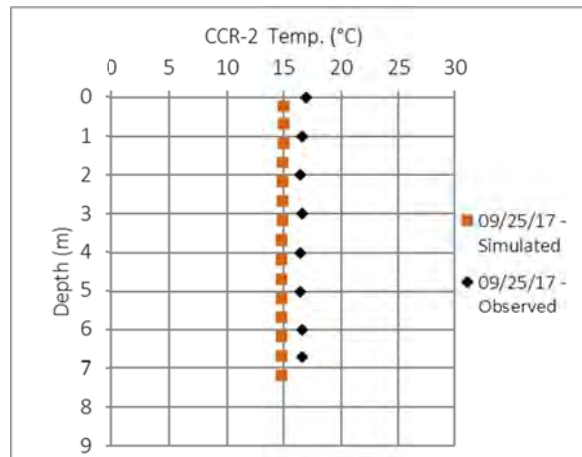
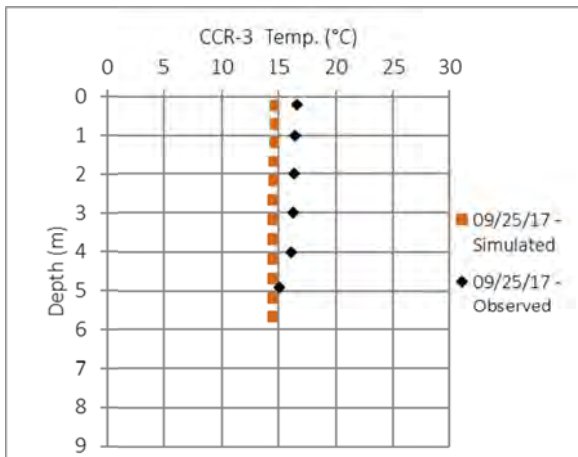
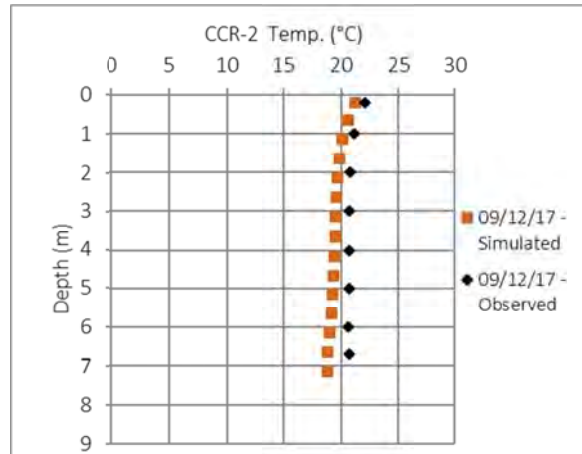
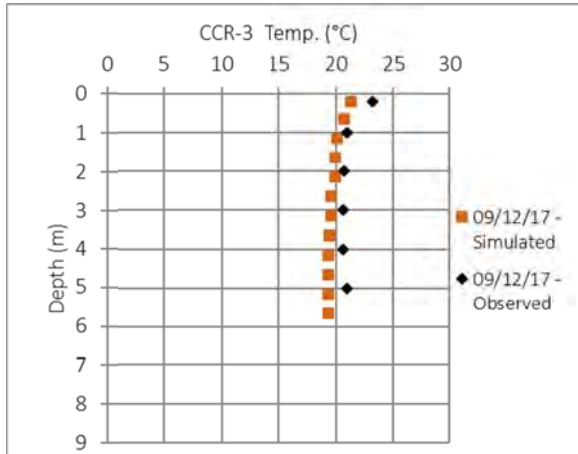
3 Wa



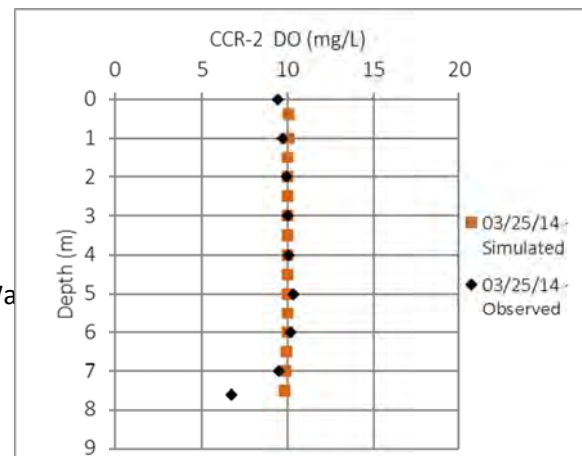
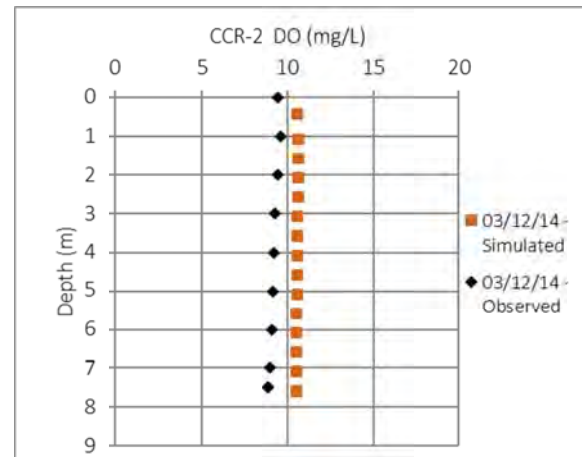
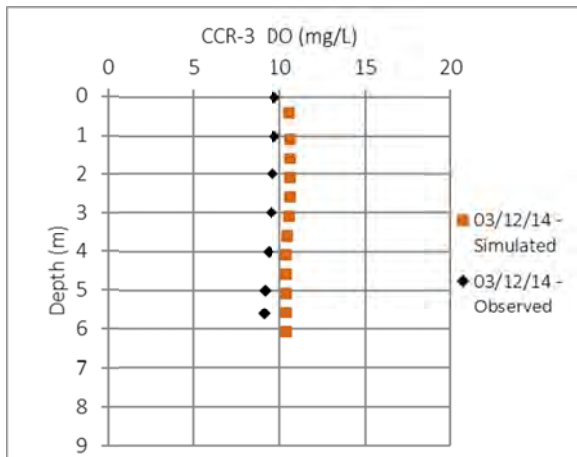
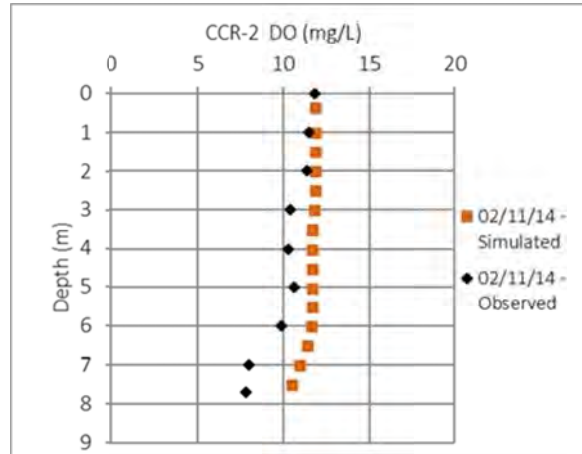
3 Wa

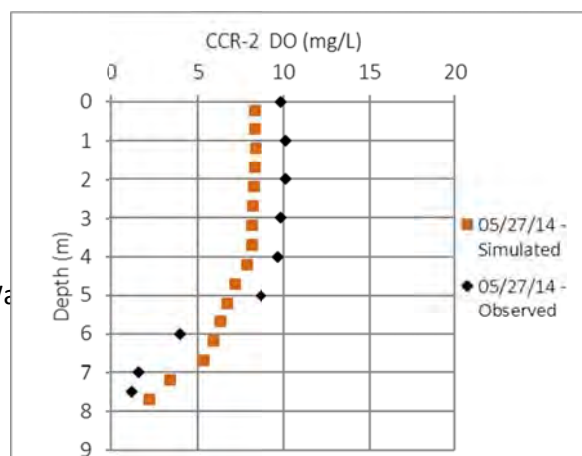
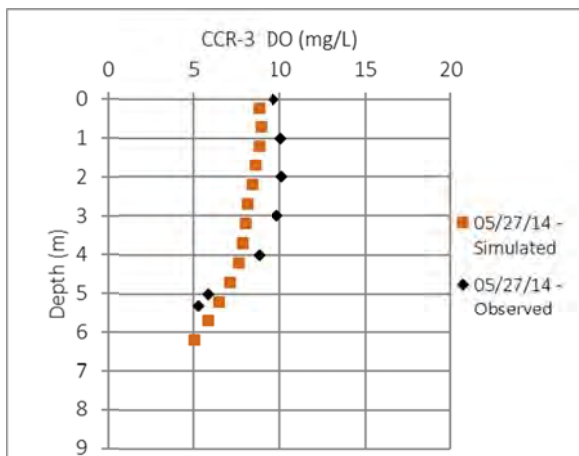
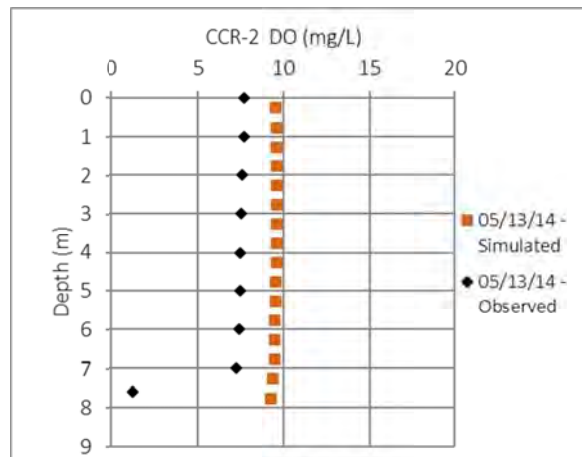
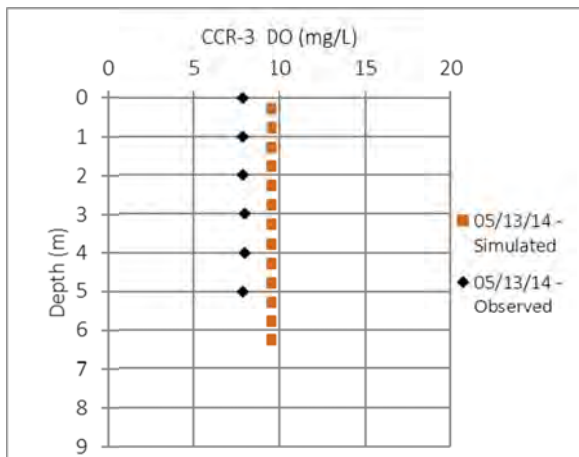
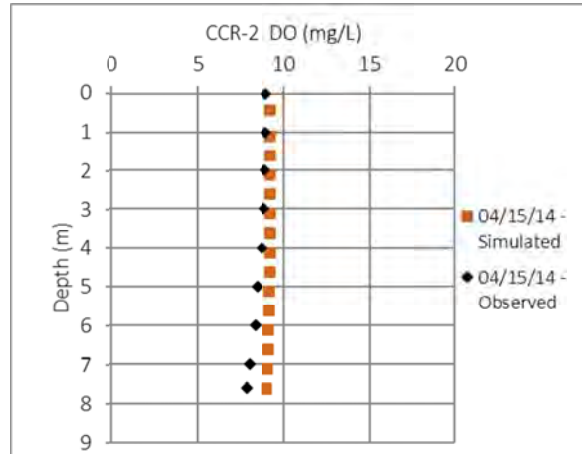
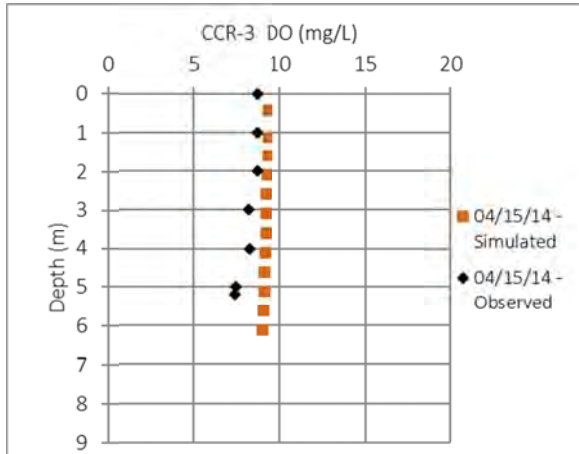


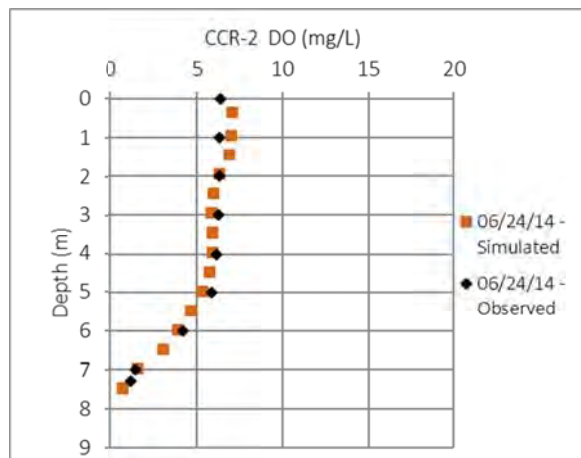
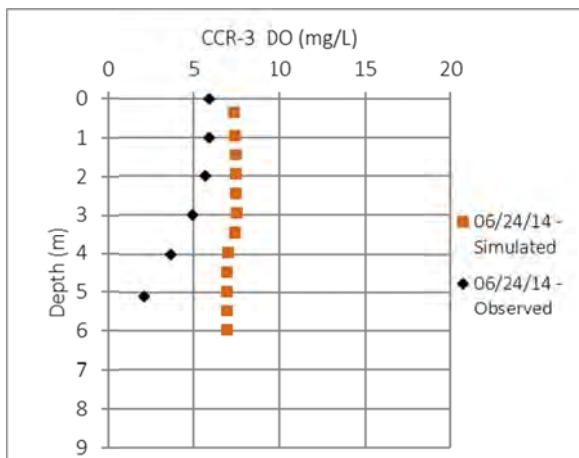
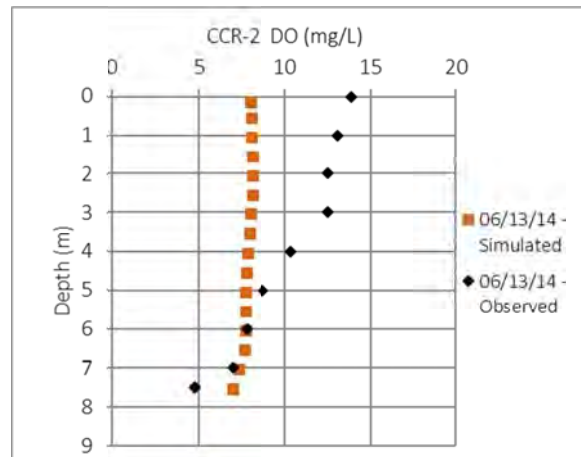
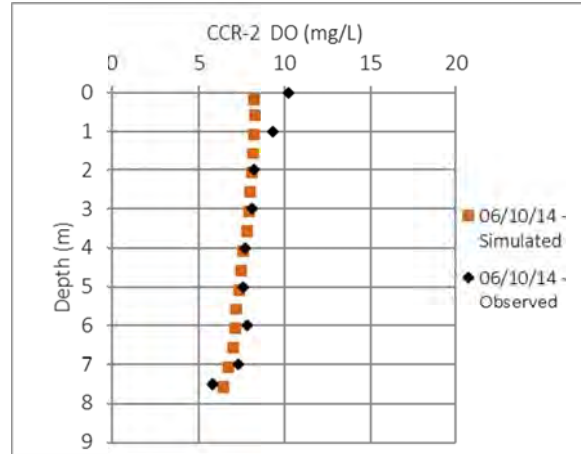
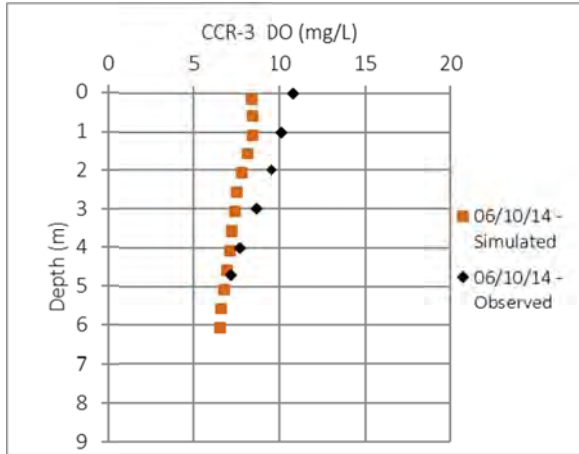
Water

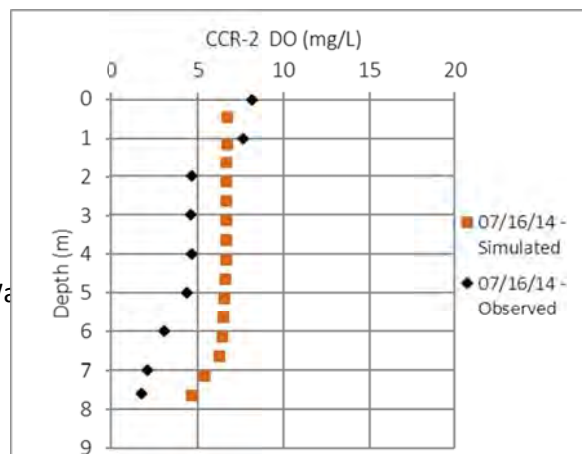
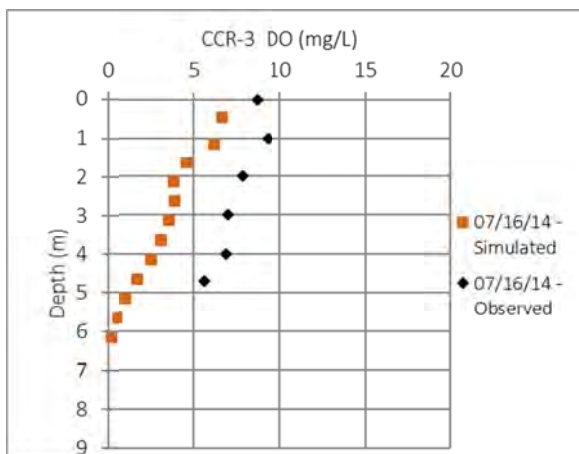
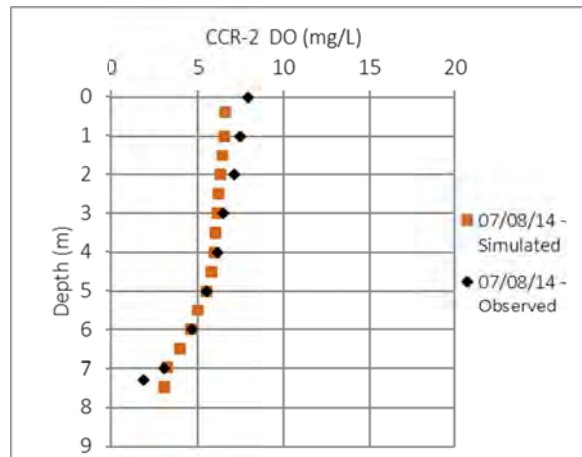
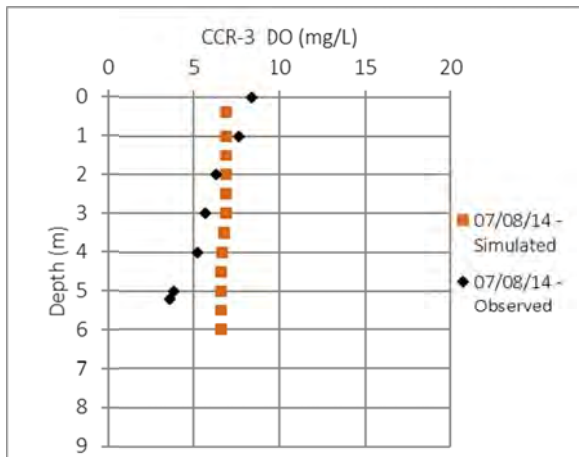
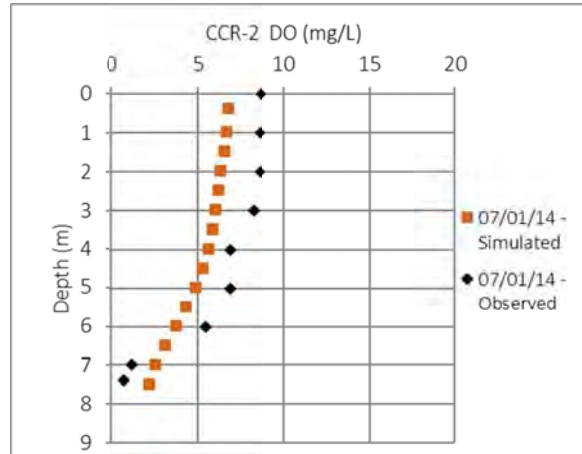
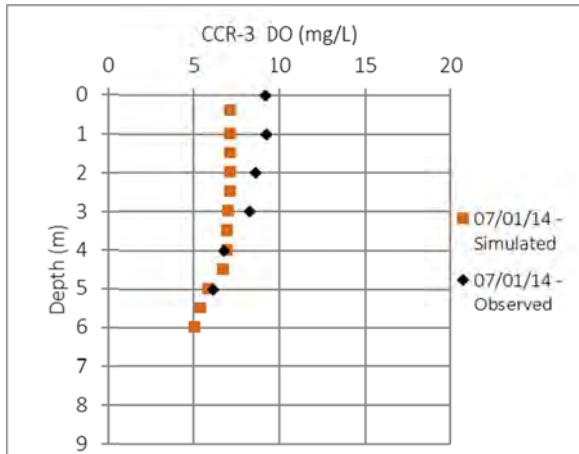


Attachment B: Dissolved Oxygen Calibration: Observed and Simulated Results

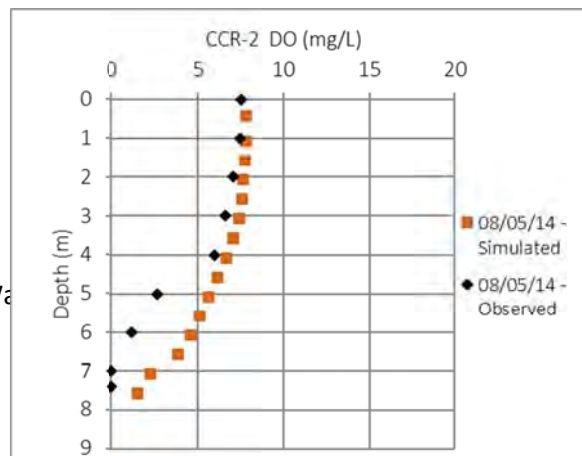
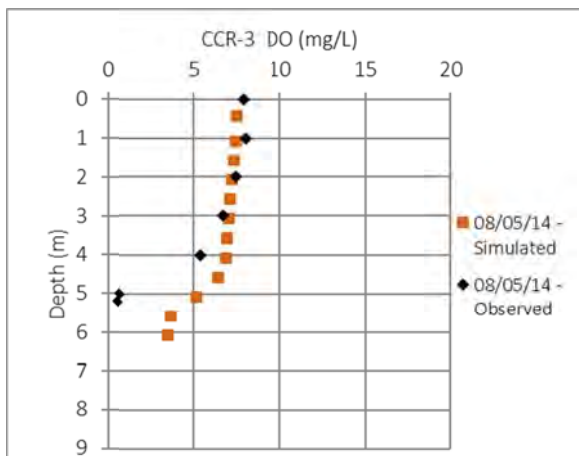
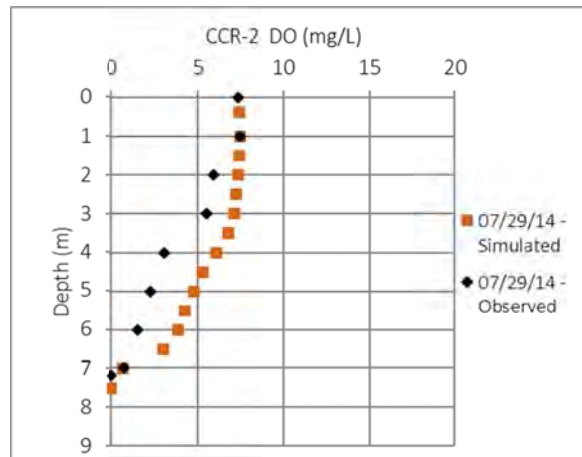
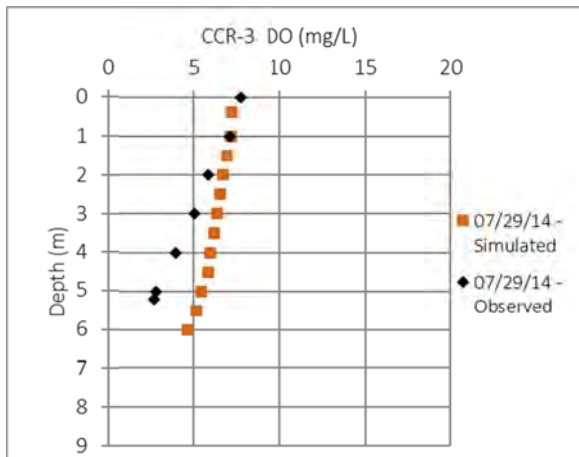
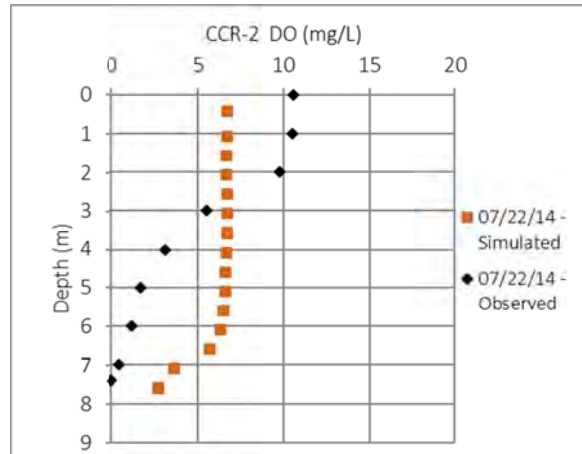
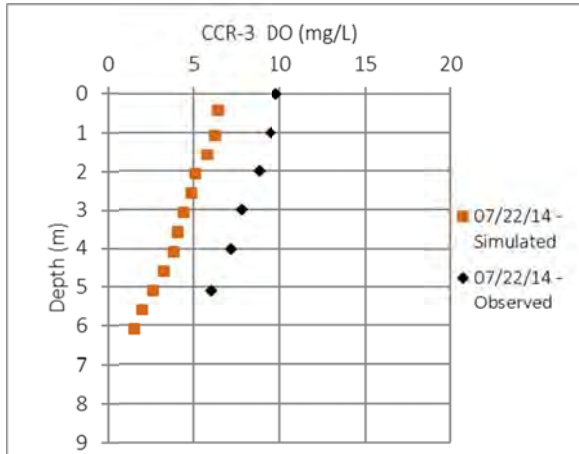




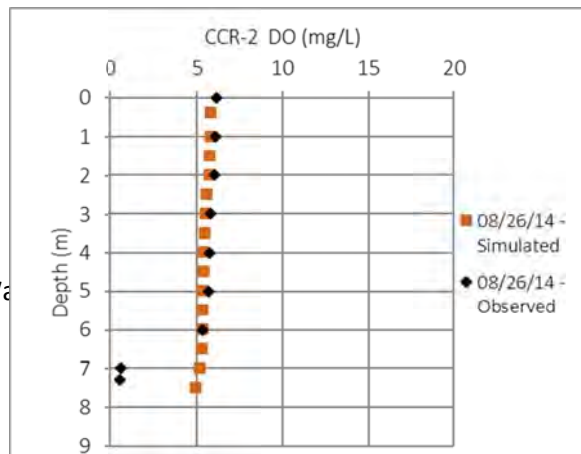
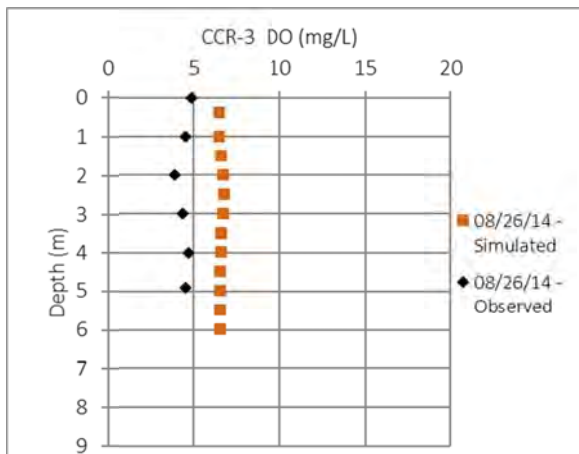
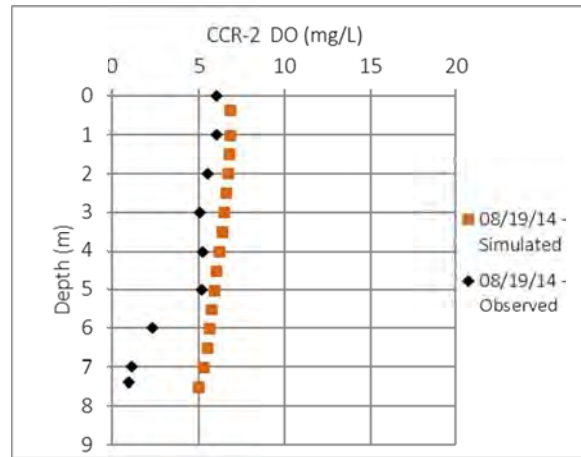
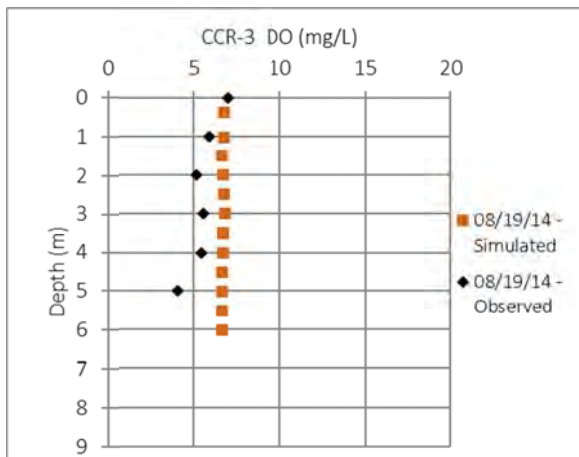
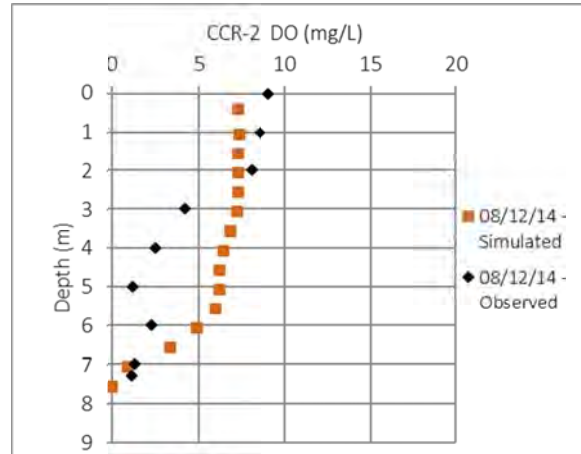
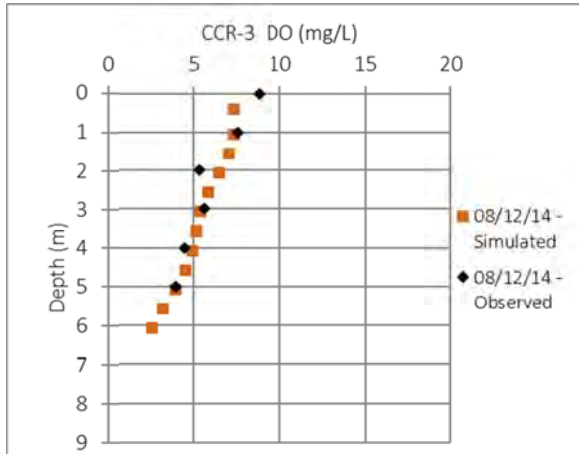




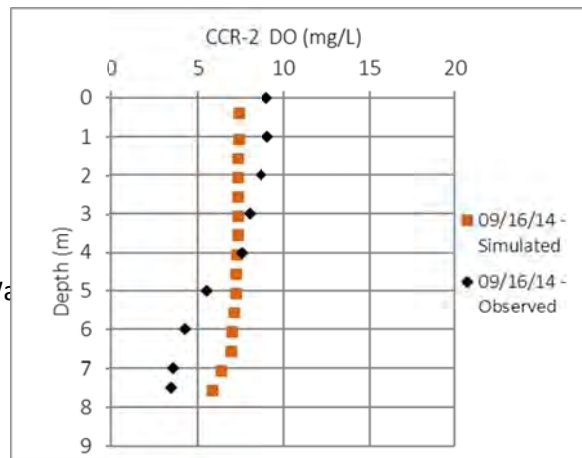
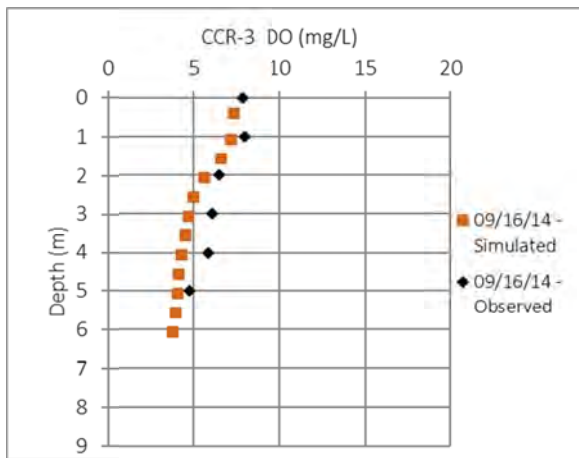
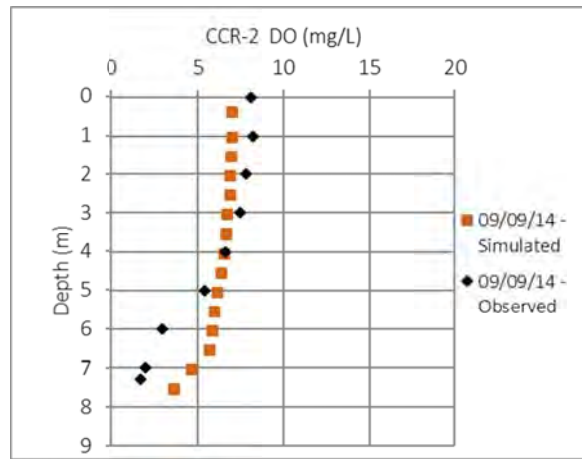
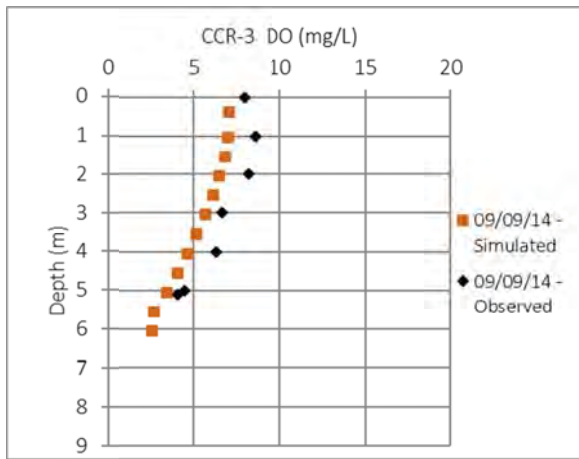
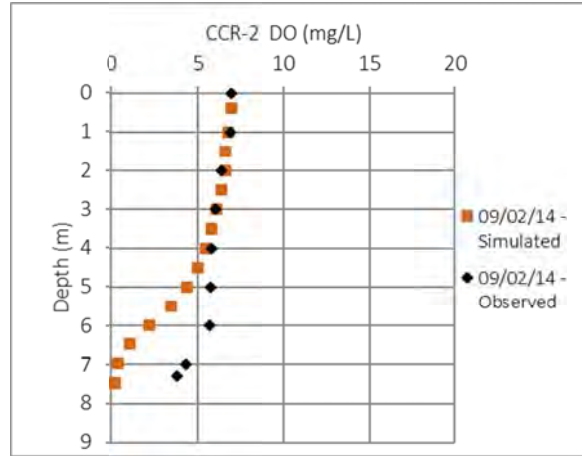
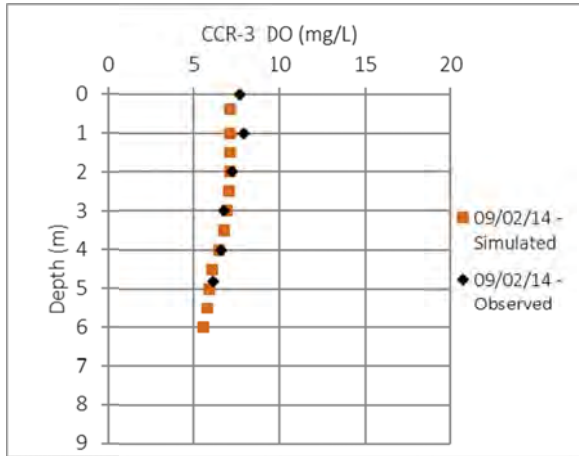
3 Wa



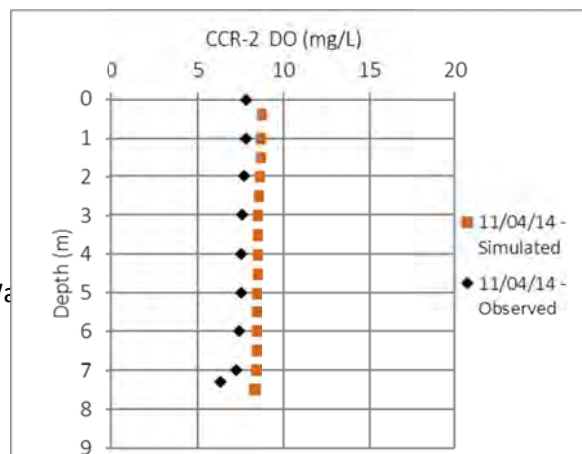
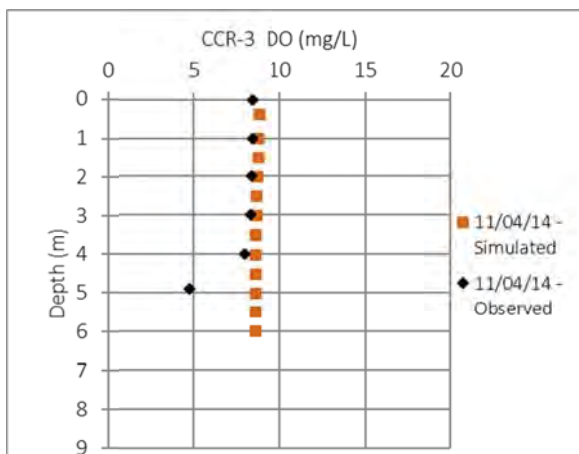
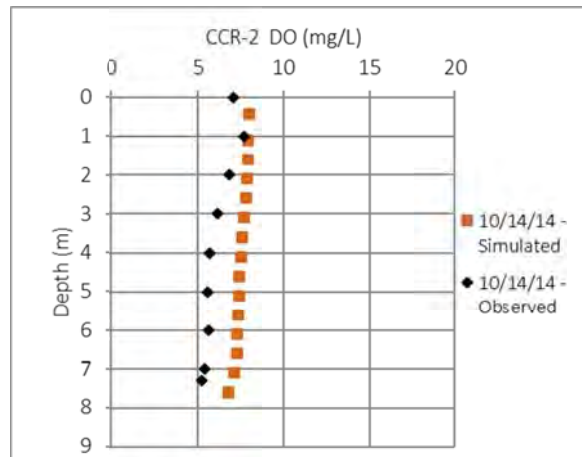
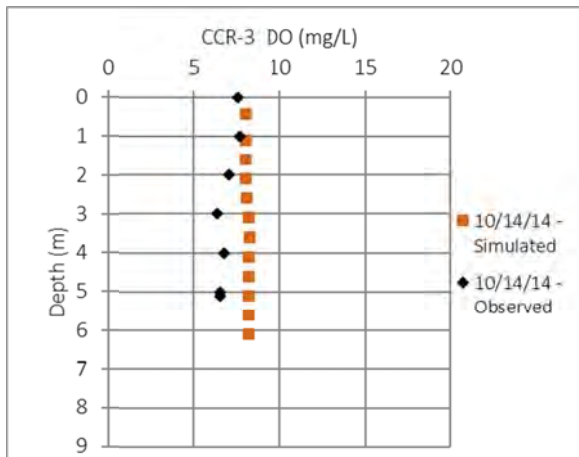
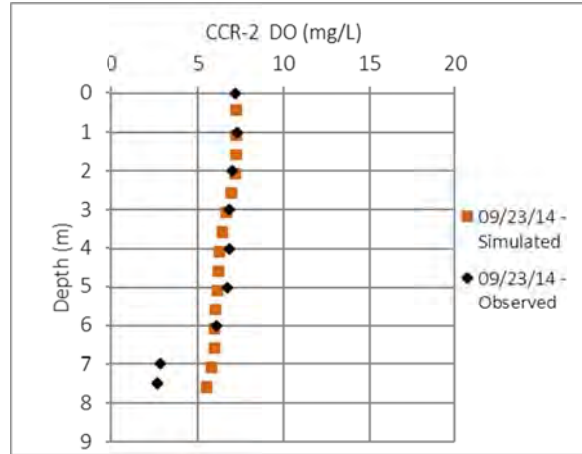
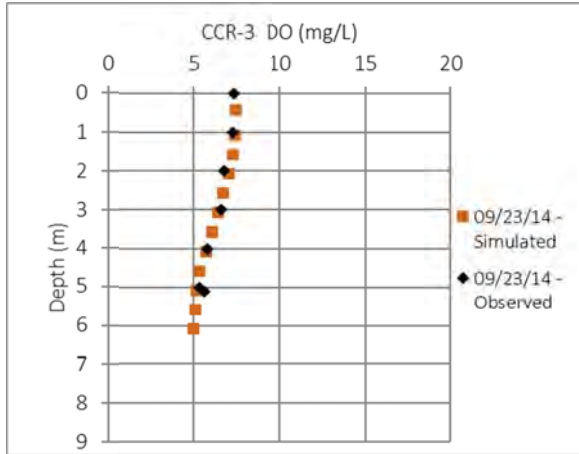
3 Wa



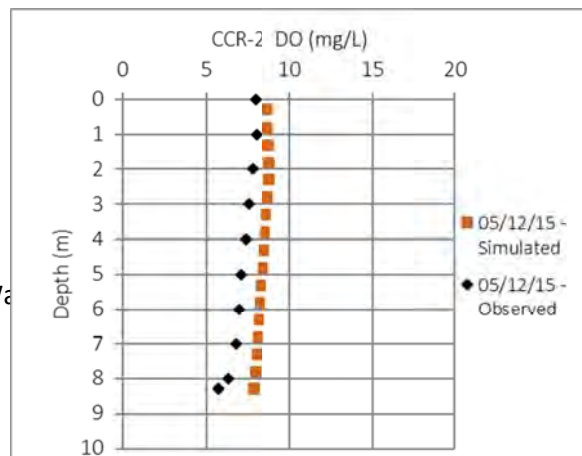
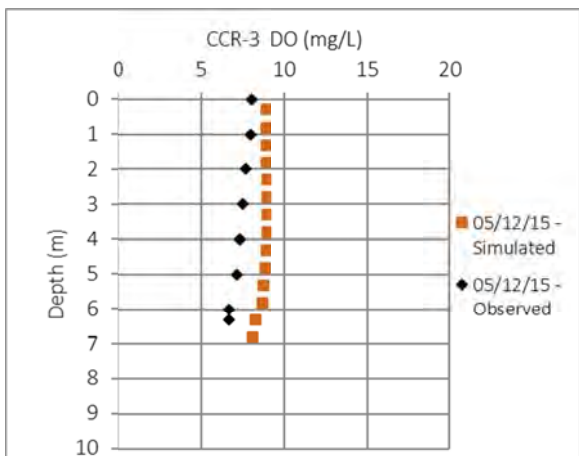
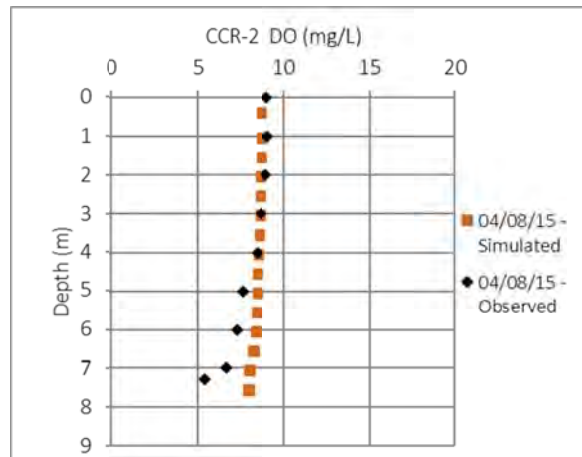
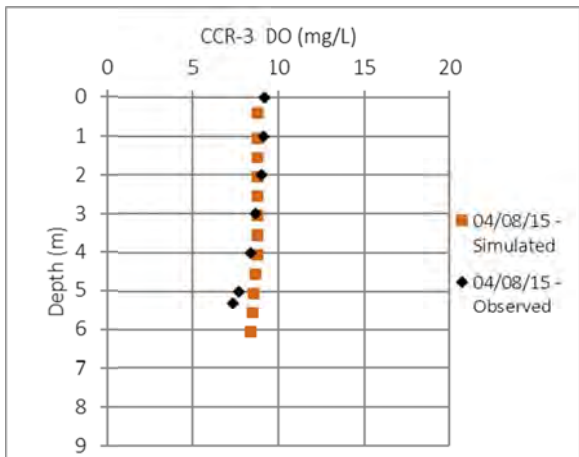
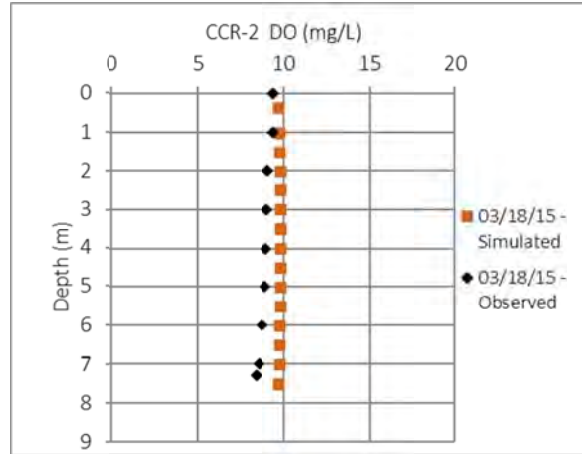
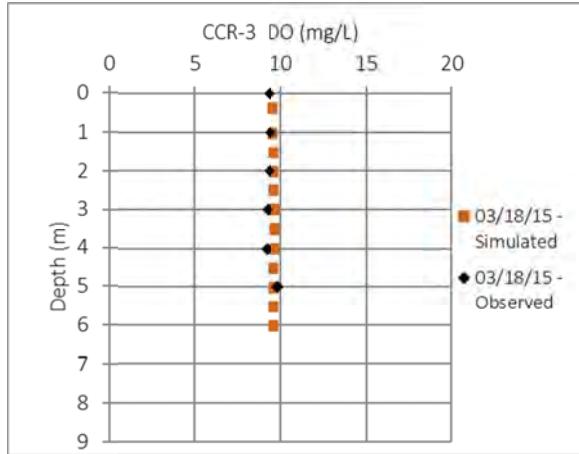
3 Wa



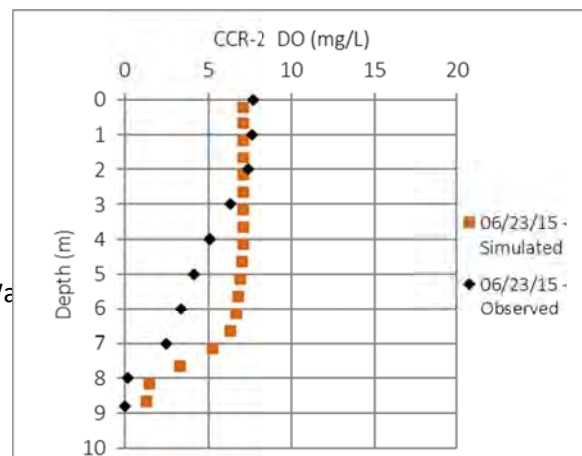
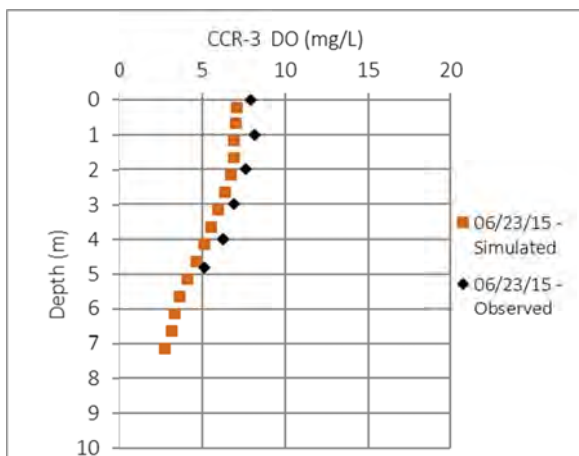
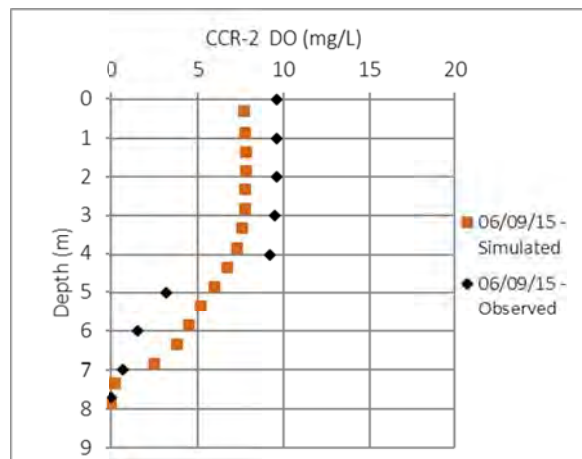
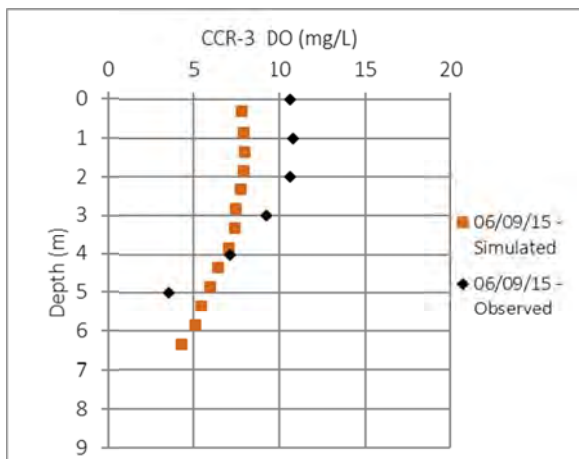
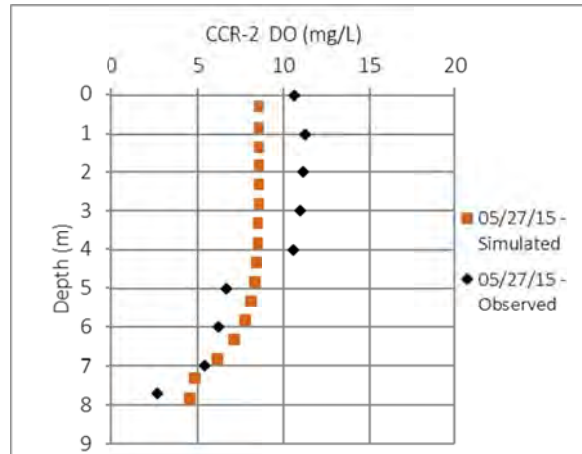
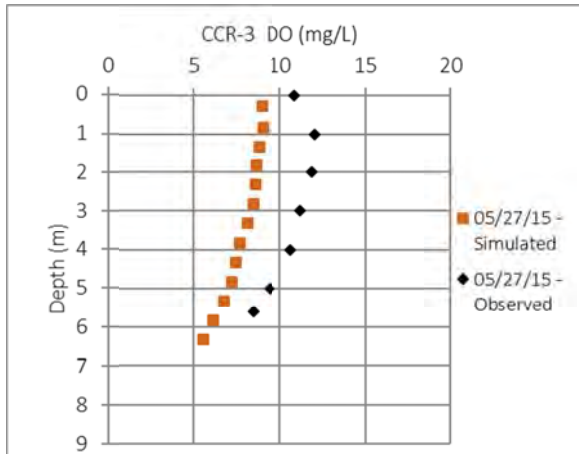
3 Wa



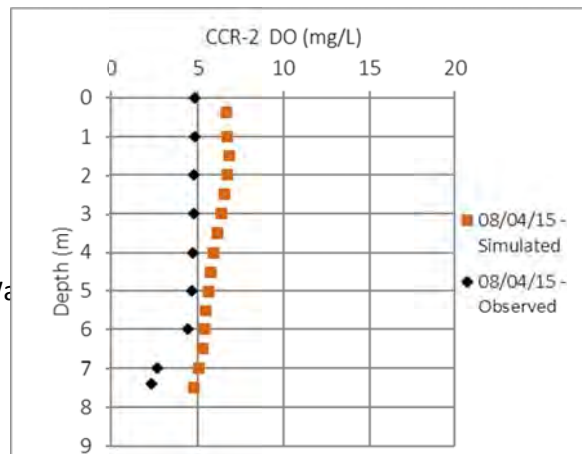
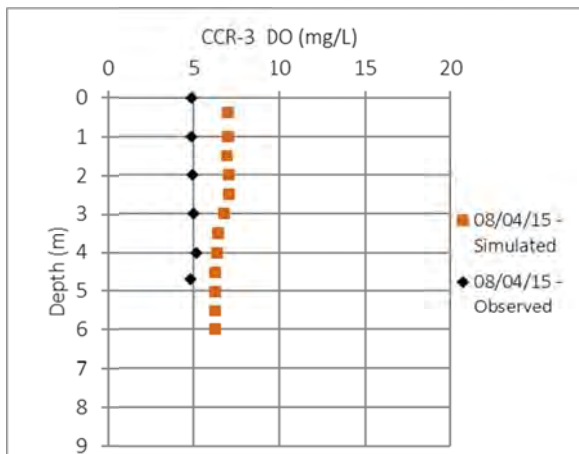
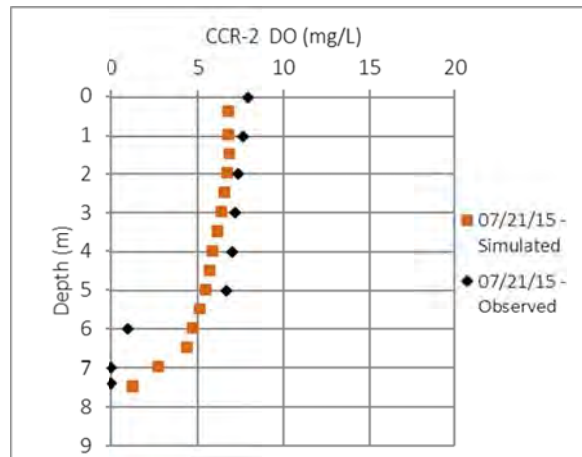
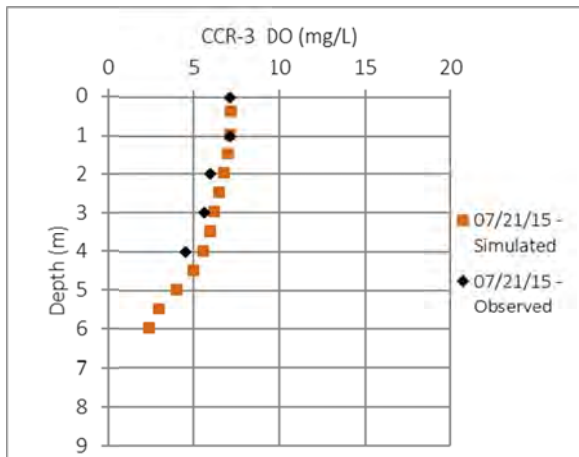
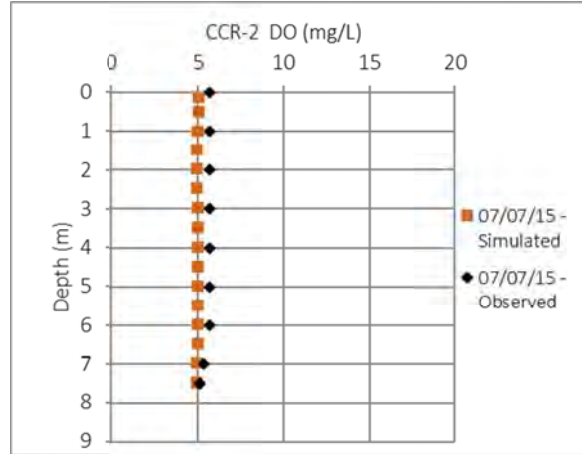
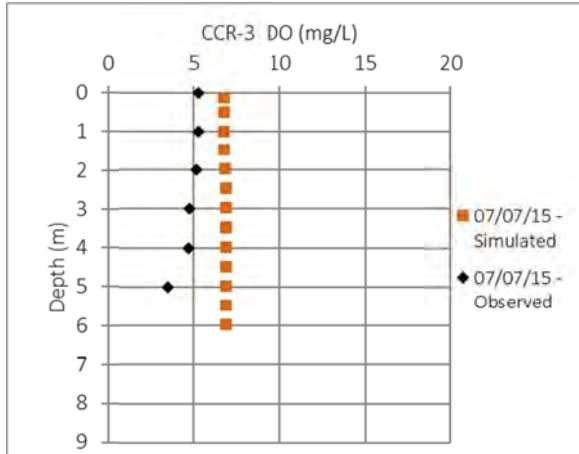
3 Wa



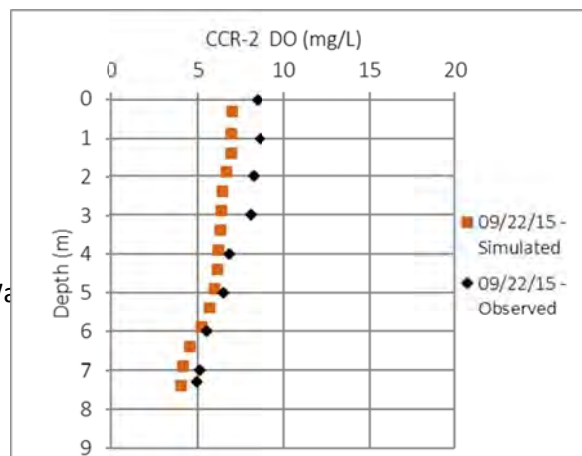
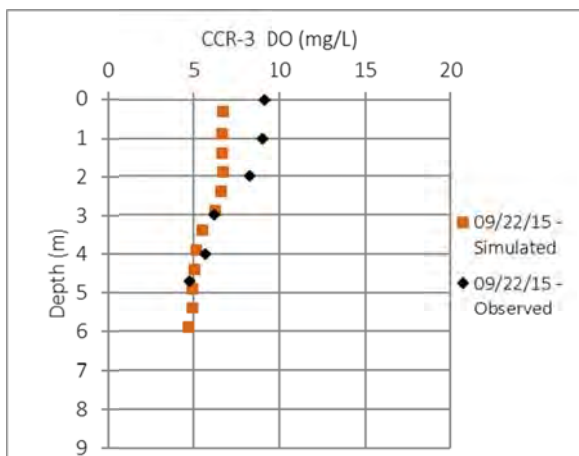
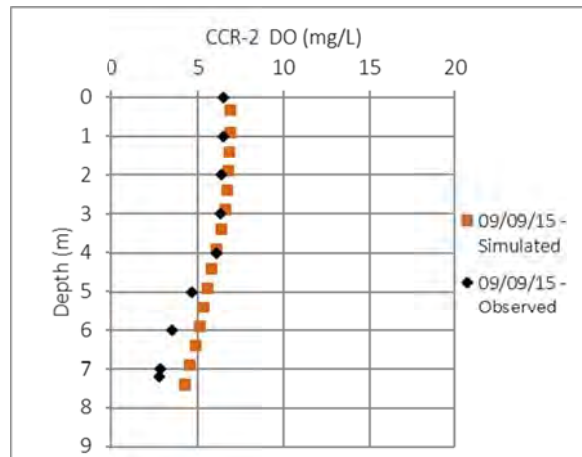
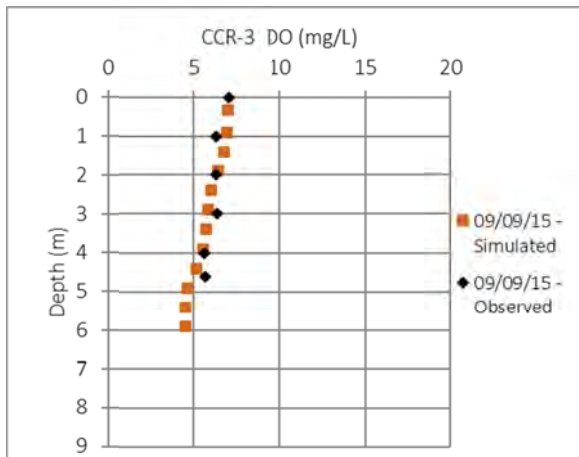
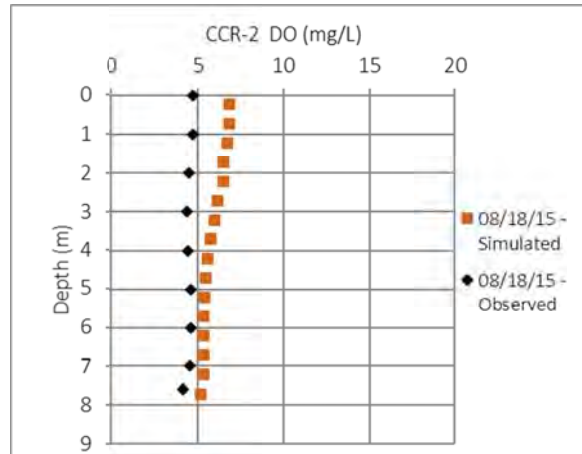
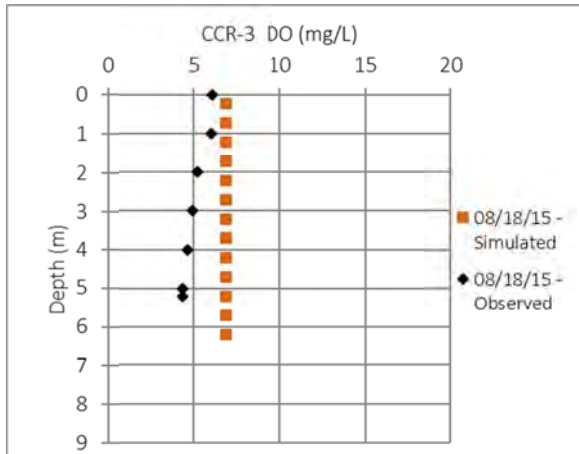
3 Wa



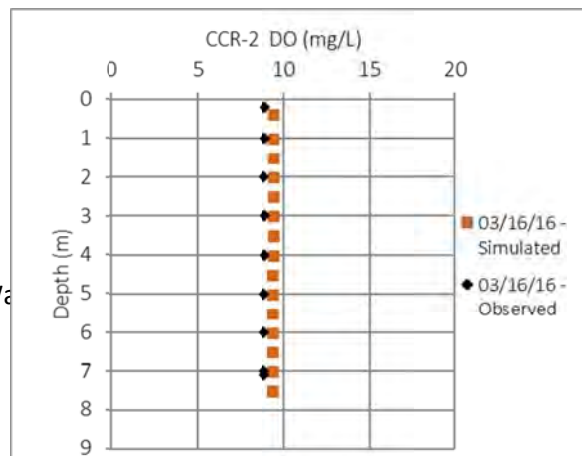
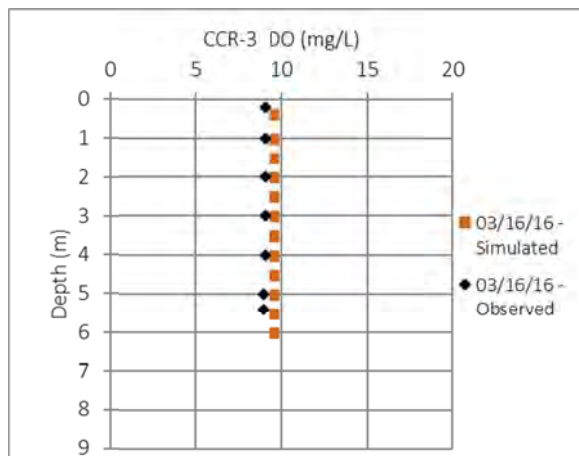
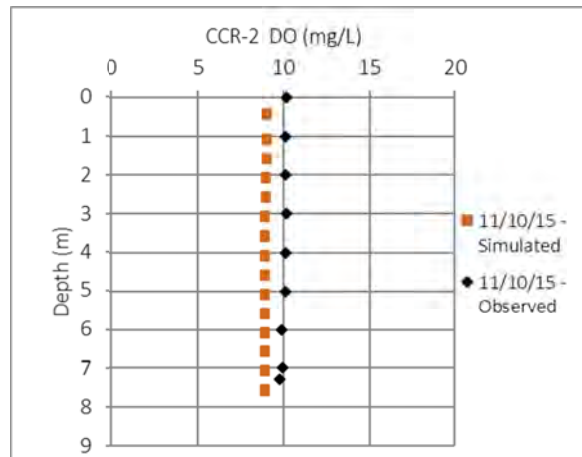
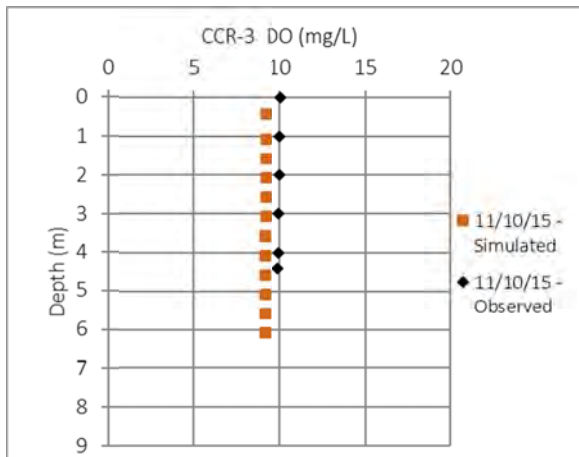
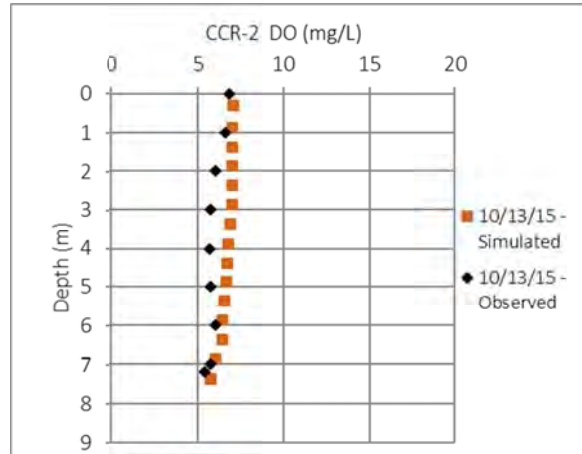
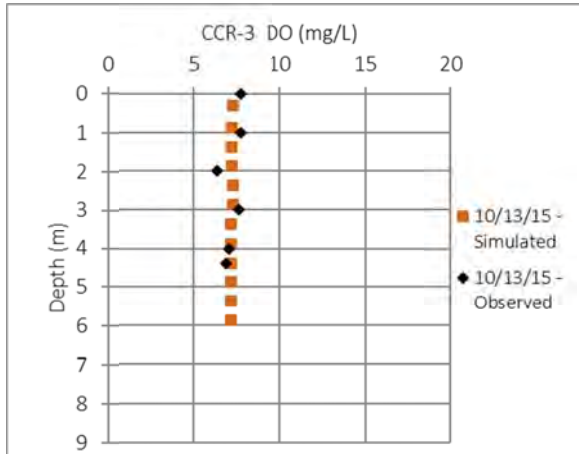
3 Wa

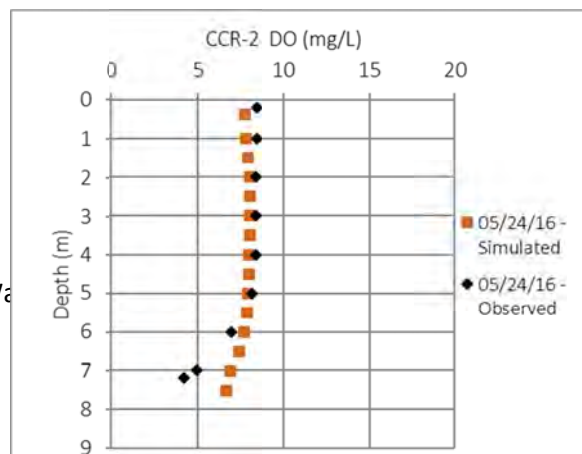
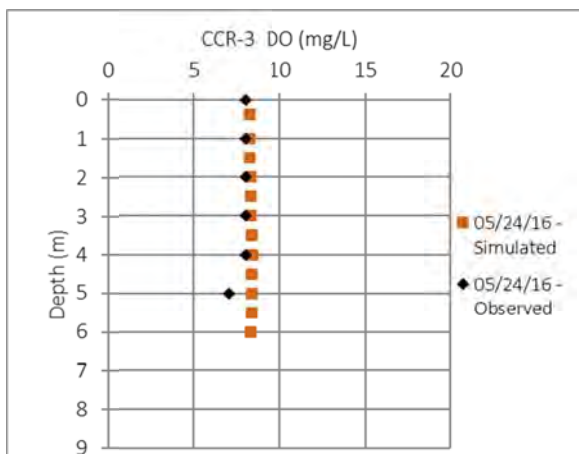
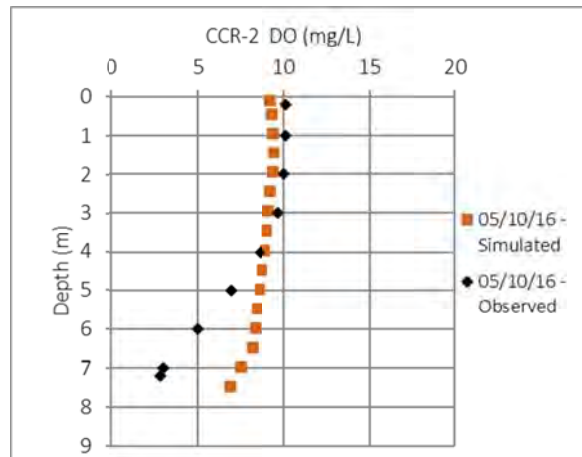
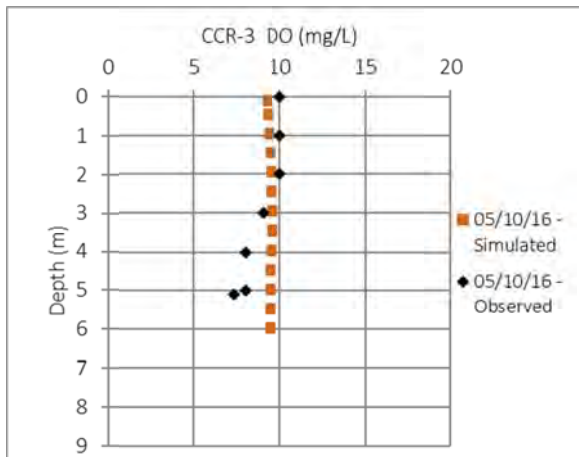
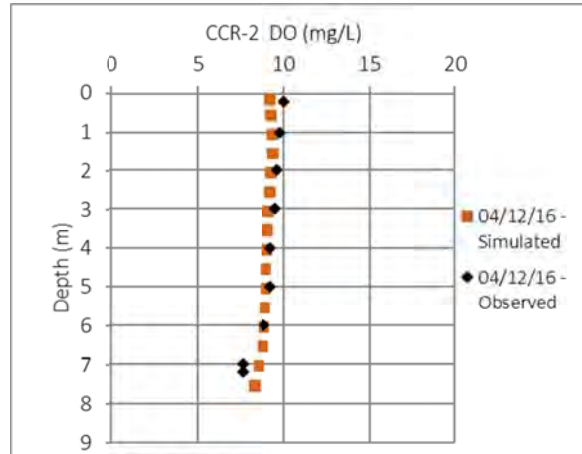
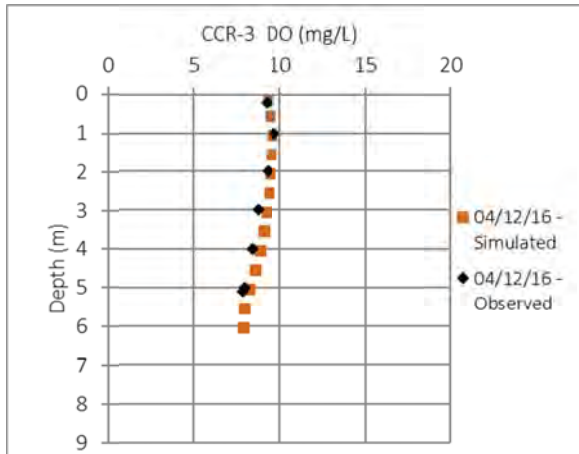


3 Wa

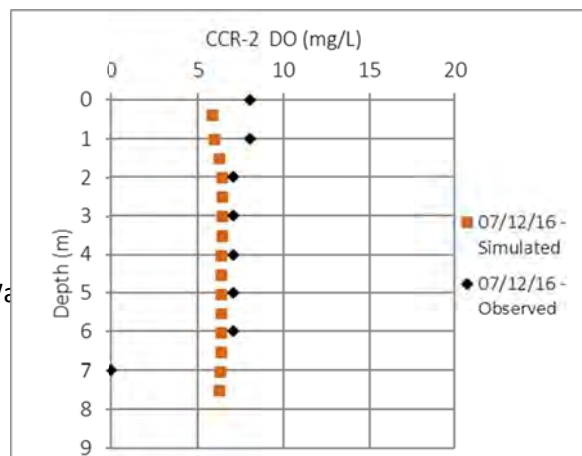
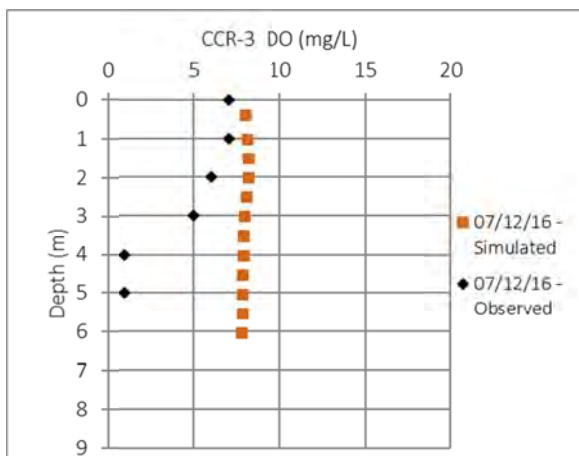
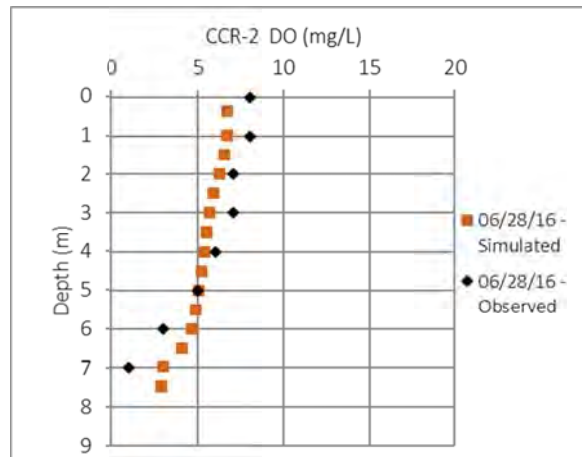
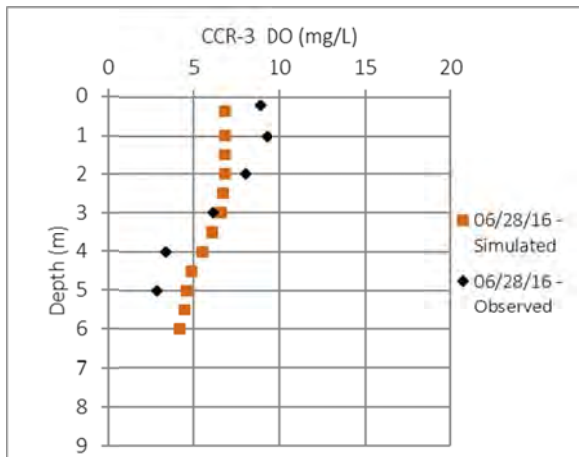
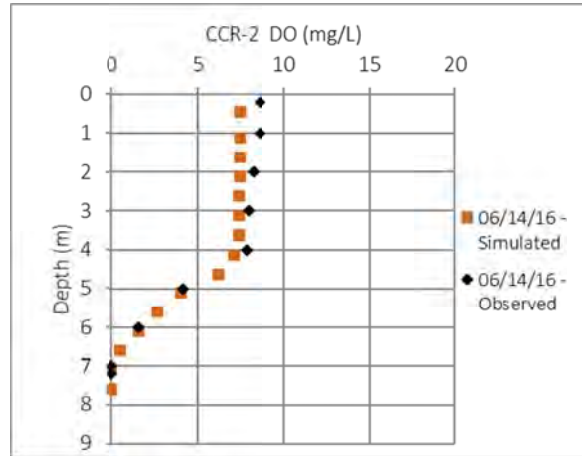
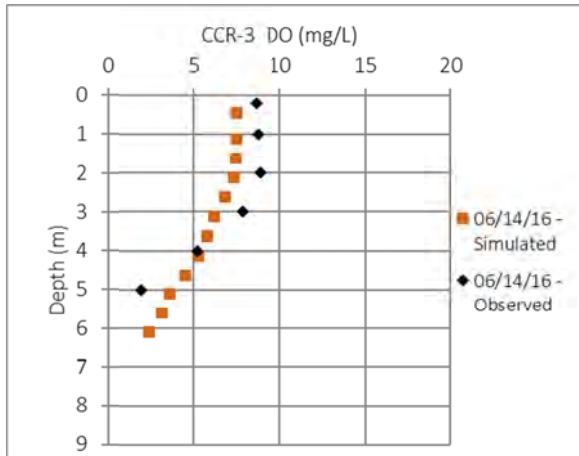


3 Wa

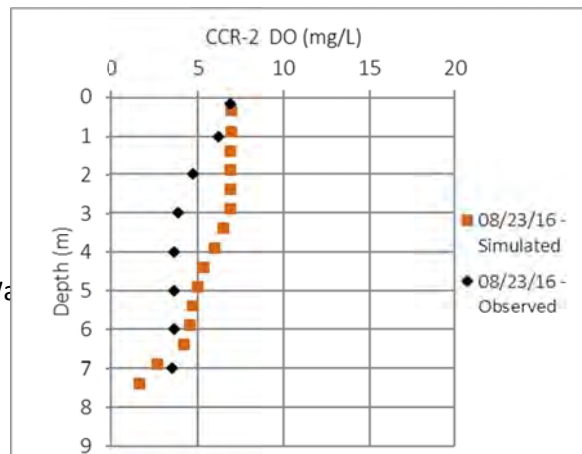
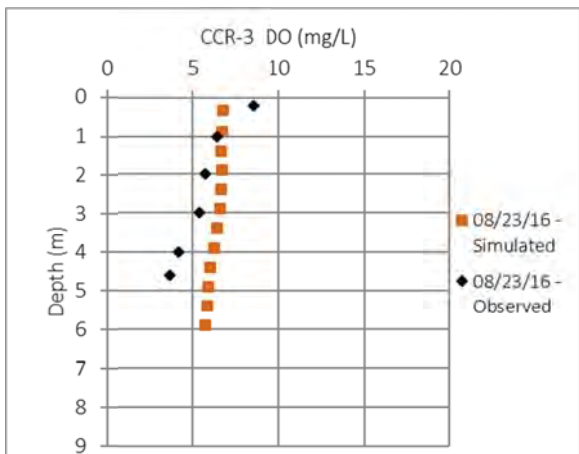
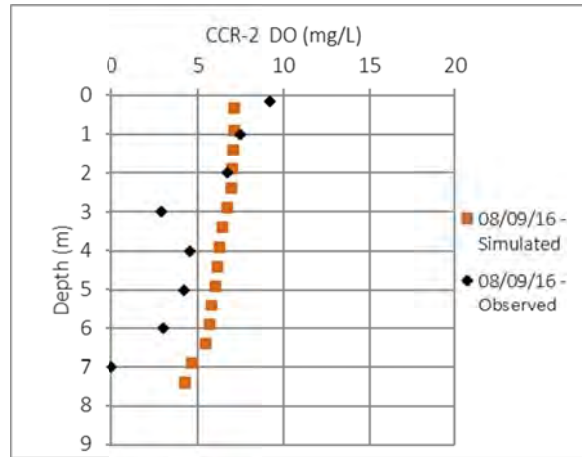
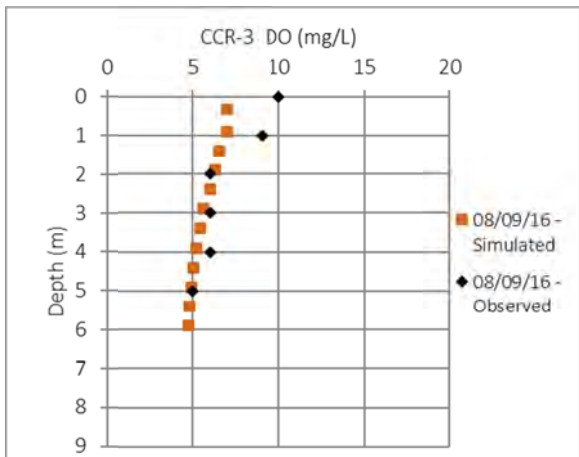
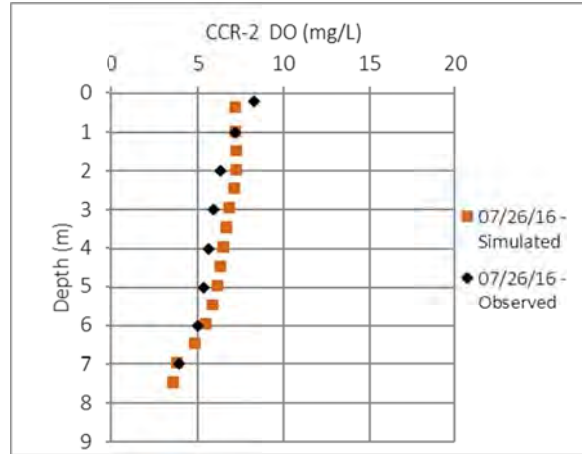
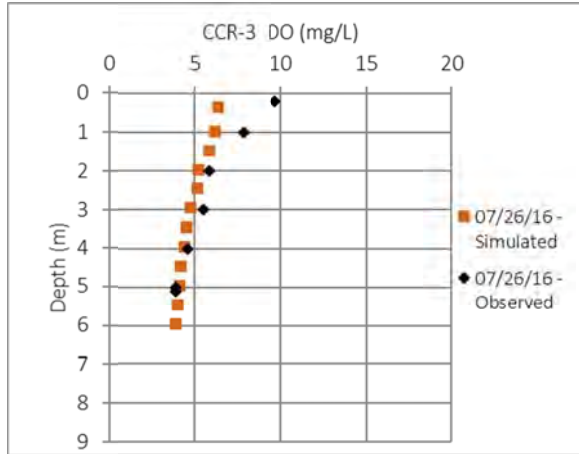




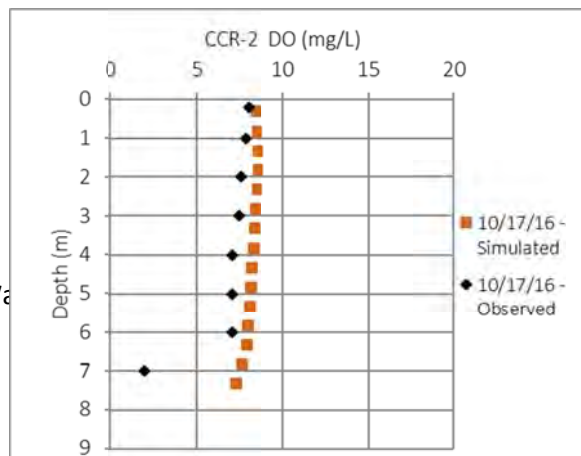
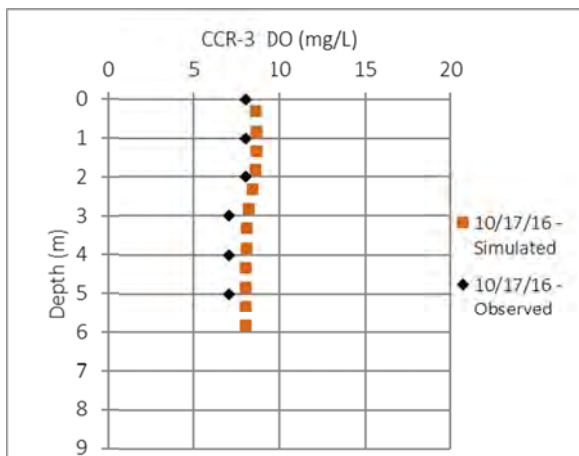
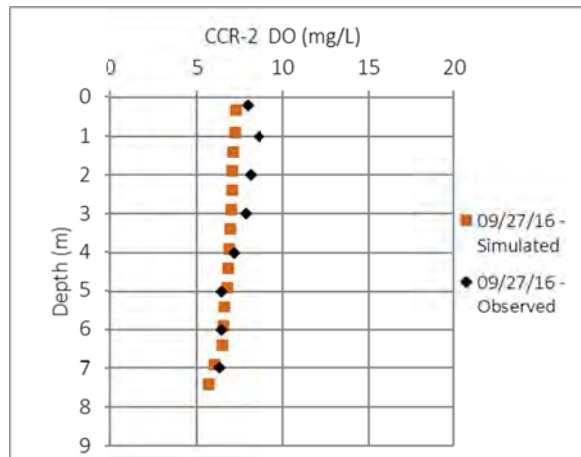
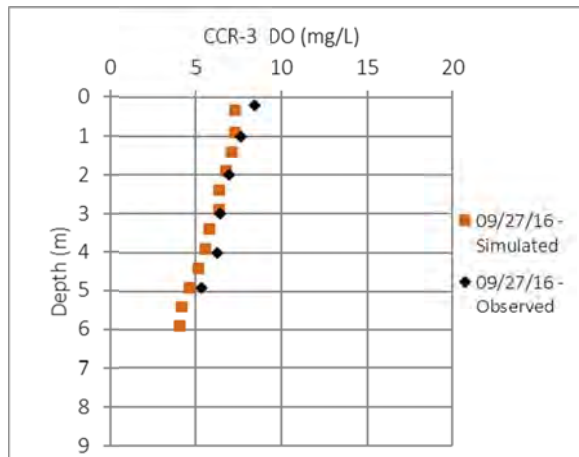
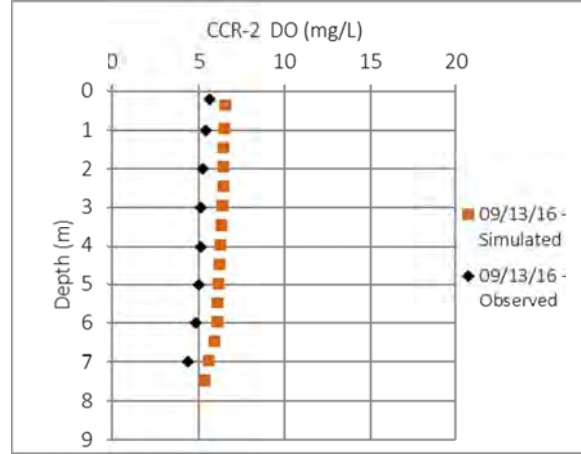
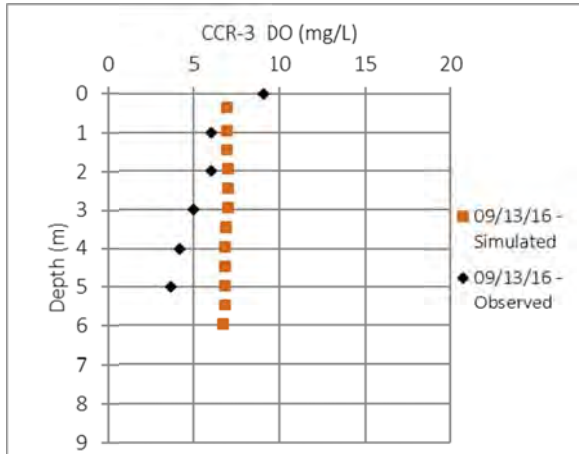
3 Wa



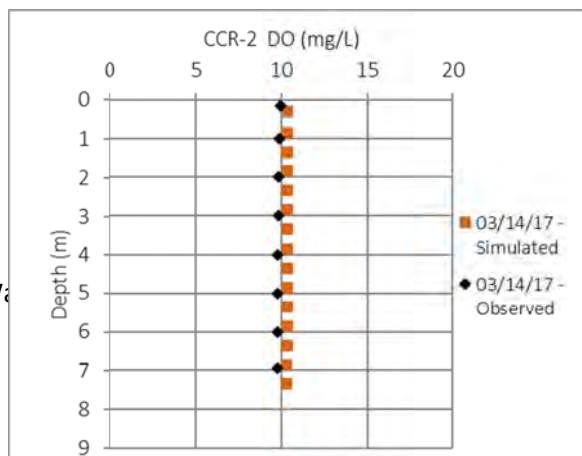
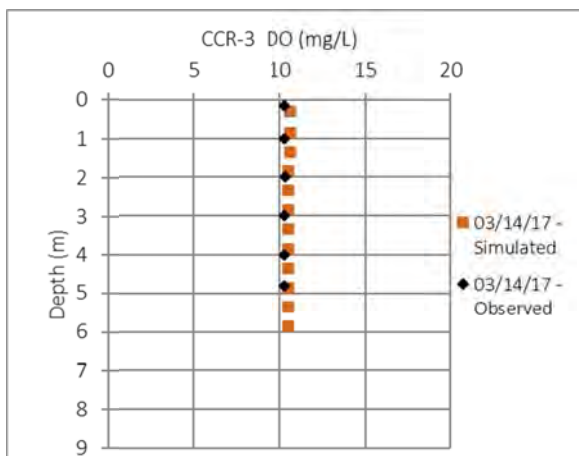
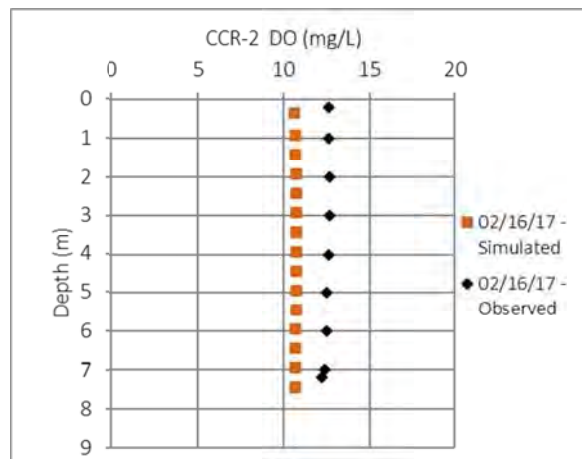
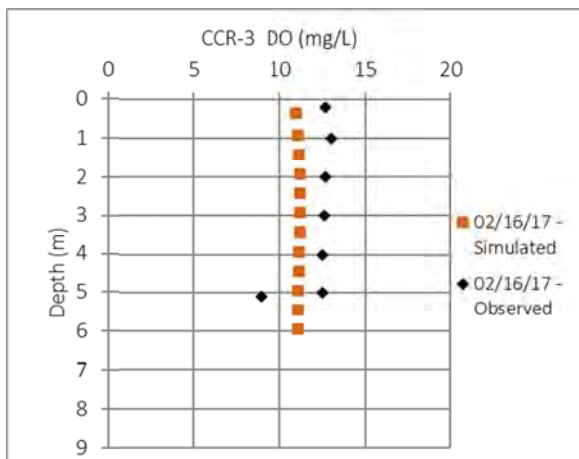
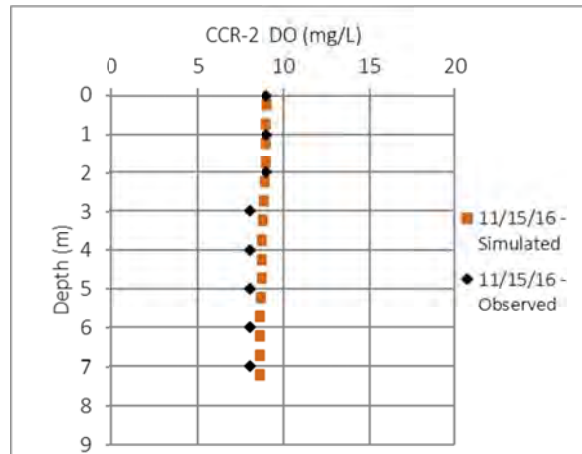
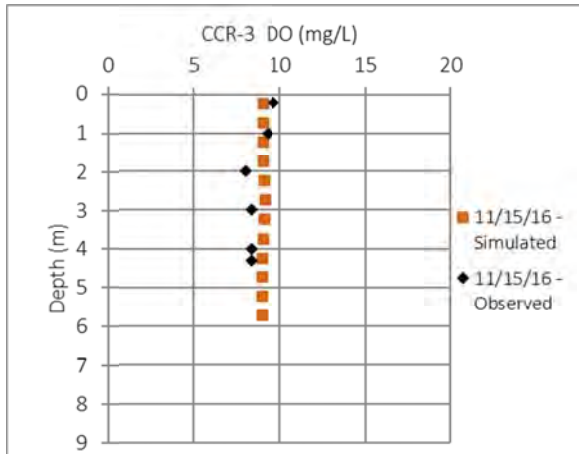
3 Wa



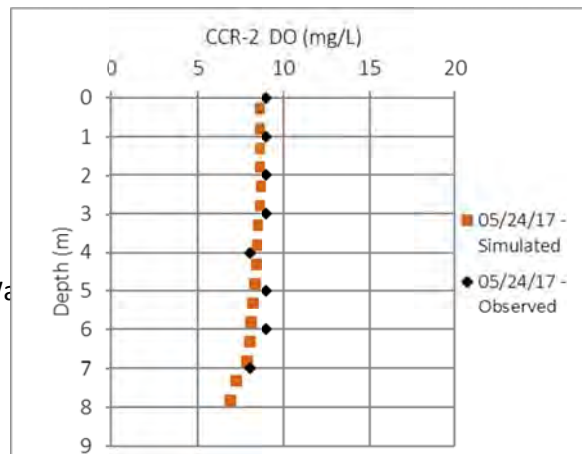
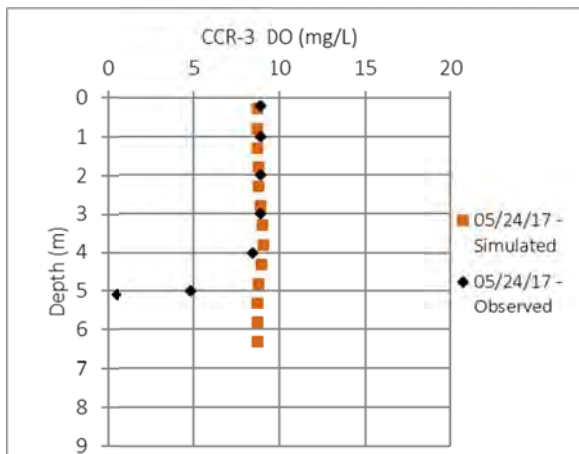
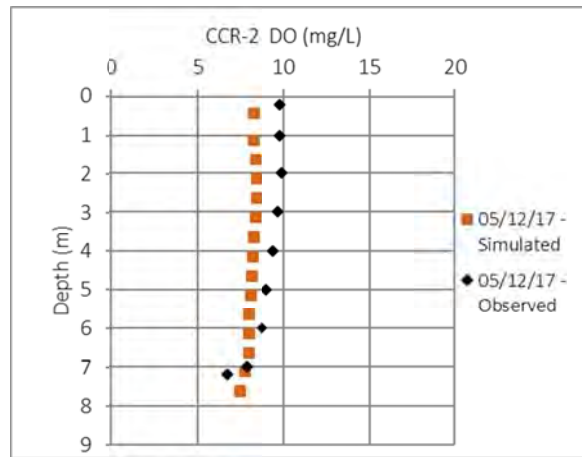
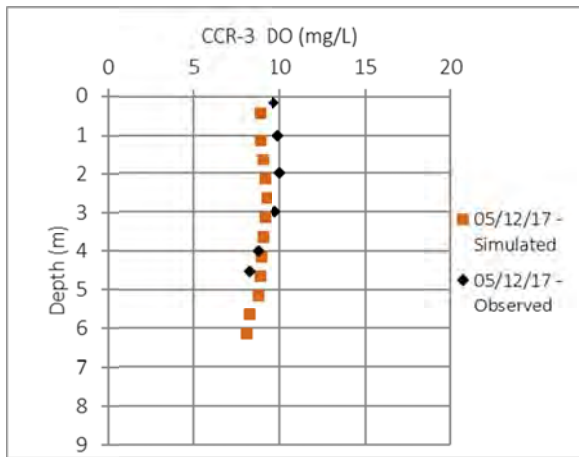
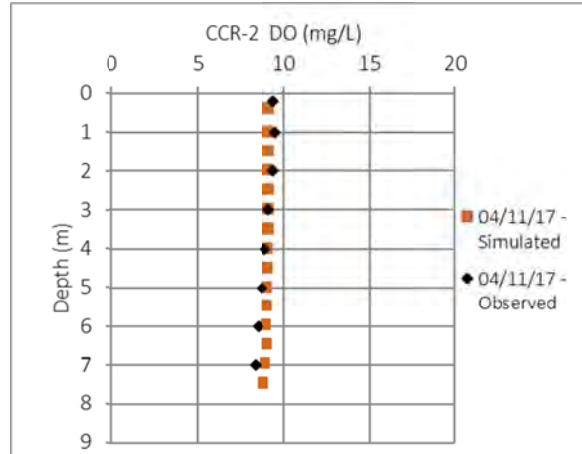
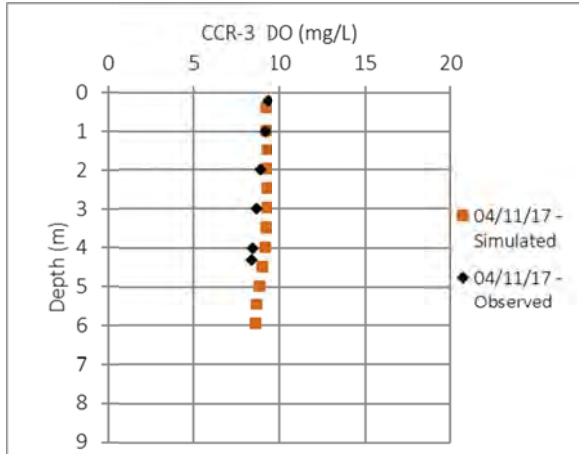
3 Wa



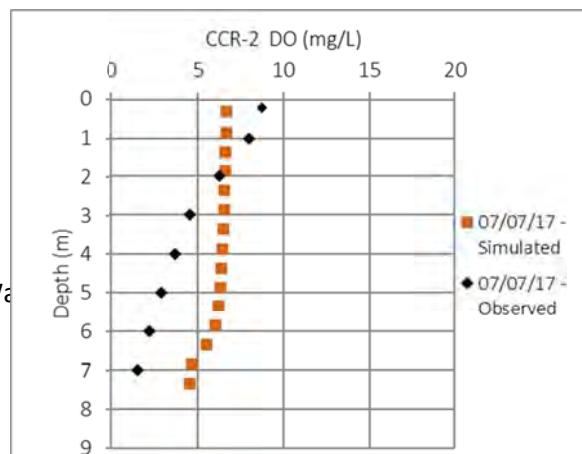
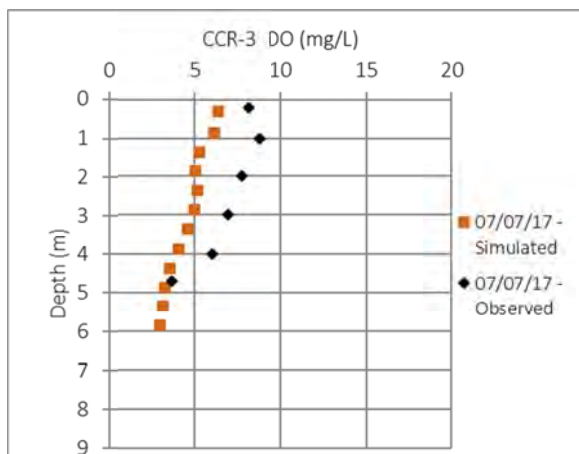
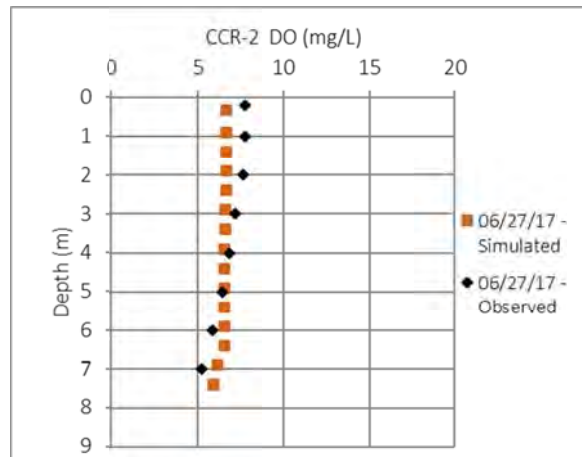
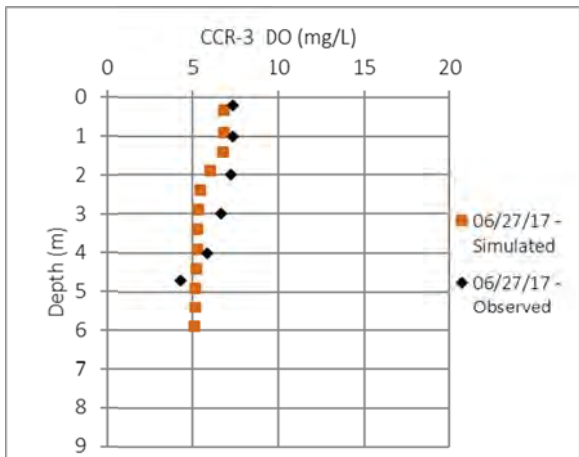
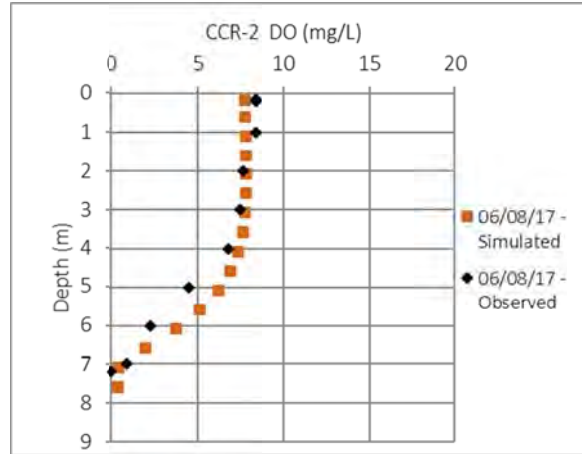
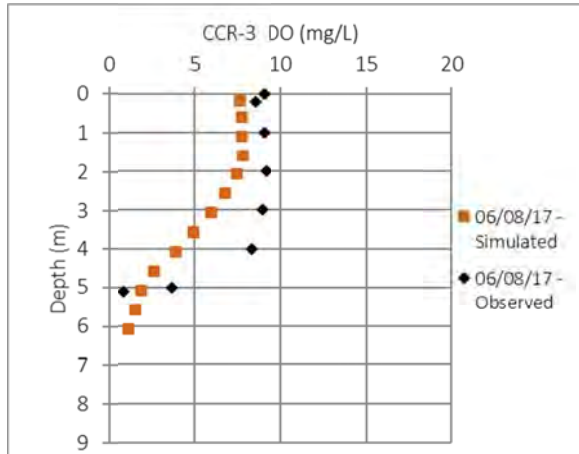
3 Wa



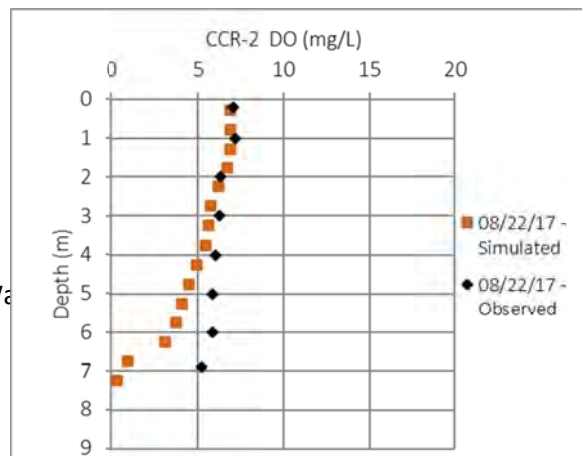
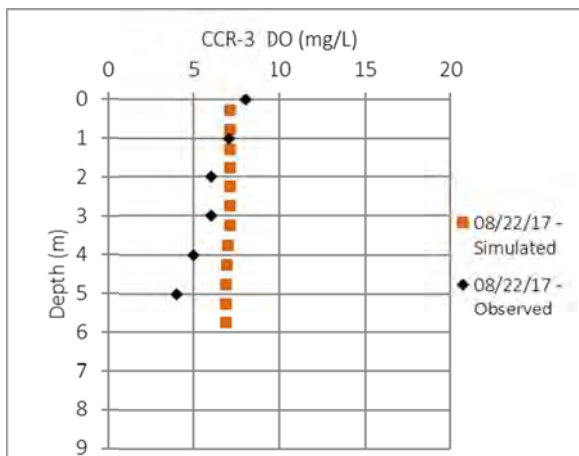
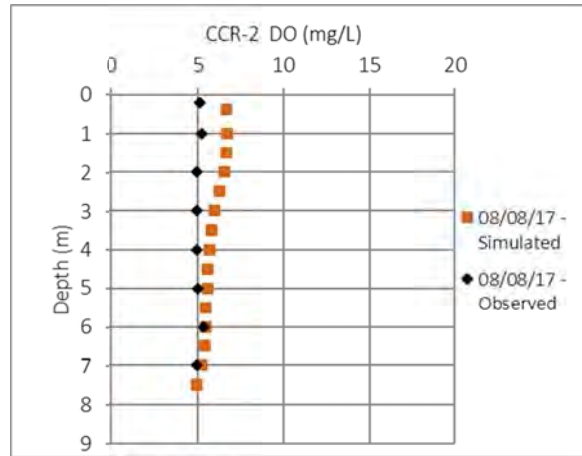
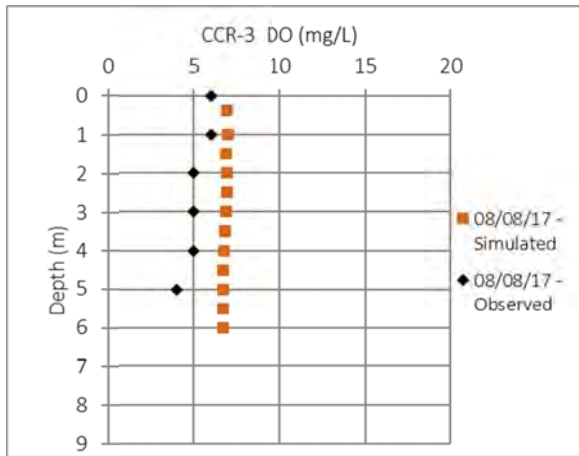
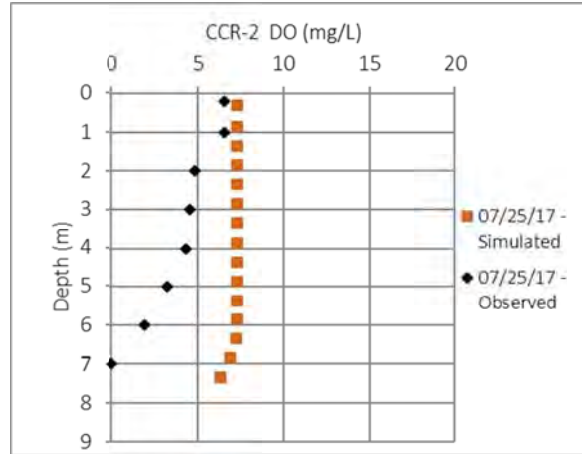
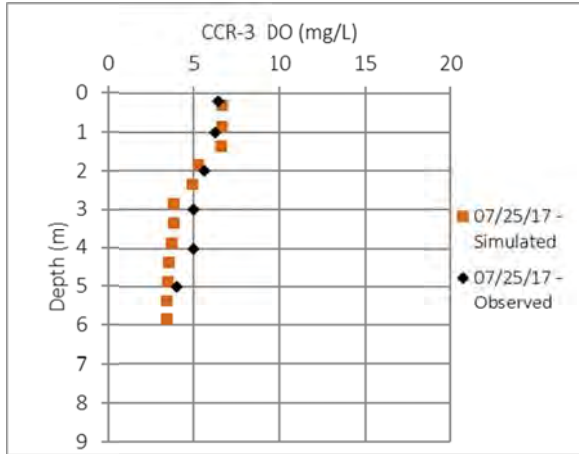
3 Wa



3 Wa



Water



3 Wa

